Investigating the Isomer-specific Effects of Conjugated Linoleic Acid on Adiposity and Insulin Resistance in *db/db* Mice

by

Ryan W. T. Hunt

A Thesis submitted to the Faculty of Graduate Studies of

The University of Manitoba

in partial fulfilment of the requirements of the degree of

Master of Science

Department of Human Nutritional Sciences

University of Manitoba

Winnipeg, Manitoba, Canada

THE UNIVERSITY OF MANITOBA

FACULTY OF GRADUATE STUDIES

*****

COPYRIGHT PERMISSION

Investigating the Isomer-specific Effects of Conjugated Linoleic Acid on Adiposity and Insulin Resistance in *db/db* Mice

By

Ryan W. T. Hunt

A Thesis/Practicum submitted to the Faculty of Graduate Studies of The University of Manitoba in partial fulfillment of the requirement of the degree

Of

Master of Science

ABSTRACT

Conjugated linoleic acid (CLA) has been shown to reduce adiposity in humans and in some animal models. *Trans (t)-10, cis (c)-12* CLA can lead to severe fat ablation and worsen insulin resistance in lean and *ob/ob* mice as opposed to improving insulin sensitivity without changes in adiposity in *fa/fa* Zucker rats. In order to investigate whether this is a species or genotype specific effect, seven-week old *db/db* mice were randomly assigned to groups fed *ad libitum* either 0.4% *c9, t 11* CLA, 0.4% *t10, c12* CLA or a control diet for six weeks. A weight-matched group were fed restricted amounts of a control diet to match the body weight of the *t10, c12* CLA fed mice. Serum glucose, insulin, triglycerides and leptin concentrations were assayed and protein levels of select insulin signalling mediators and leptin in the epididymal adipose tissue were analyzed by Western blotting.

Mice fed *t10, c12* CLA ceased to gain weight while simultaneously increasing their feed intake. HOMA-IR revealed no differences in insulin resistance among any of the *db/db* mice. Levels of the phosphorylated p85 subunit of phosphatidylinositol 3-kinase were highly elevated in epididymal fat of *db/db* mice and were highest in the *t10, c12* CLA fed group. Serum leptin concentrations of *c9, t11* CLA fed mice were higher than both control and *t10, c12* CLA fed mice. However, the *t10,* c12 CLA-fed mice had the greatest concentration of leptin when expressed per mass of visceral adipose tissue. Elevated leptin protein levels were also seen in epididymal adipose tissue of the *t10, c12* CLA fed mice.

Protein kinase C (PKC) describes a group of enzymes that have gained much attention for their ability to phosphorylate cell surface receptors and insulin signalling mediators thereby altering normal insulin signalling. To investigate possible mechanisms for the action of CLA on insulin signalling, the levels of the protein kinase C (PKC) isoforms from all classes (conventional, novel and atypical) were quantified in the epididymal adipose tissue of the mice as well as in mature 3T3-L1 adipocytes treated with CLA. PKCα, βI, θ, ε, μ and ζ/λ were all found at varying levels and subcellular locations in the epididymal adipose tissue of lean and *db/db* mice and 3T3-L1 adipocytes.

These results demonstrate that the *t10, c12* isomer of CLA depletes adipose tissue of *db/db* mice without worsening insulin sensitivity while influencing the activity of a variety of PKC isoforms in adipose tissue. This is one of the first studies to determine the presence of these enzymes in the adipose tissue of *db/db* mice and their ability to be modulated by CLA.

TABLE OF CONTENTS

ACKNOWLEDGEMENTS

This thesis would not have been possible without the expert guidance and opportunities to learn in a fantastic environment that were provided by Dr. Taylor and Dr. Zahradka. Thanks to Dr. Aukema and Dr. Anderson for their time, guidance and for volunteering to be on my committee. Thanks to Jodi, Pat and Sue from Human Ecology and Human Nutritional Sciences at the University of Manitoba and CCARM for all of their hard work and help with all things administrative. Thanks to the Dairy Farmers of Canada and the National Sciences and Engineering Research Council for funding my project.

Many thanks to Danielle and Erin for their help with animal care, to Azadeh Yeganeh for teaching me how to tame the adipocytes and to Brenda Wright for all of her weekend assistance. Thanks to Lesslee Tworek for her teaching, patience and motivating "pats" on the back. To all of the other members of the Zahradka and Taylor laboratories: Danielle, Raissa, Heather, Vanessa, Sherif, Suresh, Gayatri, Nazanin, Maria and Jordan, you have made my time here very enjoyable and made every day at the lab something to look forward to. Many thanks to everyone at CCARM, the St. Boniface Research Centre and my fellow nutritional science grad students for sharing your skills, knowledge and friendship.

Thank you to my parents for their love and support over the last two exciting years. A huge thank you to the Tramleys for all of their support, I don't know what I would have done without you guys. Thanks to my Nanna and Pappa for giving me a place to write and to my Grandparents for all of their encouragement. Finally, much love to Ally and Harvey for believing in me and cheering me on to the finish line.

DEDICATION

To all of my family

LIST OF TABLES

LIST OF FIGURES

LIST OF ABBREVIATIONS

ANOVA	One-way analysis of variance
aPKC	Atypical protein kinase C (PKCζ/λ)
BMI	Body mass index
c	*Cis*
CLA	Conjugated linoleic acid
cPKC	Conventional or classic protein kinase C (PKCα, βI, βII)
CS	Calf serum
DAG	Diacylglycerol
*db*CTL	*db/db* mice fed 0% CLA diet
*db*c9, t11	*db/db* mice fed 0.4% (w/w) *c9, t11* CLA diet
*db*PW	*db/db* mice fed 0% CLA in restricted amounts to match body weight of *db*t10, c12 group
*db*t10, c12	*db/db* mice fed 0.4% (w/w) *t10, c12* CLA diet
ddH_20	Distilled, deionized water
DEX	Dexamethasone
DMEM	Dulbecco's Modified Eagles Medium
FBS	Fetal bovine serum
GLUT-4	Glucose transporter- 4
GSK	Glycogen synthase kinase
HOMA-IR	Homeostasis model assessment-insulin resistance
IL	Interleukin
ITT	Insulin tolerance test
IRS	Insulin receptor substrate
JAK	Janus kinases
LA	Linoleic acid
lnCTL	Lean mice fed 0% CLA diet

LPL	Lipoprotein lipase
LXR	Liver X receptor
MIX	1-methyl-3-isobutylxanthine
NOD	Non-obese diabetic
nPKC	Novel protein kinase C (PKCδ, ε, θ, μ)
ObRb	Long-form leptin receptor
OGTT	Oral glucose tolerance test
PDK1	3-Phosphoinositide-dependent kinase
PI (3,4) P_2	Phosphatidylinositol 3, 4-bisphosphate
PI (3,4,5) P_3	Phosphatidylinositol 3, 4, 5-trisphosphate
PI3K	Phosphatidylinositol 3-kinase
PI4P	Phosphatidylinositol 4-phosphate
PPAR	Peroxisome proliferator activated receptor
PKB/Akt	Protein kinase B
PKC	Protein kinase C
PS	Phosphatidylserine
SH-2	Src homology- 2
SOCS3	Suppressor of cytokine signalling
SREBP	Sterol regulatory element binding protein
STAT	Signal transducers and activators of transcription
t	*Trans*
T2DM	Type 2 diabetes mellitus
T1DM	Type 1 diabetes mellitus
TG	Triacylglyceride
Tyr	Tyrosine
UCP	Uncoupling protein
ZDF	Zucker diabetic fatty

LITERATURE REVIEW

Introduction

The direct health care costs associated with overweight and obesity were estimated to be $6 Billion annually in Canada in 2006 with Type 2 Diabetes Mellitus (T2DM) contributing approximately $1.02 Billion (1). With the incidence of T2DM increasing at an alarming rate, Health Canada now estimates that the annual health care costs associated with T2DM could be as high as $9 Billion per year (Health Canada, 2006). With the prevalence of T2DM and obesity increasing among youth (2), further understanding of the pathology of these conditions and their prevention is of great importance.

Management of T2DM initially involves dietary and lifestyle changes, followed by the use of oral or injectable agents to control blood glucose levels. This regimen is followed by insulin injections if pancreatic function has been significantly compromised. Increased body fat, particularly visceral fat, is a critical risk factor in the development of diabetes (3). There is a strong link between decreased visceral adipose tissue and improved insulin sensitivity in both humans and rodents (4, 5). As a means to help control body fat levels or control body weight, many individuals have turned to various natural health products or nutraceuticals for assistance. The fatty acid isomers of conjugated linoleic acid (CLA) have been marketed as a weight-loss product for a number of years; however, CLA has yielded mixed results in human trials. A main concern regarding the use of CLA has been its potential to reduce insulin sensitivity in mice as well as in men with insulin resistance (6). Leptin receptor deficient *fa/fa* Zucker

rats fed a CLA mixture have improved peripheral glucose utilization without any changes in body weight (7). Conversely, leptin deficient *ob/ob* mice and lean mice exhibit lipodystrophy: a significant depletion of adipose tissue depots, redistribution of adipose tissue to the liver and/or muscle, and increased insulin resistance when given CLA (8, 9). We propose that the different responses to CLA observed in rodent models may be explained by the fact that one animal model is leptin receptor deficient while the other is leptin deficient (*ob/ob*). Furthermore, the changes in glucose utilization (*fa/fa* Zucker rats) in response to CLA may be attributed to an altered leptin feedback mechanism mediated by Protein Kinase C (PKC). Thus, leptin receptor deficient *db/db* mice may show improved glucose utilization along with decreased adiposity following feeding of a CLA-rich diet, however, this has not been experimentally tested. The following literature review aims to present the current state of knowledge on this topic.

Adipose tissue as an endocrine organ

Once thought to be strictly a storage site for excess energy, white adipose tissue is now recognized to be a major secretory endocrine organ that releases a number of hormones and other signalling molecules called adipokines. Adipokines have been implicated in the development of T2DM and cardiovascular disease in response to increased levels of visceral obesity (10-13). A disrupted balance between adipokines may play a key role in the development of these chronic diseases due to leptin resistance and the impaired feedback mechanisms that may result from hyperleptinemia. Interestingly, a deficiency of leptin that results from a lack of adipose tissue can also lead to insulin resistance; for example, lean mice that are given CLA experience both lipodystrophy as well as a worsening of glucose utilization (9). Obese individuals or

animals that have become leptin resistant and have extremely high circulating levels of leptin may also become insulin resistant.

Leptin and the leptin receptor

The *ob* gene encodes for leptin, an adipokine that triggers the hypothalamus to suppress appetite. With increased body fat stores, increased leptin secretion from adipose tissue elevates leptin in the blood and this leads to decreased appetite via certain anorexigenic peptides in the hypothalamus (14). Conversely, decreased adipose tissue leads to decreased leptin levels and an increase in appetite.

Leptin is a hormone and, as such, it operates by binding to a cell surface receptor. ObRb is the receptor isoform expressed primarily in the hypothalamus, but it is also found in the cell membranes of adipocytes, macrophages, pancreatic β-cells, skeletal muscle, adrenal and liver cells. Due to alternative splicing, five other leptin receptors (ObRa-f) can be synthesized and these isoforms are present in differing amounts in a variety of cell types, yet their functions remained largely unknown (15). ObRa, ObRc and ObRd possess shortened cytoplasmic domains whose functions remain to be fully elucidated. ObRe is the soluble circulating leptin binding protein found in the plasma (16, 17).

The long-form receptor (ObRb) is a transmembrane receptor and the only leptin receptor capable of triggering intracellular signal transduction pathways. It is also the only leptin receptor required for normal energy homeostasis (18). Interestingly, ObRb is linked by an unknown mechanism to insulin signalling, since a mutation in the leptin

receptor is a model for T2DM in mice (*db/db* mice) or for the metabolic syndrome in rats (*fa/fa* rats) (14, 15).

ObRb is a member of the class I cytokine receptor family, which may lead to cross-talk with other cytokines such as interleukin-6 (IL-6) (19). The janus kinase (JAK) and signal transducers and activators of transcription (STAT) signal transduction pathway known as JAK/STAT is one of the main signalling cascades activated by leptin (20). Binding of leptin to the leptin receptor leads to the activation of JAK2, which phosphorylates numerous tyrosine residues found in the cytoplasmic domain of ObRb (21). The phosphorylation of Tyr1138 on the leptin receptor leads, in turn, to STAT-3 phosphorylation, an event that promotes STAT dimerization and transport to the nucleus where it acts as transcription factor (20) for various neuropeptides that influence energy balance and appetite through the melanocortic/melanocortinergic pathway (21).

Another action of phosphorylated STAT-3 is the increased expression of a suppressor of cytokine signalling (SOCS3) which binds to phosphorylated Tyr985 and blocks JAK2 activity, thus repressing further leptin receptor signalling. When leptin was administered peripherally for 48 hours, mRNA coding for SOCS3 was increased four-fold in the hypothalamus and three-fold in the liver of *ob/ob* mice (22). STAT-3 phosphorylation was significantly decreased in the livers of *db/db* mice, although this was reversed by inhibiting the production of SOCS proteins (23). Increased levels of SOCS3 may be one of the main mechanisms responsible for leptin resistance; SOCS3 mRNA and protein levels are significantly increased in mice that have lowered leptin sensitivity from diet-induced obesity (21). Currently, the focus of research regarding

leptin signalling has been limited to the brain and liver, with very little currently known about leptin signalling in adipose tissue.

Insulin signalling

In response to increased blood glucose and certain amino acids following a meal, insulin is secreted by β-cells present in the islets of Langerhans of the pancreas. Circulating insulin binds to insulin receptors that are present in insulin sensitive tissues, such as muscle, liver and the adipose tissue. The insulin receptor is composed of an extracellular ligand-binding domain consisting of two α-subunits and two β-subunits that make up the intracellular tyrosine kinase (24). Upon binding of insulin to the α-subunit, the intracellular tyrosine kinase becomes partly activated; it then undergoes autophosphorylation, which enhances its catalytical activity and serves to form docking sites for a variety of different proteins that are responsible for propagating the insulin response (25).

The primary target substrates for phosphorylation are the insulin receptor substrate proteins 1-4 (IRS1 to IRS4). IRS proteins initially attach to specific phosphorylated tyrosines. Once bound to the insulin receptor, the IRS proteins are phosphorylated by the intrinsic tyrosine kinase of the receptor at multiple tyrosine residues. The tyrosine phosphorylated sites of IRS enable it to form a complex with the Src homology-2 (SH-2) domain of the regulatory p85 subunit of phosphatidylinositol 3-kinase (PI3K) (26). When PI3K associates with an IRS protein, PI3K is activated and moves to the plasma membrane where it phosphorylates phophatidylinositol-4-phosphate (PI4P), creating PI (3, 4) P_2 and PI (3, 4, 5) P_3 in the cell membrane (24). PI (3, 4) P_2 and PI (3, 4, 5) P_3 assist with the recruitment of 3-phosphoinositide-dependent kinase

(PDK1) and protein kinase B (PKB/Akt) to the cell membrane; this exposes threonine 308 on PKB/Akt to phosphorylation from PDK1. When activated by insulin, PKB phosphorylates glycogen synthase kinase (GSK-3), partially inactivating it; this allows for the activation of glycogen synthase and leads to increased glycogen synthesis (27). GSK-3 activity may be constantly elevated in the adipose tissue and skeletal muscle of diabetic rats and mice (28, 29).

Insulin promotes glucose transport into cells through the insulin dependent glucose transporter-4 (GLUT-4). GLUT-4 resides primarily in intracellular membranes and moves to the cell surface where it transports glucose into adipose and muscle cells in the presence of insulin (30). This process can occur over a period of greater than twenty minutes. When overexpressed, PKB and PI3K have been shown to increase the movement of GLUT-4 transporters to the plasma membrane (31), although there is a PI3K independent pathway responsible for the recruitment of GLUT-4 to the plasma membrane that has not yet been fully elucidated. Translocation of GLUT-4 to the membrane can also occur independently of insulin. Atypical PKC ζ / λ has been shown to induce translocation of GLUT-4 (32). The roles of PKCs in insulin signalling will be discussed in detail in a later section.

Leptin and insulin resistance

Obese individuals typically have increased circulating levels of leptin. In parallel with insulin resistance, which correlates negatively with increased body fat, elevated serum leptin levels correlate positively with the inhibition of glucose uptake (33). It is hypothesized that leptin may decrease insulin secretion from pancreatic β-cells by regulating the amount of triglycerides and free fatty acids present in these cells (10).

Leptin can modulate insulin signalling in cells that express leptin receptors through several mechanisms, including: 1) a reduction in insulin dependent tyrosine phosphorylation of IRS-1 by decreasing IRS mobility, and 2) increased activity of IRS-1-associated phosphatidylinositol 3-kinase (34). These are changes that may occur in obese individuals, and further research is needed to examine these mechanisms. In obese individuals, Ser-318 phosphorylation of IRS-1 in muscle tissue is up-regulated when leptin levels are elevated. Ser-318 phosphorylation of IRS-1 is suggested to be the key target for modulating leptin-induced insulin resistance (33). When Ser-318 is phosphorylated on IRS-1, further stimulation by insulin is hindered in overweight mice and humans, whereas a response to insulin is still possible in lean humans or mice fed a low fat diet. This serine phosphorylation site is known to inhibit the coupling of IRS-1 to the insulin receptor which leads to a decrease in the availability of IRS molecules, thus hindering insulin signalling (33).

Conjugated linoleic acid (CLA)

CLA is the name for a group of positional and geometrical isomers of linoleic acid (LA; C18:2 n-6) in which the two double bonds are conjugated as opposed to being separated by a methylene (CH_2) group. Double bonds separated by a single bond are considered to be conjugated. CLA can be found naturally in the fat of ruminant animals and dairy products; it can also be produced synthetically from the partial hydrogenation of sunflower and safflower oil (35). The majority of CLA obtained from the diet is in the form of the *c9, t11* isomer, or rumenic acid. This isomer, which is abundant in dairy products, accounts for 90% of the dietary CLA intake by humans (36). Of the seventeen CLA isomers identified, the two isomers that have garnered the majority of attention for

their biological effects are the naturally abundant *c9, t11* isomer and the *t10, c12* isomer which is predominantly produced synthetically (36). Typically, CLA supplements contain mixtures consisting of approximately 40% of both the *c9, t11* and the *t10, c12* isomers. The *c9, t11* and *t10, c12* isomers are also available as highly purified (95%) single isomers and are used largely for research studies. Naturally occurring CLAs are found in triglyceride form while the synthetic isomers are usually free fatty acids, unless synthesized into triglyceride form (37).

First identified for their anti-mutagenic properties, fatty acids derived from linoleic acid present in grilled beef seemed to offer anti-carcinogenic protection rather than a pro-carcinogenic effect as was expected from pan fried hamburger meat (38). Recent consumer interest regarding CLA has focused on its potential use as a weight loss agent while research has expanded to investigate the role of CLA in diabetes/insulin sensitivity, cancer, heart disease and immune function, as well as adiposity.

CLA controversy

CLA has received considerable attention for its various physiological effects, in particular its ability to reduce body fat gain, enhance lean body mass, decrease inflammation and ameliorate diabetic symptoms in some rodent models while exacerbating symptoms in others (39). In humans, several clinical trials have examined the potential weight loss effects of CLA which has led to a mixture of results regarding its efficacy. Studies where CLA was found to decrease body fat in humans all utilized high quality mixtures of CLA containing mostly the *c9, t11* and the *t10, c12* isomers (>90%) which were administered in doses of 1.8-6 g/d (39, 40). Some studies have shown moderate decreases in body fat and even an increase in lean body mass, perhaps

leading to an improved overall body composition. The fat loss from CLA has mostly been attributed to the *t10, c12* isomer which can result in fat loss between 0 and 1.0 kg, with 6.0 g of CLA day appearing to be the maximal efficacious dose (35, 40). Furthermore, the benefits of CLA for weight control may only be occurring in humans who are gaining body weight and CLA may not have an effect on already accrued adipose tissue (40, 41). The losses in body fat in human studies are quite moderate in comparison to the losses that occur in some mouse models.

Several CLA studies have been completed in mice (Table 1). Lean mice seem particularly susceptible to CLA and can experience excessive weight loss and lipodystrophy (9). Obese, *ob/ob* mice, which are unable to produce leptin also experience significant reductions in adipose tissue when fed CLA, however, this can be accompanied by a worsening of hyperglycemia and hyperinsulinemia (8). Zucker Diabetic Fatty (ZDF) rats, which lack a functional leptin receptor and are already diabetic, experience a decrease in body fat in response to 1.5% CLA mixture for 14 days along with improved insulin sensitivity (42). Even when they do not have a significant decrease in body fat mass, non-diabetic *fa/fa* Zucker rats showed an improvement in glucose utilization (43) which may be correlated with a decrease in adipocyte size when fed a 1.5% CLA mixture for 8 weeks (43).

These conflicting results have caused some concern regarding the use of CLA in humans due to the possibility of increased insulin resistance accompanying potential weight loss. Although changes in insulin sensitivity have not been seen in healthy individuals (39), CLA had an adverse effect on fasting glucose levels and insulin sensitivity in studies of humans with T2DM (44), or metabolic syndrome (6). It is

Table 1: Overview of mouse studies and dietary CLA[1,2]

Animal Model	Age, sample Size, length of treatment, gender	Total Dietary Fat (Source) (w/w)	Dose of CLA (w/w)	Isomer, Form	Purity	Assessments	Results	Reference
C57Bl/6J Lean mice	7 weeks 5 mice/group 8 months Female	10% High Oleic Safflower Oil	1%	Mixed FFA	*c9,t11*-34% *t10,c12*-36%	Adipose ITT	Ablation of all adipose tissue ↓ Insulin sensitivity	(9)
Ob/ob mice	Age unspecified 6/group 3 and 11 weeks Female (Harlan, UK)	2.5% High Oleic Sunflower Oil + Standard Chow	Exp.1:1.5% Exp.2:2.5% Exp.3:2.5% Exp.4:2.5%	Mixed FFA	**Exp.1,2:** - *c9,t11*-36% *t10,c12*-38% **Exp.3**: *c9,t11*-90% *t10,c12*-90% **Exp.4:** *c9,t11*-40% *t10,c12*-40%	White adipose OGTT	↓ Adipose tissue and body weight CLA and t10, c12 isomer. ↑AUC in CLA and *t10,c12* CLA fed mice	(47)
Ob/ob mice	6 weeks 8/group 6 Weeks Male (Harlan, UK)	13% *	0.58% 0.11% 0.01%	9, 11 10, 12 Other FFA	*	HOMA-IR Adipose Serum TGs	↓ HOMA-IR No Δ in adipose ↓ SerumTGs	(45)

Animal Model	Age, sample Size, length of treatment, gender	Total Dietary Fat (Source) (w/w)	Dose of CLA (w/w)	Isomer, Form	Purity	Assessments	Results	Reference
Ob/ob mice	12 weeks 10/group 4 Weeks Male (Harlan, UK)	6.5% Soybean Oil	1.5%	Mixed TG	*c9,t11*-39.2% *t10,c12*-38.5%	Epi-fat Serum leptin ITT	↓ Epi-fat No Δ leptin ↓ Insulin Sensitivity	(48)
Ob/ob mice	6 weeks 8/group 4 Weeks Male (Harlan, UK)	6.5% Soybean Oil	1.5% CLA	Mixed TG	*c9,t11*-39.2% *t10,c12*-38.5%	Epi-fat Fasting glucose ITT HOMA-IR	↓ Epi-fat ↑Fasting glucose ↑ Insulin resistance	(46)
Db/db mice	8 weeks 7/group 5 and 11 weeks Male (Institute of animal reproduction, Japan)	MF Diet + 1.2% Safflower Oil	1.2%	Mixed TG	*c9,t11* -35% *t10,c12*-38%	White adipose OGTT Serum insulin Serum glucose	↓ Adipose tissue and body weight ↑ Glucose tolerance	(37)

1. Abbreviations: Epi-fat, epididymal adipose tissue; FFA, free fatty acids; HOMA-IR, homeostasis model assessment-insulin resistance; ITT, insulin tolerance test; OGTT, oral glucose tolerance test; MF, modified fat: TG, triacylglycerides. 2. * Not reported

difficult to apply the results from animal studies to humans because it is not understood what the main difference between a mouse and a rat is that leads to these opposing responses to CLA feeding.

CLA and ob/ob mice

Ob/ob mice have a mutation in the leptin gene that prevents them from producing and secreting the hormone leptin. Feeding *ob/ob* mice a *c9, t11* CLA-rich diet, however, has been shown to improve fasting serum glucose, insulin and triacylglycerol concentrations and increase adipose tissue plasma membrane GLUT-4, with no changes in body weight or adiposity (45). However, feeding 50:50 mixtures of the two CLA isomers results in decreased body weight and epididymal adipose mass (46). In response to *t10, c12* CLA as a single isomer or in CLA mixtures, *ob/ob* mice exhibit decreased white adipose tissue mass with increased fasting serum glucose (45, 46). These increases in blood glucose levels are coupled with reduced insulin sensitivity and elevated fasting insulin concentrations (8, 46).

CLA and fa/fa Zucker rats

The *fa/fa* Zucker rat is morbidly obese as well as insulin resistant and considered a model for the metabolic syndrome was discovered thirty-five years ago. A spontaneous mutation in the rat, $Lepr^{fa}$ results in a dysfunctional ObRb that has reduced binding affinity for leptin (49). A 50:50 mixture of CLA given to *fa/fa* Zucker rats does not result in decreased body weight, however, they still experienced an improvement in oral glucose tolerance and higher adipose GLUT-4 mRNA levels (7). Studies involving this animal model have shown that the *t10, c12* isomer of CLA induces weight loss while improving muscle glucose transport and decreasing fasting serum glucose and insulin

concentrations (50). When given the *c9, t11* isomer on its own, *fa/fa* Zucker rats did not experience any changes in body weight, adiposity, muscle glucose metabolism, or insulin levels (50). *Fa/fa* rats fed a CLA mixture had a 23% reduction in serum leptin vs. the control, lean Zucker rats. The adipocytes of the *fa/fa* control rats were also significantly larger than those of the CLA fed *fa/fa* rats (43). Decreased adipocyte size suggests an improvement adipocyte function, as shown by improved ability to mobilize stored lipids (43), and secrete adipokines such as leptin that regulate appetite, and increased fatty acid oxidation in muscle and liver (21). There also exists a strong relationship between smaller adipocytes and increased insulin sensitivity (51, 52).

Although they exhibit a similar phenotype, *ob/ob* mice and *fa/fa* Zucker rats are of different species, and they also have different mutations. Which factor underlies the opposite effects observed when they are fed CLA is not known. A more suitable mouse model for comparing the effects of CLA between rats and mice is the *db/db* mouse, which has a mutation that leads to a shortened cytoplasmic domain on the ObRb rendering them unable to propagate a proper leptin signal resulting in a similar phenotype to that of the *fa/fa* Zucker.

CLA and db/db mice

C57BL/6J mice with a mutation in the leptin receptor ($Lepr^{db}$) are characterized by obesity, hyperglycemia, hyperinsulinemia, hyperleptinemia and dyslipidemia. The *db/db* mice also show insulin resistance according to glucose tolerance tests (53). The autosomal recessive *db/db* mutation thus makes C57BL/6J mice a suitable model for severe T2DM (15).

There is only one known study in which 8 week old *db/db* mice were given a 1.2 % CLA mixture for 11 weeks (37; Table 1). Although they utilized the triglyceride (TG-CLA) form of CLA, it is accepted to be equivalent to the free fatty acid form of CLA (54) that is most frequently employed in animal studies. The *db/db* mice experienced significant weight loss consistent with the results for *ob/ob* mice. Epididymal and abdominal fat pad weight was decreased in the *db/db* mice along with an increase in liver weight (8, 37). The *db/db* mice fed CLA had improved blood glucose and plasma insulin levels during an oral glucose tolerance test. Interestingly, these improvements are consistent with the results obtained with the administration of a CLA mixture to *fa/fa* Zucker rats (43) rather than *ob/ob* mice.

Unfortunately, the study done by Hamura et al. (2001) did not use a paired-weight control group of *db/db* mice matched to the body weight of the CLA-fed *db/db* mice. This makes it more difficult to determine whether the improvements in oral glucose tolerance and insulin levels were due to the CLA and not due to a decrease in body weight. The study also failed to explore any of the mechanisms behind the improved glucose and insulin levels or any changes regarding insulin signalling. Important adipokines that originate from adipose tissue, such as leptin, also were not measured, therefore leaving further questions that have yet to be addressed.

CLA and 3T3-L1 adipocytes

Fully differentiated 3T3-L1 adipocytes are a useful cell model to evaluate insulin action and other cellular responses in adipocytes. Mouse-derived immature pre-adipocytes are identical to fibroblasts; however, when treated with insulin, 1-methyl-3-isobutylxanthine (MIX) and dexamethasone (DEX), 3T3-L1 adipocytes will differentiate

over a four to six day period into mature fat cells. Over this time, lipid droplets appear inside the cell as an indication that the cells are differentiating (55).

Nine days after inducing differentiation, 3T3-L1 adipocytes treated with 100 μM of the *t10, c12* isomer of CLA showed both reduced expression of leptin mRNA as well as decreased leptin secretion (56), similar to the reduced serum leptin levels seen in *fa/fa* rats following administration of a CLA mixture (43). This is in contrast to the results obtained by Brown et al. (2004), who found that treatment with 30 μM of *t10, c12* isomer of CLA for 1, 2 and 3 weeks increased leptin gene expression along with a time-dependent decrease in triglyceride accumulation in newly differentiated human adipocytes from stromal vascular cells (57). Ciglitazone, an activator of peroxisome proliferator activated receptors (PPAR)-γ and an anti-hyperglycemic agent that leads to triglyceride accumulation was used to treat the 3T3-L1 adipocytes in conjunction with the *t10, c12* CLA. The ciglitazone-induced triglyceride accumulation was inhibited by the *t10, c12* isomer in 3T3-L1 adipocytes, which the researchers hypothesized was due to the isomer blocking preadipocyte differentiation through a PPAR-γ dependent mechanism (58).

In 3T3-L1 adipocytes, the *c9, t11* isomer of CLA may improve insulin-stimulated glucose transport though an anti-inflammatory mechanism or through improved translocation of GLUT-4 to the cellular membrane, which then promotes the shuttling of glucose into the cell (45). 3T3-L1 adipocytes treated with a mixture of *c9, t11* (40%) and *t10, c12* (40%) CLA isomers at concentrations of 50-200 μM decreased basal glucose uptake 20-30% over a time frame up to 96 hours. However, insulin-stimulated glucose uptake was only inhibited slightly at 200 μM, the highest concentration of CLA

employed in the study (59). Although CLA and its effects on leptin and glucose transport in 3T3-L1 adipocytes have been studied, there is a lack of investigation as to the particular cell signalling mechanisms that are stimulated by treatment with CLA.

Proposed mechanisms for differential responses to CLA

Despite the conflicting results among different animal models and cell types in response to treatment with CLA, a consistent mechanism that explains the action of CLA has yet to be fully elucidated. Several mechanisms have been examined in an attempt to explain the effects of CLA on lipid metabolism. Proposed mechanisms involving PPAR and the sterol regulatory element binding protein (SREBP) have received the most attention.

PPARs (α, β/δ and γ) are nuclear receptors that function as transcription factors when activated by endogenous signals like fatty acids to regulate a number of genes important to lipid and triglyceride metabolism (60). The distribution of the various PPAR targets varies among tissues; PPARα is abundant in liver, muscle and brown adipose tissue, while PPARγ is highest in adipose tissue (61). Due to their unique chemical structure, CLA isomers may be important signalling molecules through their ability to act as ligands for multiple PPARs. PPARγ seems to be activated solely by the *t10, c12* isomer while PPARα may be activated by both the *t10, c12* and the *c9, t11* isomer (47). Activation of PPARγ by CLA is thought to have an insulin sensitizing effect similar to the PPARγ agonists, the thiazolindinediones, which are used as drugs in the management of T2DM. Unfortunately these drugs lead to triglyceride accumulation in adipocytes, which is not seen with CLA treatment (47, 56, 57). In *fa/fa* Zucker rats, CLA did not alter the gene or protein levels of two of PPARγ's targets: uncoupling protein 2

(UCP-2) and lipoprotein lipase (LPL) (43). CLA's mechanism of action may also be due to the activation of hepatic PPARα which enhances hepatic fatty acid oxidation (62). In the liver of *ob/ob* mice, neither PPARα nor one of its target genes, carnitine palmitoyl transferase-1α, showed differences in mRNA expression between CLA isomer fed and control mice (46). The mechanisms involving either PPARα or PPARγ and CLA do not appear to explain the different responses observed in mice and rats; however, they may still play a large role in the some of the effects of CLA on adiposity.

SREBP-1c belongs to a group of nuclear transcription factors (SREBPs) found in insulin sensitive tissues like the liver, muscle and adipose tissue. When activated by insulin, SREBP-1 regulates a number of genes involved in lipid metabolism and glucose utilization (63). SREBP-1c can also be activated by the Liver-X-Receptor-α (LXR-α) that is stimulated by cholesterol derivatives (63). Elevated SREBP-1c activity leads to states of lipid accumulation or lipodystrophy as well as insulin resistance; however, SREBP-1c knock-out mouse models have lower fasting glucose levels (63). Overexpression of SREBP-1c is found in the livers of *ob/ob* mice, *fa/fa* Zucker rats and *db/db* mice (23, 63). Because of the link between increased lipids and decreased insulin sensitivity, SREBP-1c may be an important transcription factor that could explain the effects seen in mice and rats if it is regulated differently between the two species in response to CLA. In *ob/ob* mice, the *c9, t11* isomer has been shown to improve serum lipid profiles; this may be due to reduced activation of hepatic SREBP-1c and LXR-α mRNA expression. The *t10, c12* isomer had no effect on hepatic SREBP-1c or LXR-α mRNA levels in the *ob/ob* mice which may explain the hyperlipidemia as well as the increased diabetic effect seen with this treatment (8). Stringer (2006) found that in the

fed state, dietary CLA isomers had no effect on hepatic SREBP-1 activation although there was improved hepatic steatosis in *fa/fa* Zucker rats. Full length SREBP-1 was significantly increased in the liver of fed-state *fa/fa* Zucker rats given *c9, t11* and *t10, c12* CLA isomers, however, the amount of activated SREBP-1 did not change due to CLA (64). Because CLA did not increase SREBP-1 levels in multiple animal models, there is no obvious way to explain the genotype or species-specific responses to CLA. Therefore, the mechanism of how CLA improves insulin resistance and hepatic lipid levels in *fa/fa* Zucker rats requires further exploration.

Protein kinase C (PKC)

A group of isoenzymes known as PKC is gaining attention for their ability to influence insulin signalling (65). At this point, the direction of the cellular response, specifically whether insulin signalling is downregulated or upregulated, appears to be dependent upon which isoforms are either present or activated within the particular cell type. Furthermore, exploration into the effects of CLA on PKC within the context of insulin signalling has been extremely limited to date.

PKC is a family of eleven or more isozymes, some of which are able to regulate the insulin signalling pathways by either promoting or inhibiting insulin's actions (65). The PKC isoforms have been placed into three different groups according to the substrates that they require for activation. The classical or conventional PKCs (cPKCs) include the isoforms α, βI, βII and γ which are activated by a product of lipid oversupply, diacylglycerol (DAG), as well as intracellular Ca^{2+} and phosphatidylserine (PS). These isoforms are widespread throughout the body. Novel (nPKC) PKC isoforms, δ (widespread), ε (brain, heart), η (heart, skin, and lung), θ (muscle, brain, blood cells) and

μ (lung epithelial cells) are activated by DAG and PS but do not require Ca^{2+}. The atypical PKC (aPKC) isoforms ζ (widespread) and ι/λ (kidney, brain, and pancreas) do not require Ca^{2+} or DAG for activation (66). The isoforms found in adipose tissue, however, have not been well characterized. Consequently, their role in insulin or leptin signalling in adipocytes has also not been adequately defined.

PKC isoforms are able to interact with various upstream and downstream targets of the insulin signalling cascade which can lead to various effects on glucose utilization (65) as summarized in Table 2. The activation of DAG-sensitive PKC isoforms (conventional and novel) may provide a link between impaired lipid metabolism and decreased insulin sensitivity and glucose utilization. Activated atypical PKC isoforms have been shown to act downstream of PI3K and may provide an insulin sensitizing effect in adipocytes (66).

Table 2: Effect of PKC isoforms on insulin signalling

PKC Isomer	Insulin Signalling Substrate	Effect on Glucose Utilization
PKCα	Insulin receptor substrate (IRS)	↓ Glucose uptake and ↑Insulin resistance
PKCβI PKCβII	Insulin receptor GLUT-4 transporter	↑Insulin resistance ↑ Glucose uptake
PKCδ	Insulin receptor, IRS	↑ Glucose uptake, ↑ Insulin receptor endocytosis
PKCε	Glycogen synthase kinase (GSK), PKB/Akt	Hinders glucose uptake, ↑ Insulin resistance
PKCθ	Insulin receptor	↑ Insulin resistance
PKCζ/λ	IRS PKB/Akt, GLUT-4 vesicle	↑Insulin resistance ↑ Glucose uptake independently of insulin

Adapted from Sampson et al (2006)

Effects of CLA on PKC

There is limited evidence to support the view that CLA will affect PKC activity in regards to insulin resistance. Based on two studies using prostate and mammary epithelial cells, CLA has been shown to activate several PKC isoforms (α, δ, μ and ζ) (67). Song et al (2004) showed that the *c9, t11* and *t10, c12* isomers were equipotent in stimulating changes in PKC distribution in human prostate cancer cells. Activation of the cPKC and nPKC isoforms occurs when they are localized in the membrane, and cytosolic PKC is typically considered inactive (68). However, in normal rat mammary epithelial tissue, CLA was found to have no effect on the distribution of various PKC isoforms (69). In the same study, CLA treatment was shown to increase PKC α, δ, ε and η in membrane fractions when administered to adipocytes isolated from mammary gland tissue. These results indicate that various PKCs can be modulated by CLA; however, the effects of CLA on PKC isoforms that are present in adipose tissue as well as their relationship with insulin sensitivity remain to be explored.

Effects of leptin on PKC

Few studies have investigated whether leptin is able to alter the activity of PKC with respect to insulin signalling, especially in adipocytes. Leptin appears to activate PI3K through JAK2 which leads to the association of IRS1 or IRS2 to p85-PI3K, thereby enhancing glucose uptake (18). Stimulating HEK-293 kidney cells with leptin results in increased levels of phosphorylated PKCδ and PKCε, with no rise in intracellular Ca^{2+}, which is to be expected as these novel PKCs are not dependent on Ca^{2+} for activation. Interestingly, the second messengers PI (3, 4) P_2 and PI (3, 4, 5) P_3 that are phosphorylated by active PI3K, have been shown to activate both PKCδ and PKCε in

insect cells (95), which may suggest a PKC mediated mechanism for leptin and insulin signalling pathways to communicate. Further investigation into how these two signalling pathways may cross-talk and can influence insulin sensitivity through an ObRb-PI3K-PKC pathway is required especially in adipose tissue and other insulin sensitive tissues.

Summary of current state of knowledge

PKC isoforms, leptin and CLA have all been shown to modulate insulin sensitivity (Figure 1) in various conditions. On the other hand, the evidence regarding the effects of CLA on PKC and leptin remain to be fully explored. Some evidence indicates that CLA is able to alter the activity of some PKC isoforms as well as reduce the secretion of leptin from adipose tissue. CLA appears to have an insulin sensitizing effect in rats (*fa/fa*) and mice (*db/db*) that lack a leptin receptor while it appears to promote insulin resistance in mice (*ob/ob*) that cannot produce leptin. The mechanism for this difference is currently unknown. The differences in insulin sensitivity may be due to differences in secreted leptin, mediated by changes in PKC as a result of feeding CLA isomers.

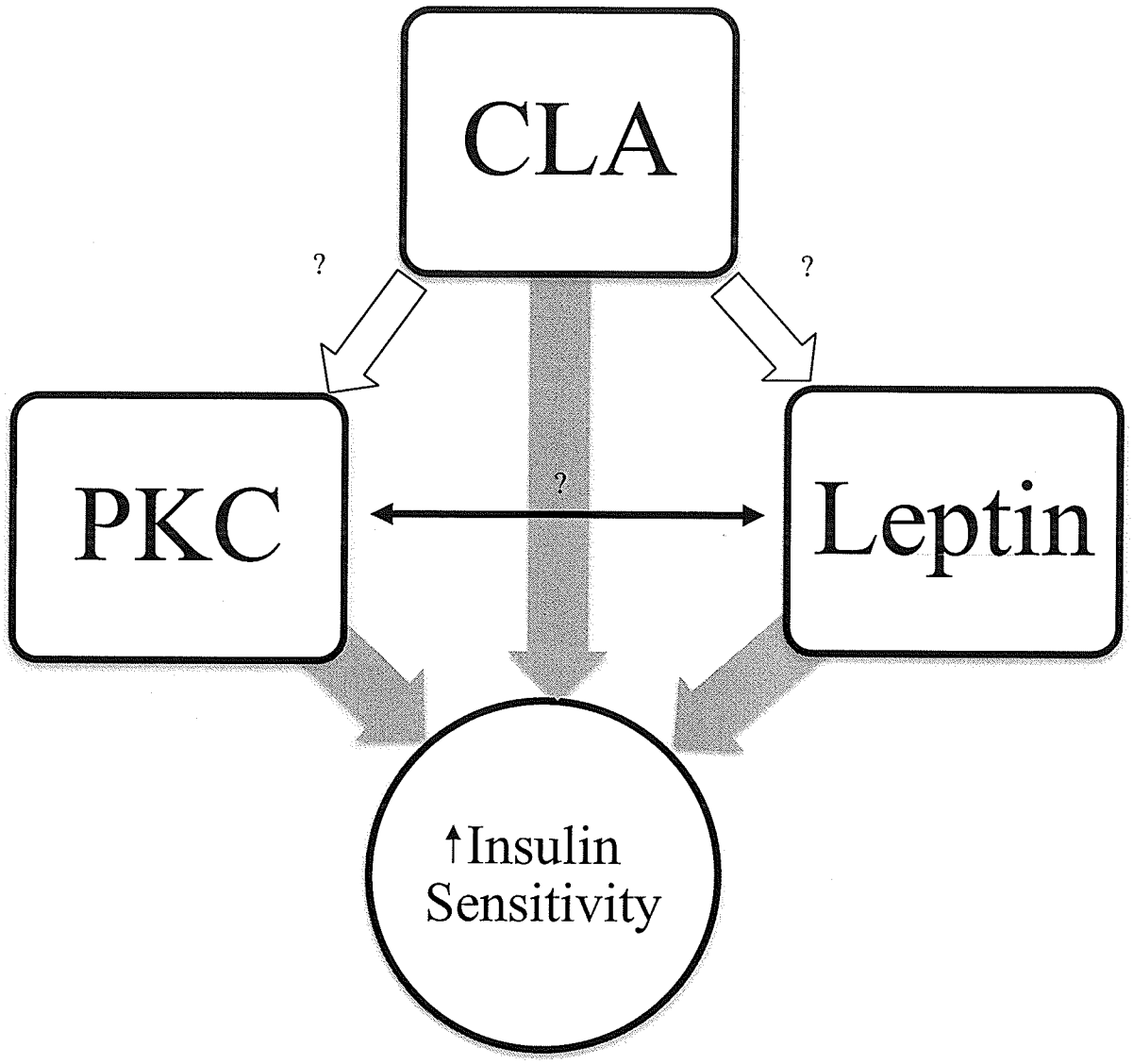

Figure 1: Potential direct and indirect effects of CLA on insulin sensitivity

STUDY DESIGN AND RATIONALE

This study will include *in vitro* and *in vivo* models to investigate how CLA improves glucose utilization with or without reducing adiposity due to changes in leptin that are potentially mediated by various PKC isoforms. The *db/db* mouse, a model for obesity and T2DM, will be used to study the effects of CLA on mice that do not have a functional leptin receptor. The effects of CLA on the mouse-derived 3T3-L1 adipocytes, which do have a functioning leptin receptor, will be used to compare how CLA may modulate leptin levels and PKC activity in adipocytes.

The dietary study (*in vivo*) model will last for six weeks and will involve four groups of leptin receptor deficient, *db/db* mice: i) a control group fed 0% CLA, ii) group fed 0.4 % (w/w) *c9, t11* CLA, iii) group fed 0.4 % (w/w) *t10, c12* CLA and iv) paired weight control group. The study will also include a lean control group that will receive the 0% CLA diet. Both isomers will be compared, as it is the *t10, c12* isomer that has been labeled as being responsible for decreased adiposity while simultaneously inducing insulin resistance, although, both *t10, c12* and *c9, t11* CLA isomers are typically available in equal amounts when taken as a nutraceutical. The paired weight control group will receive the control diet and will not be fed *ad libitum*. This group will have their calories adjusted so that their body weight is equivalent to the CLA group with the lowest body weight. That way, if the *db/db* mice experience changes in glucose utilization or leptin levels that are significantly different from the control groups the changes be attributed to the CLA and not just from changes in body weight and adiposity. Changes in levels of serum and adipose leptin are important and may indicate that intake of CLA results in decreased production of leptin even in animals that lack a leptin

receptor, suggesting an altered feedback mechanism. Changes in adiposity will be assessed by weighing peri-renal and epididymal adipose tissue.

To examine whether changes in glucose utilization have occurred, fasting blood will be collected to measure serum insulin and glucose. The homeostasis model of insulin resistance (HOMA-IR) will be used to calculate the level of insulin resistance using the fasting levels of serum glucose and insulin; this will give us an overall view of the glucose utilization of *db/db* mice given CLA. Although it would be preferable to assess oral glucose tolerance, the repeated blood sampling of fasted mice via the sephaneous vein is very difficult. Any changes in insulin sensitivity will be explained at the molecular level by assessing the levels of phosphorylated PKB/Akt, PI3K and PDK-1 in adipose tissue; this will help to determine whether there are any changes in insulin signalling as a result of CLA feeding.

Activation of certain isoforms of PKC by CLA in adipose tissue or in 3T3-L1 adipocytes has been relatively unexplored. The PKC isoforms α, β, δ, ε, θ, ζ/λ have all been shown to have both inhibitory and stimulatory effects on insulin signalling by acting on various substrates of the insulin signalling pathway (65); CLA has been shown to activate PKC α, β, δ and ζ in prostate cancer cells as well as in mammary gland tissue adipocytes (67, 69). Exploration of the effects of CLA on PKC α, β, δ, ε, θ, ζ/λ in mature 3T3-L1 adipocytes and adipose tissue of the mice will provide further information as to how changes in insulin signalling may occur as a result of CLA. In order to measure the level of PKC activation, cytosolic and membrane PKC have to be separated from each other and then compared as membranous PKC is regarded as being the activated form (68).

The pairing of these two models will help to explain the mechanism for the changes in insulin sensitivity that accompany fat loss in rodents fed CLA.

HYPOTHESES

1. The *t10, c12* isomer of CLA will reduce weight gain and adiposity as well as improve glucose utilization in *db/db* mice, an effect similar to what occurs in *fa/fa* Zucker rats. These effects will be due to their genotype (leptin receptor mutation) and not due to differences between species (rat vs. mouse).
2. Activation of PKC in adipose tissue will contribute to the mechanism whereby the *t10, c12* CLA isomer improves utilization of glucose in adipose tissue due to a dysfunctional leptin receptor.

OBJECTIVES

1. To investigate the effects of a dietary *c9, t11* or *t10, c12* CLA isomers on body weight, adiposity, fasting serum glucose, insulin and leptin. Epididymal adipose tissue of *db/db* mice will be explored for the protein levels of leptin, key mediators in insulin signaling (p-Akt, p-PI3K and p-PDK-1) and PKC α, β δ, ε, θ, μ and ζ/λ.
2. To compare the effects of leptin, linoleic acid and *c9, t11* or *t10, c12* CLA on PKC α, β δ, ε, μ and ζ/λ, and leptin levels in treated 3T3-L1 adipocytes.

MATERIALS AND METHODS

STUDY 1 - ANIMAL STUDY

Animals and diet

Six-week old male C57BLKS/J mice, homozygous for the diabetes spontaneous mutation (*Lepr*^{db}) [*db/db* mice], and ten C57BLKS/J mice [lean controls; lnCTL] were obtained from the Jackson Laboratory (JAX Mice and Services, Bar Harbor, Maine). The experiment was designed for n=10 per group (40 *db/db* + 10 lean controls), however, Jackson Laboratories sent one extra *db/db* mouse which was assigned to the *t10, c12* CLA group. The mice were allowed to acclimatize for 5-9 days to the housing conditions (stainless steel hanging cages, 12 hour light/dark cycle with controlled humidity and temperature) and diet (control diet containing 0% CLA) [Table 3]. The *db/db* mice were randomly assigned to diets containing 0% CLA [*db*CTL], 0.4% (w/w) *c9, t11* CLA [*db*c9, t11] or 0.4% (w/w) *t10, c12* CLA [*db*t10, c12] and fed *ad libitum,* or were randomly assigned to the paired weight control group [*db*PW] fed the 0% CLA diet in restricted amounts to maintain a body weight equivalent to the *t10, c12* CLA-fed mice. The lnCTL group was fed the 0% CLA diet *ad libitum*. Fresh diet was provided three times weekly. The *db*PW mice received restricted amounts of 0% CLA diet daily, beginning on the second week. Weekly body weights were obtained, with the *db*t10, c12 CLA and *db*PW groups being weighed more often in order to determine the degree of diet restriction required. The dietary intake of the *db*PW mice was not different from the lnCTL group. In order to more accurately measure the feed intake of the mice, the diet was mixed with water creating a paste diet. The diet was stored in small portions at -20°C and thawed before feeding. Feed intake was corrected for spillage by weighing any

spilled diet underneath the individual mouse cages. Water was freely available throughout the study. The dietary intervention lasted for 6 weeks. The protocol for the animal care procedures was approved by the University of Manitoba Protocol Management and Review Committee and met the guidelines of the Canadian Council on Animal Care (70).

Table 3: Diet formulation

Ingredients (g/kg Diet)	Control Diet	*c9, t11* Diet	*t10, c12* Diet
Cornstarch[1]	363	363	363
Maltodextrin[2]	132	132	132
Sucrose[2]	100	100	100
Egg White[2]	212.5	212.5	212.5
Cellulose[2]	50	50	50
AIN-93MXG - Mineral Mix[2]	35	35	35
AIN-93VX - Vitamin Mix[2]	10	10	10
Choline[2]	2.5	2.5	2.5
Biotin Mix (200 mg biotin/kg cornstarch)[2]	10	10	10
Tert-butylhydroquinone[3]	0.014	0.014	0.014
Soy Oil[2]	85	80.57	80.57
c9, t11 CLA (90% pure) cat #: 10-1823-90 lot #: G438:12	0	4.44	0
t10, c12 CLA (90% pure) cat #: 10-1826-90 lot #: I-261:8	0	0	4.44

[1]Casco Inc. Etobicoke, Ontario
[2]Harlan Teklad 2826 Latham Drive Madison, WI
[3]Sigma-Aldrich, St. Louis, MO
[4]Larodan, Malmo, Sweden

Tissue collection

At the end of the study period, the mice were fasted from 07:00 to 13:00 and euthanized by asphyxiation with carbon dioxide and cervical dislocation. Trunk blood was drained and collected from the mice immediately following cervical dislocation and placed on ice. The blood was centrifuged (Eppendorf Centrifuge 5804, Hamburg,

Germany) at 5000 rpm for 10 minutes at 4°C, and the serum aliquoted and stored at -80°C. Epididymal and peri-renal fat pads, liver, kidneys and pancreas were dissected, weighed, and flash frozen in liquid nitrogen and stored at -80°C.

Serum biochemistry

i. Glucose

Fasting glucose was analyzed using a commercial kit (Cat. # 220-32, lot: 34381, Diagnostic Chemicals Ltd., Charlottetown, P.E.I.), the principle of which is modified from the Trinder glucose oxidase/peroxidase method (71):

1. Glucose + O_2 + H_2O $\xrightarrow{\text{glucose oxidase}}$ gluconic acid + hydrogen peroxide (H_2O_2)
2. H_2O_2 + hydroxybenzoate + 4-aminoantipyrine $\xrightarrow{\text{peroxidase}}$ quinoneimine dye + H_2O

Reagents used:

- Glucose colour reagent: a solution, reconstituted with ddH_2O, containing a buffer (pH 7.25 at 25°C), 0.25 mmol/L 4-aminoantipyrine, 20 mmol p-hydroxybenzoate, >40 000 U/L glucose oxidase (*Aspergillus niger*), >2000 U/L horseradish peroxidase, and preservatives.
- Glucose Standard: solution containing 5 mmol/L glucose and preservatives, serially diluted to produce 3 additional standards (0.625, 1.25, and 2.5 mmol/L).

Serum from the lean mice was diluted 5 times and serum from the *db/db* mice was diluted 10 times with ddH_2O. Five μL of ddH_2O, glucose standards, serum samples, and quality control were pipetted, in triplicate, into a 96-well microplate (Costar

EIA/RIA 96-well polystyrene plate, Fisher Scientific, Whitby, ON). Two-hundred μL of the reconstituted glucose colour reagent was then added to each well. After gentle shaking, the plate was incubated at room temperature for 10 minutes. The absorbance of the colour was read at 505 nm with a microplate reader (SpectraMax 340, Molecular Devices Corp., Sunnyvale, CA) using SOFTmax Pro software (version 1.2.0., Molecular Devices Corp., Sunnyvale., CA). The mean result for each sample as multiplied by the dilution factor to obtain the final serum glucose concentration in mmol/L. The standard curve of all assays had a minimum correlation coefficient of 0.9.

ii. Triacylglycerides

Serum triacylglycerides were quantified using a commercial kit (Cat # 210-75, Diagnostic Chemicals Ltd., Charlottetown, P.E.I.) with a method adapted from Fosssati & Prencipe (1982).

1. Triglycerides $\xrightarrow{\text{Lipase}}$ Glycerol + Fatty Acids
2. Glycerol + ATP $\xrightarrow{\text{Glycerol Kinase}}$ Glycerol-1-phosphate + ADP
3. Glycerol-1-phosphate + O_2 $\xrightarrow{\text{L-α-glycerol phosphate oxidase}}$ H_2O_2 + Dihydroxyacetone Phosphate
4. 4-aminoantipyrine + H_2O_2 + 3,5-dicholoro-2-hydroxy-benzenesulfonic acid $\xrightarrow{\text{peroxidase}}$ Quinoneimine Dye + HCl + $2H_2O$

The formation of the quinoneimine dye turns the samples red, the intensity of which is directly proportional to the concentration of total triacylglycerides in the sample.

Reagents used:

- RI Enzyme colour solution

- Triglyceride standard: Solution containing 2.0 mmol/L triglyceride standard diluted with a 0.9% saline solution to produce 5 additional standards (0.0625, 0.125, 0.25, 0.5, 1.0 mmol/L).

Serum from *db/db* mice fed *c9, t11* CLA was diluted 5× while the serum from all other groups were diluted 10× with a 0.9% saline solution. Ten μL of 0.9% saline solution, triglyceride standards, serum samples and quality control were pipetted in triplicate into the wells of a microplate (Costar EIA/RIA 96-well polystyrene plate, Fisher Scientific, Whitby, ON). One hundred μL of RI enzyme colour solution was added to each well followed by 140 μL of ddH_2O, and the plate was mixed and incubated for 5 minutes at 37°C in a microplate reader (SpectraMax 340, Molecular Devices Corp., Sunnyvale, CA). The plate was mixed and the absorbance read at a wavelength of 515 nm using SOFTmax Pro software (version 1.2.0., Molecular Devices Corp., Sunnyvale., CA). The mean result for each sample was multiplied by the dilution factor to obtain the final serum triglyceride concentration in mmol/L. The standard curve of all assays had a correlation coefficient of 0.9 or greater.

iii. Cholesterol

Fasting serum cholesterol was quantified using a commercial kit (Cat. # 225-26, Diagnostic Chemicals Ltd., Charlottetown, P.E.I), which has been adapted from Allain et al (1974) and Roschlau et al (1974):

1. Cholesterol Esters $\xrightarrow{\text{Cholesterol esterase}}$ Cholesterol + Fatty Acids
2. Cholesterol + O_2 $\xrightarrow{\text{Cholesterol oxidase}}$ Cholesterol-3-one + H_2O_2
3. H_2O_2 + 4-aminoantipyrine + Phenol $\xrightarrow{\text{Peroxidase}}$ Quinoneimine + $4H_2O$

The quinoneimine dye turns the samples a colour, the intensity of which is directly proportional to the concentration of total cholesterol in the sample.

Reagents used:

- Cholesterol colour reagent: solution containing phosphate buffer (pH 6.7 at 25°C), 1.6 mM 4-aminoantipyrine, >5560 U/L horseradish peroxidise, >400 U/L cholesterol oxidase (*Norcardia sp.*), a preservative, and a stabilizer.
- Cholesterol phenol reagent: solution containing 40 mM phenol, a surfactant, and a stabilizer.
- Cholesterol working reagent: equal volumes of cholesterol colour reagent and cholesterol phenol reagent, mixed gently.
- Cholesterol standard: solution of 5 mM cholesterol, a surfactant, and a preservative; serially diluted to produce 3 additional standards (0.625, 1.25, 2.5 mM).

Serum samples were diluted 2× using 1× PBS (Cat #37572, Thermo Scientific, Rockford, IL) working solution. Ten μL of cholesterol standards, serum samples, ddH_2O and the quality control were pipetted, in triplicate, into the wells of a microplate (Costar EIA/RIA 96-well polystyrene plate, Fisher Scientific, Whitby, ON). Two-hundred μL of working reagent was added to each well, and the plate was mixed for 30 seconds before being incubated at 37°C for 5 minutes. The absorbance of the colour in each well was read at 505 nm using a microplate reader (SpectraMax 340, Molecular Devices Corp., Sunnyvale, CA) using SOFTmax Pro software (version 1.2.0., Molecular Devices Corp., Sunnyvale., CA). The mean result for each sample was multiplied by the dilution factor

to obtain the final serum cholesterol concentration in mmol/L. The standard curve of all assays had a correlation coefficient of 0.9 or greater.

Enzyme immunoassay

i. Leptin

Fasting serum leptin was quantified using a mouse/rat enzyme immunoassay kit (Cat # 22-LEPMS-E01, Alpco Diagnostics., Salem, New Hampshire).

Reagents used:

- 96-well microtiter plate coated with anti-mouse/rat leptin antibody
- Antibody conjugate: Biotinylated anti-mouse/rat leptin antiserum, diluted 1:100 with dilution buffer. Also contains a preservative.
- Enzyme conjugate: Horse-radish peroxidase conjugated streptavidin diluted 1:100 with the dilution buffer immediately before use. Also contains a preservative.
- Wash buffer: Diluted 1:20 with ddH_2O just prior to use. Also contains a preservative.
- Tetramethylbenzidine (TMB) substrate solution
- Stop solution: 0.2 M Sulfur Acid (H_2SO_4)
- Standards A-G: Each reconstituted with 1 mL dilution buffer to yield concentrations of 25, 50, 100, 200, 400, 800, and 1600 pg/mL of recombinant mouse leptin.

- Control: Lyophilized mouse serum, reconstituted with dilution buffer. Actual leptin concentration of 1265 ± 190 pg/mL.

Fasting termination serum from *db/db* mice was diluted 100× and serum from lean mice was diluted 10× with dilution buffer. One hundred μL of dilution buffer, standards (A-G), quality control and diluted samples are were pipetted in duplicate into the wells of the 96-well microtiter plate that was coated with anti-mouse/rat leptin antibody, and incubated for one hour on an orbital shaker (DS-500, VWR, Henry Troemner, Thorofare, NJ), rotating at 90 rpm. After the incubation period, the plate was washed 3 times with 250 μL of wash buffer with a microplate washer (Wellwash AC 870, Ref # 5161020, Thermo Labsystems, Woburn, MA). One hundred μL of antibody conjugate was pipetted into each well and the plate was incubated for another hour while being shaken at 90 rpm. The plate was washed 3 times with 250 μL of wash buffer with the microplate washer (Wellwash AC 870, Ref # 5161020, Thermo Labsystems, Woburn, MA). One hundred μL of the enzyme conjugate solution was pipetted into each well. The microtiter plate was covered, and shaken at 90 rpm for 30 minutes before being washed 3 times with 250 μL of wash buffer. In the dark, 100 μL of the TMB substrate solution was added to each well and incubated for 30 minutes. The reaction was terminated with 100 μL of the stop solution and the absorbance was read with a ThermoMax microplate reader (Molecular Devices Corp, Sunnyvale, CA) at 450 nm with a reference filter of ≥590 nm. The standard curve regression line was described using a four parameter logistic lin-log curve-fit calculated by Softmax Pro Software (Version 2.34, Molecular Devices Corp, Sunnyvale, CA). The absorbance values of the samples, when multiplied with their respective dilution values, were used to calculate the leptin concentrations of the mouse

serum samples. The correlation coefficient of the standard curve was ≥ 0.95. The determined and calculated concentration of the recombinant mouse leptin control was between 1075 and 1455 pg/mL.

ii. Insulin

Fasting serum insulin concentrations were determined using a mouse insulin high range enzyme immunoassay (Cat. # 80-INSMSH-E01, Alpco Diagnostics., Salem, New Hampshire)

Reagents used:

- Insulin microplate: 96 well plate coated with mouse monoclonal anti-insulin antibody
- Antibody conjugate: Horseradish peroxidase labeled monoclonal anti-insulin antibody
- Wash buffer: Diluted 1:20 with ddH_2O just prior to use. Also contains a preservative.
- Tetramethylbenzidine (TMB) substrate solution
- Stop solution: 0.2 M Sulfur Acid (H_2SO_4)
- Insulin standards A-E: Each reconstituted with 1 mL dilution buffer to yield concentrations of 3, 7.5, 30, 75, 150 ng/mL and zero standard (0 ng/mL)
- Mammalian insulin high control: lyophilized insulin reconstituted with 0.6 mL of ddH_2O; yields a concentration of 4.77 ng/mL (3.61-5.91 ng/mL) insulin.

Five μL of the standards (A-E), high insulin control and diluted serum samples were pipetted in duplicate into the 96-well microplate. Seventy-five μL of working strength conjugate was pipetted into each well and the plate was placed on the orbital shaker (DS-

500, VWR, Henry Troemner, Thorofare, NJ) and agitated at 90 rpm at room temperature. After a 2 hour incubation period, the plate was washed six times with 250 μL of the reconstituted wash buffer with a microplate washer (Wellwash AC 870, Ref # 5161020, Thermo Labsystems, Woburn, MA). One hundred μL of the TMB substrate was pipetted into each well and incubated at room temperature on an orbital shaker while being agitated at 90 rpm. After 15 minutes, the reaction was terminated with 100 μL of the stop solution. The microplate was read with a ThermoMax microplate reader (Molecular Devices Corp, Sunnyvale, CA) at the absorbance wavelength 450 nm with a reference wavelength of 620-650 nm. Using Softmax Pro Software (Version 2.34, Molecular Devices Corp, Sunnyvale, CA), the standard curve was plotted on a log/log scale and the sample concentrations were determined by plotting the absorbance of each unknown sample against the standard curve.

HOMA-IR

The fasting serum insulin and glucose concentrations were used to calculate the level of insulin resistance with the homeostasis model assessment formula (74).

$$[\text{Fasting glucose (mmol/L)}] \times [\text{Fasting insulin } (\mu\text{U/mL})] / 22.5.$$

Fasting serum insulin was converted from ng/mL to μU/mL:

$$\text{Insulin (ng/mL)} / 0.0417 = \text{Insulin } (\mu\text{U/mL})$$

Western blotting

Western blotting was used to identify the proteins of interest using polyclonal and monoclonal antibodies with a method adapted from Gallagher et al (2008). The adipose tissue samples are solubilised and separated by sodium dodecylsulfate polyacrylamide gel electrophoresis (SDS-PAGE). The samples are then transferred to polyvinylidene

difluoride (PVDF) membrane which allows access for the primary antibodies to bind to the proteins of interest, after non-specific binding sites have been blocked with bovine serum albumin. The antigen-antibody complexes are then tagged with horseradish peroxidase that is attached to a secondary antibody. The protein of interest can then be illuminated using the appropriate chemiluminescent substrates and captured on autoradiographic film.

i. Protein extraction from whole epididymal adipose tissue

In order to quantify the levels of various proteins present in the adipose tissue of the mice, the protein is first released from the tissue by homogenization in a detergent-containing solution and this is then followed by centrifugation to remove insoluble materials and make the proteins available for analysis by Western blotting.

Reagents used:

- 3× Sample Buffer: 3% SDS, 30% glycerol, 0.2 M Tris-HCl pH 6.8, ddH2O
- Liquid N_2

In a mortar, 200 mg of epididymal adipose tissue is covered in liquid N_2 and allowed to freeze so that it can be ground into a fine powder with a pestle. Three times sample buffer was added to the powder, and this was stirred into a uniform paste which was then allowed to sit for a minimum of 15 minutes to permit lysis of the cells. One and a half mL of the suspension was pipetted into a microfuge tube and centrifuged (Eppendorf Centrifuge 5804, Hamburg, Germany) at 12000 rpm for 5 minutes. The supernatant was removed and put into another tube and sonicated (Sonic dismembrator, Model 100, Thermo Fisher Scientific Inc., Ottawa, ON) for 15 seconds to shear the DNA in the sample and thus decrease its viscosity. The samples were stored at -80°C.

ii. Subcellular fractionation of epididymal adipose tissue

In order to identify the distribution of the various PKCs in the epididymal adipose tissue of the mice, the cellular components were fractioned so that the microsomal (activated) and cytosolic (inactive) PKCs were separated from each other.

Reagents used:

Homogenization Buffer:

- 0.25 M Sucrose
- 0.5 mM Tris
- 3 mM $CaCl_2$
- 1 mM EDTA
- 0.5 mM EGTA
- 25% Glycerol

Nuclear Extraction Buffer:

- 175 mM K_2HPO_4
- 0.1 mM EDTA

Protease Inhibitor Cocktail Set III (Cat # 539134, EMD Sciences, INC., Darmstadt, Germany)

- AEBSF, Hydrochloride
- Aprotinin, Bovine Lung, Lyophilized
- Bestatin
- E-64, Protease Inhibitor
- Leupeptin, Hemisulfate
- Pepstatin

Two hundred mg of epididymal adipose tissue was suspended in homogenization buffer approximately 2.5× the volume of the tissue sample. For every 10 mL of homogenization buffer, 2 μL of set III protease inhibitor cocktail (Cat # 539134, EMD Sciences, INC., Darmstadt, Germany) was added to prevent the breakdown of the cellular proteins. The tissue and homogenization buffer were then homogenized (Polytron PT

1600 E, Kinematica AG, Littau-Lucerne, Switzerland) on low speed for 10-15 seconds. The samples were then centrifuged (Eppendorf Centrifuge 5804, Hamburg, Germany) at 2000 rpm for 10 minutes at 4°C. The supernatant was transferred to an ultracentrifuge (Beckman Coulter Optimax Max Ultracentrifuge) tube and spun at 38000 rpm for 40 minutes. The supernatant, which consists of the cytosolic fraction, was collected and stored at -80°C. The remaining pellet, which consists of the microsomal fraction, was resuspended in 100 μL of homogenization buffer and stored separately at -80°C.

iii. Quantification of protein samples

A protein assay was used to quantify the protein concentration of the epididymal adipose tissue and 3T3-L1 adipocyte whole cell and subcellular fractions. The reaction between the reagents and proteins produces a coloured product whose colour intensity, when measured by spectrometric analysis at 550 nm, is directly proportional to the amount of protein in each sample. The results from each assay are compared to a standard calibration curve in order to calculate the quantity of protein.

Reagents used:

- Pierce protein assay reagent A (Cat #23223, Thermo Scientific, Rockford, IL): sodium bicarbonate, bicinchoninic acid and sodium tartrate in 0.2 M sodium hydroxide
- Pierce protein assay reagent B (Cat #23224, Thermo Scientific, Rockford, IL): cupric sulphate
- Protein standard: 2 mg/mL bovine serum albumin standard (Cat # 23209, Thermo Scientific, Rockford, IL) diluted with ddH_2O for tissue samples or with 2×

Sample buffer for cell lysates to produce 6 standards (0.2, 0.4, 0.6, 0.8, 1.0 and 2.0 mg/mL)

- ddH_2O
- 2× sample buffer (0.5 M Tris HCl pH 6.8; 10% SDS; Glycerol (Cat # BP229-1, Fisher,)

The protein extracts derived from the adipose tissue were diluted with ddH_2O. Subcellular fractions and samples from the 3T3-L1 adipocytes were diluted with 2× sample buffer. Ten microlitres of ddH_2O or 2× samples buffer, the standards and samples were pipetted, in triplicate, into the wells of a 96-well microplate (Cat #167008, Nunclon, Roskilde, Denmark). A ratio of 221 μL of reagent A to 4 μL of reagent B was mixed in a volume to allow 200 μL to be pipetted into each well. The plate was incubated at 37°C for 30 minutes. The plate was read at 550 nm on a microplate reader (Thermomax, Molecular Devices Corp, Sunnyvale, CA) and Softmax Pro Software (Version 2.34, Molecular Devices Corp, Sunnyvale, CA) was used to determine the final protein concentration in each sample.

iv. Sodium dodecylsulfate polyacrylamide gel electrophoresis

After quantification of the protein extracts from the adipose tissue, SDS-PAGE was used to separate the various proteins according to their molecular mass. Polyacrylamide gel with SDS, loaded with the tissue or cell samples has a current passed through it that draws the denatured and negatively charged proteins though the gel; the higher molecular mass proteins migrate slower through the gel than those that have a lower molecular mass.

Reagents used:

7.5-12% separating gel:

- 20% acrylamide
- 10% SDS
- 1.5 M Tris-HCL pH 8.8
- 10% ammonium persulfate
- N, N, N', N'-Tetramethylethylenediamine (TEMED) (Cat # 805615, MP Biomedicals, Solon, OH)
- ddH_2O

5-7.5% stacking gel

- 20% (wt/v) acrylamide
- 10% (wt/v) SDS
- 0.5 M Tris-HCL pH 6.8
- 10% (wt/v) ammonium persulfate
- TEMED (Cat # 805615, MP Biomedicals, Solon, OH)
- ddH_2O

- H_2O-saturated butanol
- 10% Bromophenol blue
- 2-mercaptoethanol (Cat # 6010, Omnipur, U.S.A)
- SDS-PAGE electrode buffer: 0.125 M Tris, 0.96 M glycine, 0.5% SDS

One or 1.5 mm spacers were placed between a large and a small glass plate. The plates were inserted into a sandwich clamp assembly and then placed into a casting stand. The 7.5-12% separating gel was prepared and poured between the glass plates. A Pasteur pipette was used to gently layer a small amount of H_2O-saturated butanol over top of the separating gel to make sure that the top of the gel is even. The gel was left to polymerize for approximately thirty minutes, after which the H_2O-saturated butanol was poured off and the gel rinsed with ddH_2O. The stacking gel reagents were prepared and poured on top of the separating gel. A 10 or 15 well comb was inserted and the gel was left to polymerize for 30 minutes.

When the stacking gel had polymerized, the sandwich clamp assembly was transferred to the electrophoresis apparatus and placed in a transparent buffer tank. SDS-

PAGE electrode buffer was poured into the middle of the electrophoresis apparatus as well as into the buffer tank.

The concentration of protein determined from the protein assay was used to calculate the appropriate volume of each sample. Each protein sample was mixed 1 to 1 with a solution of bromophenol blue and 2-mercaptoethanol. The bromophenol travels with the smallest proteins in the sample and helps to determine when the procedure should be stopped. The 2-mercaptoethanol, a reducing agent, removes secondary and tertiary structures of the sample's proteins. The samples were heated in a 90°C water bath for 5 minutes to further denature the proteins. Ten μg of protein per sample of whole epididymal adipose tissue sample was loaded into each well. Samples from the subcellular fractions of the adipose tissue or from the 3T3-L1 adipocytes contained 15 μg of protein. The tissue samples, an internal loading control (a tissue sample which was repeated on all gels to control for different intensities on different gels), a reference control sample to ensure that a response could be detected, and a molecular mass marker were loaded into the wells of the stacking gel using a syringe. The electrophoresis apparatus was connected to a power supply and electrophoresis conducted at 20 mA (per gel) for approximately 90 minutes, until the bromophenol blue had reached the bottom of the gel.

v. Gel transfer

After the proteins had separated by size in the polyacrylamide gel they were electrophoretically transferred to a 6.8 cm × 8 cm polyvinylidene difluoride membrane.

Reagents used:

- Transfer Buffer: 20% methanol, 0.25 mM Tris pH, 130 mM glycine, ddH_2O
- 5× Tris-buffered saline in Tween-20 (TBST) 0.1 M Tris-HCl pH 7.4, 0.25% Tween-20
- 1× TBST: 1 part 5× TBST and 4 parts ddH_2O
- Methanol (Fisher Scientific, Fair Lawn, NJ)

The glass plates from the SDS-PAGE were separated and the stacking gel discarded. The gel was removed from the glass plate by attaching it to a piece of blotting paper. The PVDF membrane was placed on top of the membrane while immersed in transfer buffer after the PVDF membrane had been equilibrated in the transfer buffer for 5 minutes. The membrane was covered with a piece of blotting paper and both sides were covered with a fiber pad. Any bubbles were pressed out and the components were placed inside a transfer cassette in the transfer buffer solution. The cassette was latched closed and placed in the electrode module with the negative side of the cassette facing the negative side of the module. The transfer buffer solution was poured into the tank after addition of an ice pack and a stir bar. The apparatus was placed on a magnetic stirrer with the stir speed at 200 rpm. Electrode wires were attached to the electrode module and current applied at 100 volts for 60 minutes. Membranes with the transferred proteins were removed and placed in a covered container with 1× TBST covering the membrane and stored at 4°C.

vi. Identification of proteins

Western blotting was used to probe for the proteins of interest on a PVDF membrane by complexing them with a primary antibody followed by a secondary antibody that is conjugated to horseradish peroxidase (HRP). When exposed to a

chemiluminescent reagent, the HRP catalyzes the oxidation of luminol which, as it decays, emits light; the intensity of the light is proportional to the amount of the targeted protein that is present.

Reagents used:

- 1×TBST
- 3% BSA in TBST (Bovine serum albumin fraction V, Cat #10735080001, Roche Diagnostics, Mannheim, Germany)
- 1% BSA in TBST
- Lumigen PS-3 detection reagent (Ref # RPN2132 V1 + V2, Lumigen PS3, GE Health, Piscataway, NJ)
- Primary (1°) antibody
- Horseradish peroxidase linked secondary (2°) antibody

The membrane was placed into a black blotting box and covered with 10 mL of 3% BSA in TBST and agitated on an orbital shaker for 1 hour. The primary antibody was added to the 3% BSA-TBST at a ratio of 1:1000 and agitated for another hour. After one hour, the 1° antibody aliquot was poured into a test tube for re-use and stored at -20°C. The membrane was washed with 1×TBST and agitated for 5 minutes; this was repeated four times. A horseradish peroxidase-linked secondary antibody, specific to the animal source of the primary antibody, was added to 1% BSA in TBST at a ratio of 1:10,000. After one hour, the 2° antibody solution was poured off and discarded. The membrane was then washed with 1×TBST by agitating it for 5 minutes; this step was repeated four times.

During the final wash, 2 mL of chemiluminescent agent (Ref # RPN2132 V1 + V2, Lumigen PS3, GE Health, Piscataway, NJ) was prepared. After the membrane was finished washing, it was covered with the chemiluminescent reagent and agitated for 30-60 seconds. The membrane was removed from the reagent, and placed between two acetate sheets. Any excess air or liquid was pressed out gently. The membrane, still between the acetate sheets, was placed into an autoradiography cassette. Autoradiographic film was placed on top of the acetate sheet and the autoradiography cassette closed; a timer was used to record the exposure time.

Band intensity was quantified by scanning densitometry (trace analysis with a GS 800 imaging densitometer, Bio-Rad Laboratories, Hercules, California) using Quantity One software (version 4.5.0, Bio-Rad Laboratories, Hercules, California). Data for each protein were expressed as an arbitrary unit by calculating the ratio of the trace analysis value of the protein of interest to trace analysis value of the Ponceau S staining or of β-Tubulin on the same blot. When multiple gels were used for adipose tissue samples, the mean for the lnCTL samples was set to 1 and the ratio for all other groups was adjusted accordingly. If multiple gels were used for the adipose tissue or 3T3-L1 adipocyte samples, an internal loading control sample was used to adjust for differences in band intensity (trace analysis of protein of interest/trace analysis of internal control/trace analysis of β-Tubulin).

vii. Loading control stain:

Ponceau solution was applied to the membrane after the gel transfer to stain proteins on the membrane and was rinsed with ddH_2O and allowed to dry before

quantification. The membranes were then rehydrated with methanol and 1×TBST prior to blocking with 3% BSA-TBST and incubation with the primary antibody.

- Ponceau S Solution: Cat # P7170-1L, Sigma-Aldrich, St. Louis, MO)

viii. Primary antibodies:

- Leptin (Cat # ab17629-100, Abcam, Inc., Cambridge, MA.), Rabbit PC, 1:1000
- ACRP30 (Cat # ab107920, Abcam, Inc., Cambridge, MA.), Rabbit PC, 1:1000
- PKCα (H-7) (Cat # SC-8393, Santa Cruz Biotechnology, Inc., Santa Cruz, CA.) Mouse MC, 1:1000
- PKCβI (C-16) (Cat # SC-209, Santa Cruz Biotechnology, Inc., Santa Cruz, CA.) Rabbit PC, 1:1000
- PKCδ (G-9) (Cat # SC-8402, Santa Cruz Biotechnology, Inc., Santa Cruz, CA.) Mouse MC, 1:1000
- PKCε (Cat # CS-2683s, Cell Signalling Technologies, Inc., Danvers, MA.) Rabbit MC, 1:1000
- PKCθ (Cat # 15170-L2, BD Transduction Labs, San Jose, CA) Mouse MC, 1:1000
- PKCμ (Cat# SC-638, Santa Cruz Biotechnology, Inc., Santa Cruz, CA.) Rabbit PC, 1:1000
- p-PKCα/βII (Cat # 9375s, lot: 3, Cell Signaling Technologies, Inc., Danvers, MA.) Rabbit PC, 1:1000
- p-PKCζ/λ (Thr410/403) (Cat # CS-9378s lot: 7, Cell Signaling Technologies, Inc., Danvers, MA.) Rabbit PC, 1:1000

- p-α-Akt (Ser473) (Cat # CS-9271, Cell Signaling Technologies, Inc., Danvers, MA.) Rabbit PC, 1:1000
- p-PDK-1 (Cat # CS-3061., Cell Signaling Technologies, Inc., Danvers, MA.) Rabbit PC, 1:1000
- p-p85α-PI3K (Cat # SC-12929 lot L2403, Santa Cruz Biotechnology, Inc., Santa Cruz, CA.) Goat PC, 1:1000
- STAT-3 (Cat # CS-9132 lot:6, Cell Signaling Technologies, Inc., Danvers, MA.) Rabbit PC, 1:1000
- p-STAT-3 (Y705) (3E2) (Cat# 9138s, Cell Signaling Technologies, Inc., Danvers, MA.) Mouse MC, 1:1000
- β-Tubulin (loading control)(Cat # ab6046-100., AbCam Inc., Cambridge, MA.), Rabbit PC, 1:1000

ix Secondary antibodies

- HRP Goat: Peroxidase-conjugated chrom-pure Goat IgG (Cat # 005-030-003, Jackson Immunoresearch Laboratories, West Grove, PA)
- HRP Mouse: Blotting grade affinity purified goat Anti-Mouse IgG (H + L) HRP (Cat # 170-6516, Bio-Rad Laboratories, Hercules, CA)
- HRP Rabbit: Blotting grade goat anti-rabbit IgG (H + L)(Human IgG adsorbed) HRP (Cat # 170-6515, Bio-Rad Laboratories, Hercules, CA)

x. Stripping of membrane blots

After probing for the primary antibody, the PVDF membrane was stripped and washed so that it could be re-probed for a new antibody and loading control.

Reagents used:

- Stripping buffer: 10% SDS; 0.5 M Tris HCl pH 6.8; ddH_2O
- 2-mercaptoethanol
- 1×TBST
- 10% Bleach

The PVDF membrane was covered with 25 mL of stripping buffer per membrane. In the fume hood, 80 μL of 2-mercaptoethanol was added for every 10 mL of stripping buffer. The container was sealed and placed in a larger container which was sealed to help reduce odour. The solution was agitated overnight. The solution was poured down the sink in the fume hood, and the membrane placed in a new container and covered with 1×TBST. The membrane was washed by agitation for 5 minutes; the washing was repeated until no odour was present. The old containers were rinsed with 10% bleach and left in the fume hood until the odor dissipated.

Statistical analysis

One-way analysis of variance (ANOVA) was used to analyze serum and Western blot data, as well as end point data for body weight and organ weights. Repeated measures ANOVA was used for analyzing weekly feed intake and weekly body weights of the mice. Duncan's multiple range test was used for multiple comparisons among groups. Statistical analysis was performed with Statistical Analysis Software (Version 9.1.3, SAS Institute Inc., Cary, NC.). The level of significance was set at $P<0.05$. Data are expressed as the mean ± standard error of the mean (SEM).

STUDY 2 – CELL CULTURE MODEL

The effects of *c9, t11* and *t10, c12* CLA isomers on the levels of leptin, p-STAT-3, PKCα, PKCβI, PKCε, PKCμ, p-PKCζ/λ and p-PKCα/βII were determined in mature, fully differentiated 3T3-L1 adipocytes.

Culturing of 3T3-L1 adipocytes

The 3T3-L1 mouse embryo fibroblasts (pre-adipocyte) (Cat # CL-173, American Type Culture Collections, Manassas, VT) were seeded on 12-well plates and grown to confluence at 37°C in Dulbecco's Modified Eagles Medium (DMEM) with 10% bovine calf serum (Cat # 16170-086, Invitrogen Corporation, Grand Island, N.Y.) [10% CS-DMEM]. Two days post-confluency (Day 0), the bovine calf serum was replaced with fetal bovine serum (Cat # 12483-020, Invitrogen Corporation, Grand Island, N.Y.) [10% FBS-DMEM] and the peadipocytes were stimulated with a cocktail containing 1 μM insulin (DIN # 02024233, Novolin, Nordisk Canada Inc, Mississauga, ON), 0.25 μM Dexamethasone (Cat # D2915, Sigma-Aldrich, St. Louis, MO) and 0.5 mM 3-iso butyl-1-methyl xanthine (Cat # I5879 Sigma-Aldrich, St. Louis, MO). On day 2, the medium was replaced with 10% FBS-DMEM and 1 μM insulin. On day 4 and every second day afterwards the media was replaced with 10% FBS-DMEM until the adipocytes were fully differentiated.

Addition of CLA to 3T3-L1 adipocytes

Twelve to sixteen days after inducing differentiation, the adipocytes were treated for 0, 1, 2, 4, 8 and 24 hours with:

- 6.25 nM Leptin

- 60 μM *t10, c12* CLA (Cat # 90145, Cayman Chemical Company, Ann Arbor, Michigan)
- 60 μM *c9, t11* CLA (Cat # 90140, Cayman Chemical Company, Ann Arbor, Michigan)
- 60 μM linoleic acid (Cat # 90150, Cayman Chemical Company, Ann Arbor, Michigan)
- 60 μM of a 1:1 mixture of *c9, t11* and *t10, c12* CLA
- 60 μM of a 1:1 mixture of linoleic acid and *t10, c12* CLA ,
- 60 μM of a 1:1 mixture of linoleic acid and *c9, t11* CLA
- 2 μL of ethanol (vehicle control)

Sixty μM was previously determined in our laboratory as an effective concentration for treating 3T3-l1 adipocytes with CLA and linoleic acid. Linoleic acid was regarded as a treatment control while leptin was used to compare the effects of leptin and CLA on leptin and PKC levels in 3T3-L1 adipocytes. Each treatment was performed in triplicate with each experimental plate containing a vehicle control designated as zero.

Cell lysing

To terminate the treatments prior to analysis, the media was aspirated and the cells were washed twice with 2 mL of 1× Phosphate Buffered Saline (PBS) (Cat # 37572, Thermo Scientific, Rockford, IL). Two hundred μL of 2× sample buffer was added to the cells and they were allowed to lyse. The cells and the solubilised material were pipetted into separate test tubes and sonicated to shear the DNA. The samples were then stored at -80°C.

Western blotting

i. *Primary antibodies*

- Leptin (Cat # ab17629-100., AbCam Inc., Cambridge, MA.), Rabbit PC, 1:1000
- PKCα (H-7) (Cat # SC-8393, Santa Cruz Biotechnology, Inc., Santa Cruz, CA.) Mouse MC, 1:1000

- PKCβI (C-16) (Cat # SC-209, Santa Cruz Biotechnology, Inc., Santa Cruz, CA.) Rabbit PC, 1:1000
- PKCε (Cat # CS-2683s, Cell Signaling Technologies, Inc., Danvers, MA.) Rabbit MC, 1:1000
- PKCμ (Cat# SC-638, Santa Cruz Biotechnology, Inc., Santa Cruz, CA.) Rabbit PC, 1:1000
- p-PKCα/βII (Cat # 9375s, lot: 3, Cell Signaling Technologies, Inc., Danvers, MA.) Rabbit PC, 1:1000
- p-PKCζ/λ (Thr410/403) (Cat # CS-9378s lot: 7, Cell Signaling Technologies, Inc., Danvers, MA.) Rabbit PC, 1:1000
- STAT-3 (Cat # CS-9132 lot: 6, Cell Signaling Technologies, Inc., Danvers, MA.) Rabbit PC, 1:1000
- p-STAT-3 (Y705) (3E2) (Cat# 9138s, Cell Signaling Technologies, Inc., Danvers, MA.) Mouse MC, 1:1000
- β-Tubulin (loading Control) (Cat # ab6046-100., AbCam Inc., Cambridge, MA.), Rabbit PC, 1:1000

ii. Secondary antibodies

- HRP Goat: Peroxidase-conjugated chrom-pure Goat IgG (Cat # 005-030-003, Jackson Immunoresearch Laboratories, West Grove, PA)
- HRP Mouse: Blotting grade affinity purified goat Anti-Mouse IgG (H + L) HRP (Cat # 170-6516, Bio-Rad Laboratories, Hercules, CA)
- HRP Rabbit: Blotting grade goat anti-rabbit IgG (H + L)(Human IgG adsorbed) HRP (Cat # 170-6515, Bio-Rad Laboratories, Hercules, CA)

Statistical analysis

One-way analysis of variance (ANOVA) was used for Western blot analysis. Repeated measures ANOVA was used for analyzing leptin levels over 24 hours. Duncan's multiple range test was used for multiple comparisons among groups. Statistical analysis was performed with Statistical Analysis Software (Version 9.1.3, SAS Institute Inc., Cary, NC.). The level of significance was set at $P<0.05$. Data are expressed as the mean ± standard error of the mean (SEM).

RESULTS

STUDY 1 - ANIMAL STUDY

Body weight and feed intake

Before the experimental diet began, all of the *db/db* mouse groups weighed approximately 7 g more than the lnCTL group, thus indicating that obesity was already present (Figure 2). After one week on the experimental diet, the *db*t10, c12 mice weighed significantly less than the *db*CTL, *db*PW and *db*c9, t11 mice, suggesting weight gain had ceased. By the sixth and final week of the experiment, the *db*t10, c12mice weighed significantly less than the *db*CTL, *db*c9, t11 and even the lnCTL group (Figure 3). At week 5 and 6, the *db*PW mice (fed restricted amounts of diet) weighed no different that the lnCTL or the *db*t10, c12 mice. The body weight of the *db*c9, t11 mice was not different from *db*CTL throughout the study. There was an n=9 for the *db*c9, t11 group due to a mouse that had overgrown teeth and could not eat. There was also a *db*CTL mouse that did not complete the study which resulted in an n=9.

There was no difference in feed intake between the lnCTL and *db*PW groups during weeks 2 to 4 of the study (Figure 4). Interestingly, weekly feed intake of the *db*t10, c12mice climbed steadily throughout the study even as body weight diminished and it was greater than the *db*c9, t11 group during weeks 4, 5 and 6 despite the large disparity in body weight between the two groups. Consequently, by the final two weeks of the study, the *db*t10, c12 had higher feed intake than all of the other groups except for the *db*CTL group. There was also no difference in feed intake or body weight between the *db*c9, t11 or *db*CTL groups.

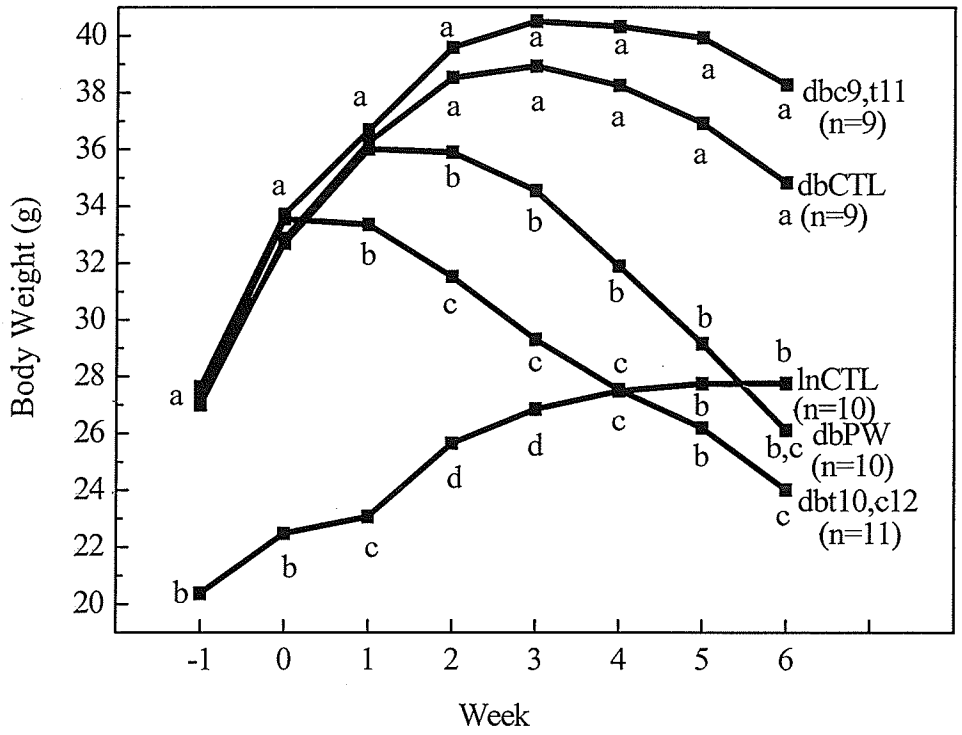

Figure 2: Weekly body weight. Weekly body weight data are presented as means. SEM was ± 0.3, 0.8, 1.1, 1.0 and 0.7 at week -1; ± 0.4, 0.7, 1.1, 1.0 and 0.5 at week 0; ± 0.4,0.6, 0.9, 0.6 and 0.5 at week 1; ± 0.6, 0.5, 0.8, 0.9 and 0.6 at week 2; ± 0.7, 0.4, 0.8, 0.9, 0.4 and 0.7 at week 3; ± 0.7, 0.4, 0.9, 0.7 and 1.0 at week 4; ± 0.6, 0.5, 1.2, 0.7 and 1.0 at week 5; ± 0.6, 0.5, 1.3, 0.8 and 0.9 at week 6 for the lnCTL, *db*CTL, *db*c9,t11, *db*t10,c12 and *db*PW groups respectively (not shown in figure). LnCTL = lean mice fed 0 % CLA diet, *db*CTL = *db/db* mice fed 0 % CLA diet, *db*c9, t11 = *db/db* mice fed 0.4 % c9, t11 CLA diet, *db*t10, c12 = *db/db* mice fed 0.4 % t10, c12 CLA, *db*PW = *db/db* mice fed 0 % CLA in restricted amounts. Statistical differences among means ($p \leq 0.05$) at each week are indicated by different lower case letters.

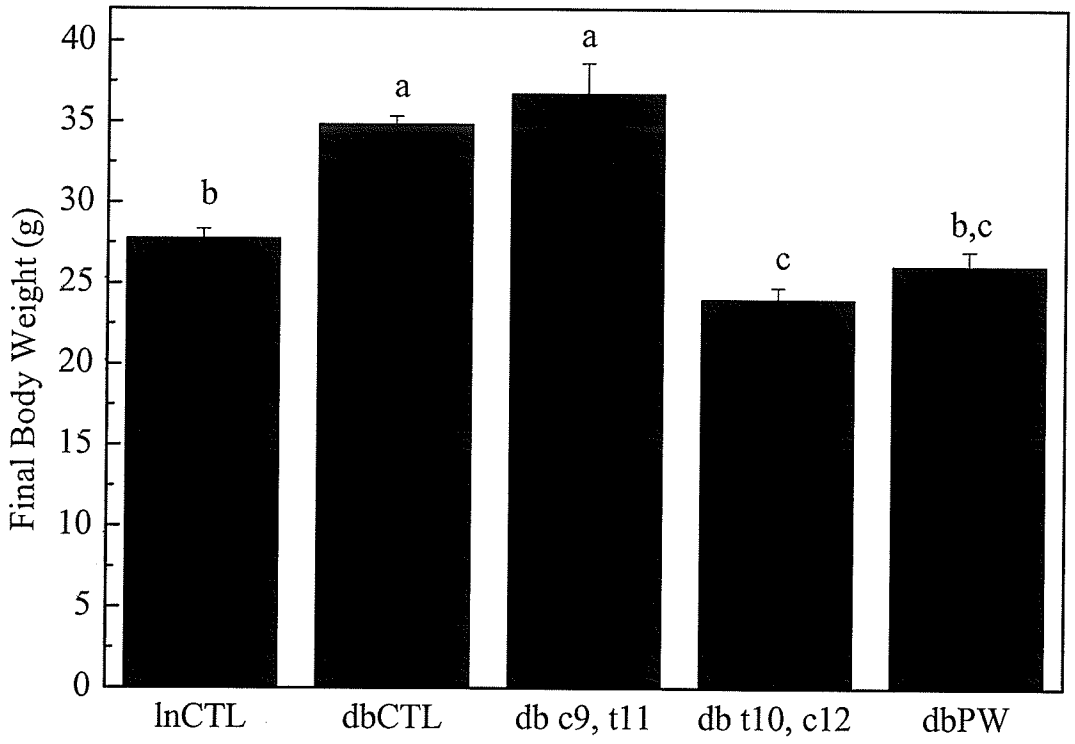

Figure 3: Final body weight. Body weights after 6 weeks of dietary intervention are presented as means ± SEM; n=9 for *db*CTL, n=10 for *db*c9, t11, *db*PW, lnCTL and n=11 for *db*t10, c12. LnCTL = lean mice fed 0 % CLA diet, dbCTL = *db/db* mice fed 0 % CLA diet, *db*c9, t11 = *db/db* mice fed 0.4 % c9, t11 CLA diet, *db*t10, c12 = *db/db* mice fed 0.4 % t10, c12 CLA, *db*PW = db/db mice fed 0 % CLA in restricted amounts. Statistical differences among means ($p \leq 0.05$) are indicated by different lower case letters.

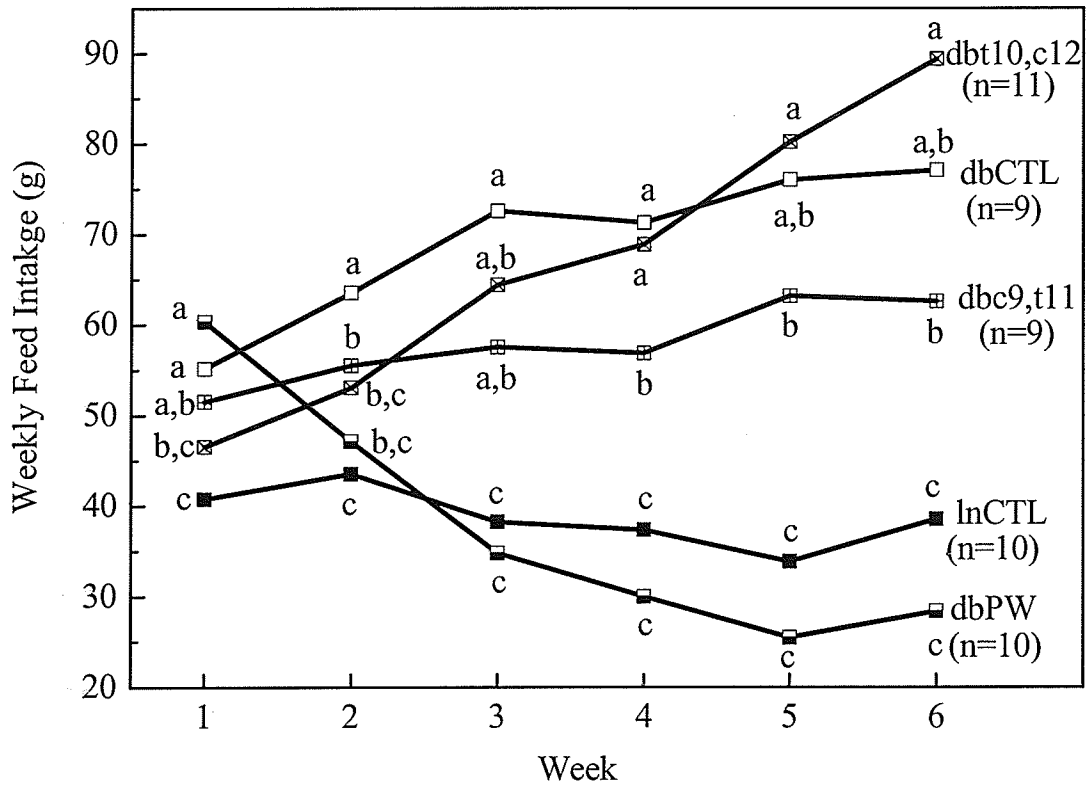

Figure 4: Weekly feed intake. Weekly feed intake data are presented as means. SEM was ± 4, 2, 2, 3 and 4 at week 1; ± 5, 3, 4, 3 and 2 at week 2; ± 3, 4, 3, 5 and 1 at week 3; ± 4, 6, 4, 4 and 1 at week 4; ± 4, 6, 7, 5 and 1 at week 5; ± 6, 6, 6, 5 and 2 at week 6 for the lnCTL, *db*CTL, *db*t10,c12, *db*c9,t11 and *db*PW groups respectively (not shown in figure). LnCTL = lean mice fed 0 % CLA diet, dbCTL = *db/db* mice fed 0 % CLA diet, dbc9, t11 = *db/db* mice fed 0.4 % *c9, t11* CLA diet, dbt10, c12 = db/db mice fed 0.4 % t10, *c12* CLA, dbPW = *db/db* mice fed 0 % CLA in restricted amounts. Statistical differences among means ($p \leq 0.05$) at each week are indicated by different lower case letters.

Liver weight

Liver tissue from the lean and *db/db* mice was dissected and weighed at termination (Figure 5a). There was no difference in absolute liver weight among the *db*CTL, *db*c9, t11 and *db*t10, c12groups. The *db*PW group that was diet restricted had a reduction in liver size compared to the other *db/db* groups. Even so, *db*PW liver still weighed more than the lnCTL group.

When the liver was represented as a percentage of body weight, the livers of the *db*10, c12 groups were far greater than all other groups (Figure 5b). There was no difference in liver as a percentage of body weight among the *db*CTL, *db*c9, t11 and *db*PW groups. The relative liver weight of the lnCTL group was lower than all other groups.

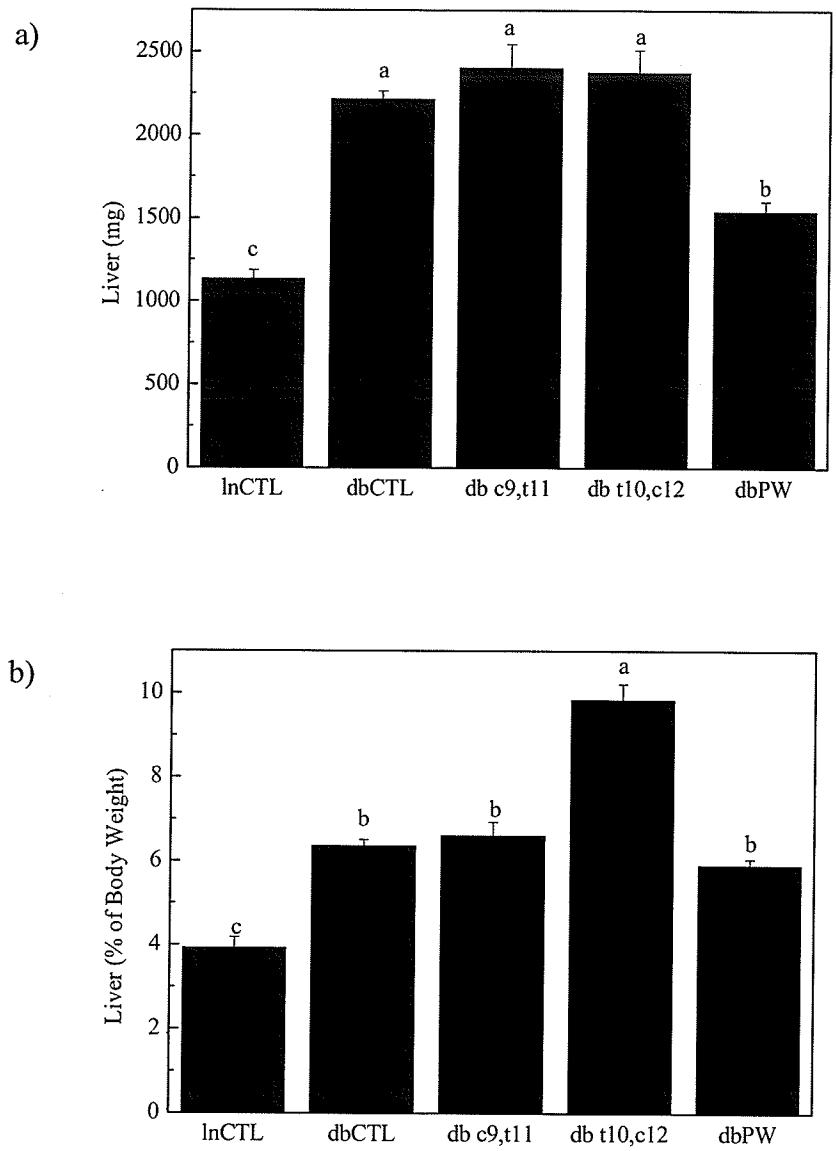

Figure 5: Liver weight. a) Absolute liver weight and b) liver weight as a percentage of body weight are presented as mean ± SEM; n=9 for *db*CTL, n=10 for *db*c9, t11, *db*PW, lnCTL and n=11 for *db*t10, c12. LnCTL = lean mice fed 0 % CLA diet, dbCTL = *db/db* mice fed 0 % CLA diet, *db*c9, t11 = *db/db* mice fed 0.4 % c9, t11 CLA diet, *db*t10, c12 = *db/db* mice fed 0.4 % t10, c12 CLA, *db*PW = db/db mice fed 0 % CLA in restricted amounts. Statistical differences among means ($p \leq 0.05$) are indicated by different lower case letters.

Pancreas weight

At termination, the pancreas from the lean and *db/db* mice was dissected and weighed (Figure 6a). There was no difference in absolute weight of the pancreas among the *db*CTL, *db*c9, t11 and *db*t10, c12mice. The pancreas weight of the lnCTL group did not differ from the *db*t10, c12or *db*CTL groups; however, the pancreas weight of the *db*c9, t11 group's was greater than the lnCTL group. The *db*PW group had the lowest pancreas weight, although there was no difference between the lnCTL and *db*PW group.

When corrected for body weight there were no differences among the lnCTL, *db*CTL, *db*c9, t11 or *db*PW mice (Figure 6b). The pancreas as a percentage of body weight was higher in the *db*t10, c12group than all other groups.

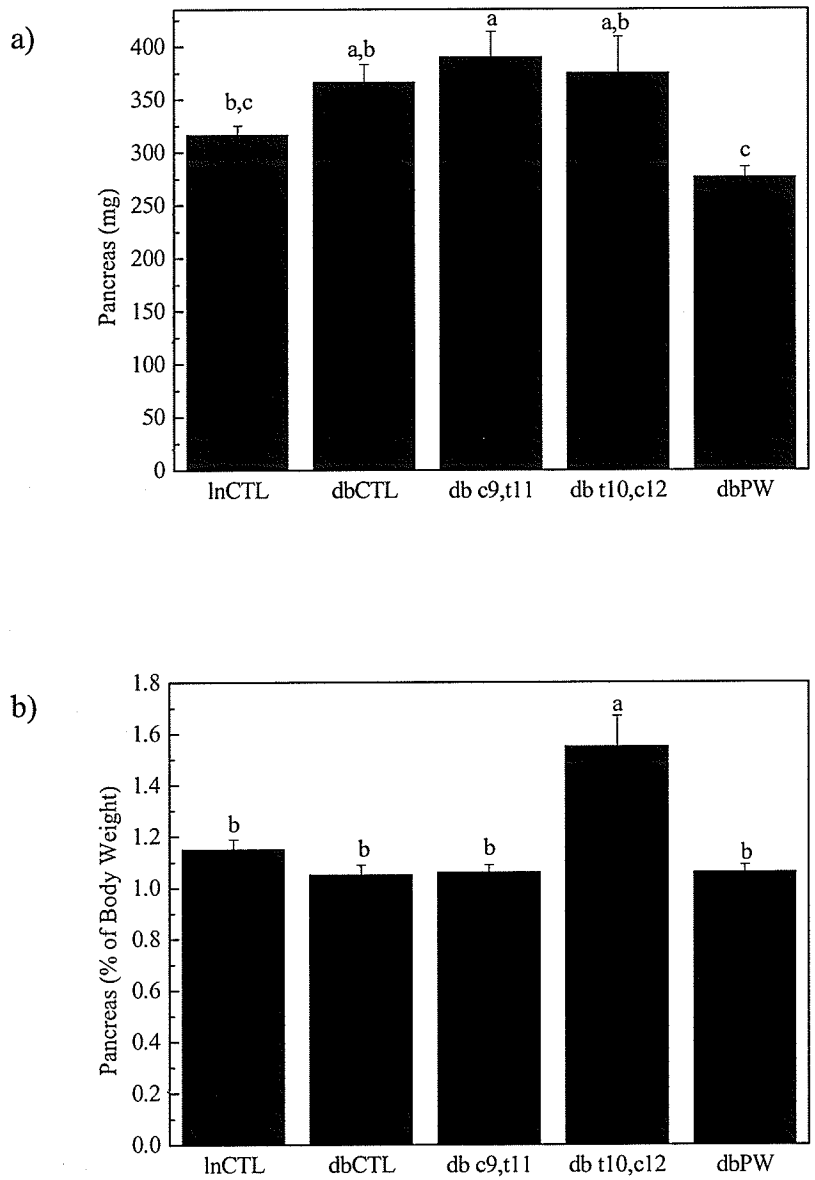

Figure 6: Pancreas weight. a) Absolute pancreas weight and b) pancreas as a percentage of body weight are presented as mean ± SEM; n=9 for *db*CTL, n=10 for *db*c9, t11, *db*PW, lnCTL and n=11 for *db*t10, c12. LnCTL = lean mice fed 0 % CLA diet, dbCTL = *db/db* mice fed 0 % CLA diet, *db*c9, t11 = *db/db* mice fed 0.4 % *c9, t11* CLA diet, *db*t10, c12 = *db/db* mice fed 0.4 % t10, *c12* CLA, *db*PW = *db/db* mice fed 0 % CLA in restricted amounts. Statistical differences among means ($p \leq 0.05$) are indicated by different lower case letters.

Kidney weight

At termination the left and right kidneys were collected and weighed prior to being frozen and stored at -80°C. The weight of the left and right kidneys of the *db*t10, c12 mice was greater than all other groups (Figure 7a and 7c). There was no difference in the weight of the kidneys between the *db*CTL and *db*c9, t11 mice. The left kidney weight of the lnCTL and *db*PW groups was lower than the other three groups although there was no difference between the lnCTL and *db*PW mice.

When corrected for body weight, no difference was found among the lnCTL, *db*CTL, *db*c9, t11 or *db*PW groups for the left kidney. The right kidney of the *db*PW as a percentage of the body weight was higher than the lnCTL, *db*CTL and *db*c9,t11 groups. The left and right kidney of the *db*t10, c12 group remained higher than all other groups.

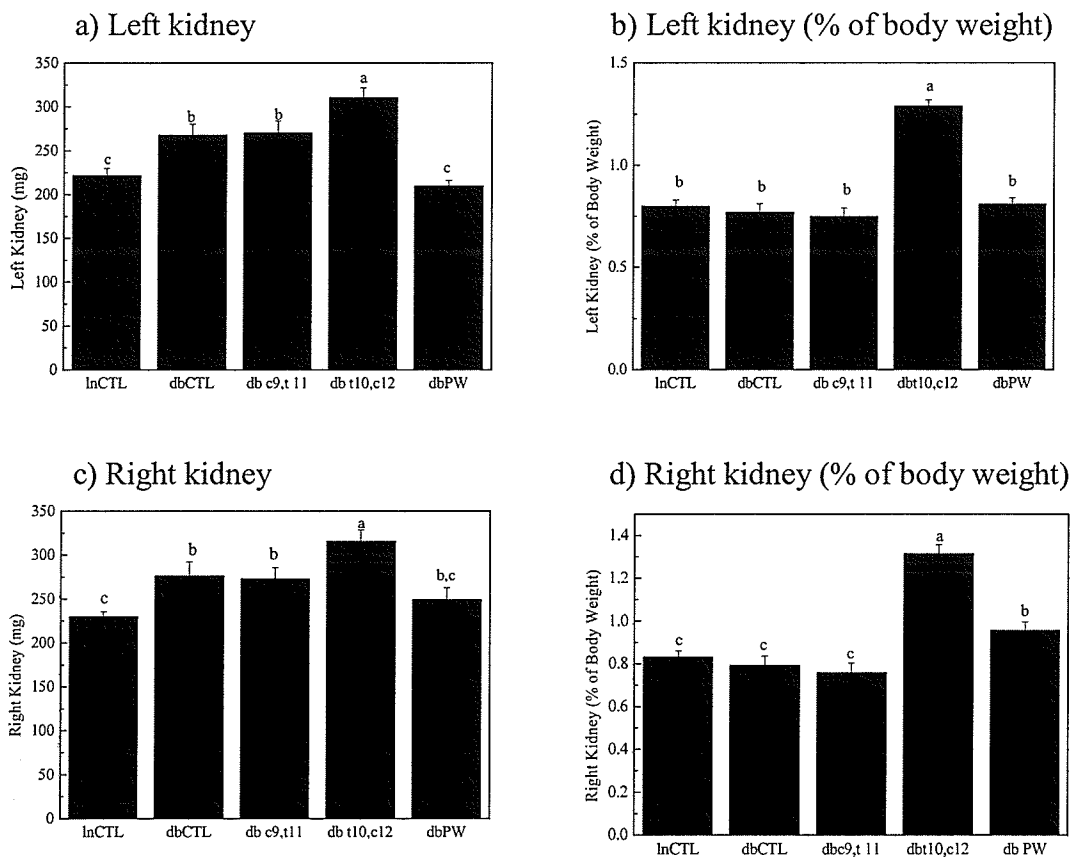

Figure 7: Kidney weight. a) Absolute left kidney weight, b) left kidney as a percentage of body weight, c) absolute right kidney weight and d) right kidney as a percentage of body weight are presented as means ± SEM; n=9 for *db*CTL, n=10 for *db*c9, t11, *db*PW, lnCTL and n=11 for *db*t10, c12. LnCTL = lean mice fed 0 % CLA diet, *db*CTL = *db/db* mice fed 0 % CLA diet, *db*c9, t11 = *db/db* mice fed 0.4 % *c9, t11* CLA diet, *db*t10, c12 = *db/db* mice fed 0.4 % t10, *c12* CLA, *db*PW = *db/db* mice fed 0 % CLA in restricted amounts. Statistical differences among means ($p \leq 0.05$) are indicated by different lower case letters.

Adipose tissue weight

Peri-renal and epididymal adipose tissue from the lean and *db/db* mice was dissected and weighed at termination. Epididymal fat pad mass was greatest in *db*c9, t11 and *db*CTL groups, while it was significantly lower in the *db*PW mice who had greater epididymal fat than the lnCTL group. The *db*t10, c12 group had the least amount of epididymal fat (Figure 8a). There was no difference in epididymal fat pad mass, expressed as a percentage of body weight, among the *db*CTL, *db*c9, t11, and *db*PW groups (Figure 8b). The lnCTL and *db*t10, c12groups had less epididymal adipose tissue relative to their body weight than the other three groups. Absolute levels of peri-renal adipose tissue were greatest in the *db*c9, t11 and *db*CTL mice. The *db*PW group had decreased peri-renal fat which did not differ significantly from the lnCTL group. The *db*t10, c12 mice had the lowest amount of total peri-renal fat, although it was not significantly lower than that of the lnCTL group. Peri-renal adipose tissue relative to body weight was greatest in the *db*CTL and *db*c9, t11 groups and was lower in the dbPW group (Figure 8d). The lnCTL and *db*t10, c12 had less peri-renal adipose tissue relative to body weight than the other groups.

Visceral fat was calculated as the sum of the peri-renal and epididymal white adipose tissue depots. Visceral adipose tissue was greatest in the *db*c9, t11 group, although it did not differ from the *db*CTL group (Figure 9). The *db*PW had less visceral fat relative to body weight than the *db*c9, t11 but it not differ from the *db*CTL group. Visceral fat relative to body weight of the lnCTL was less than the former three groups. The *db*t10, c12 group had severely depleted white adipose tissue and had less total visceral adipose tissue relative to body weight than all other groups.

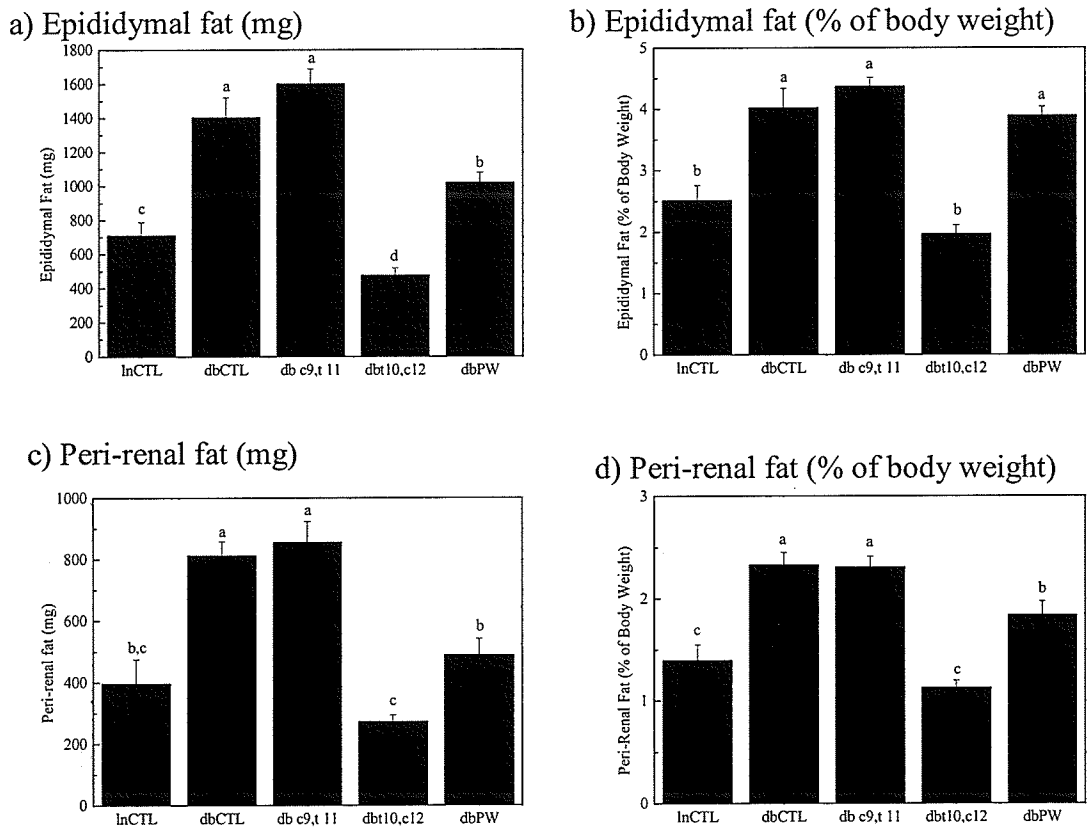

Figure 8: Epididymal and peri-renal adipose tissue. a) Absolute epididymal adipose tissue b) epididymal (as a percentage of body weight) c) Absolute peri-renal adipose tissue and d) per-renal adipose tissue (as a percentage of body weight) are presented as mean ± SEM; n=9 for *db*CTL, n=10 for *db*c9, t11, *db*PW, lnCTL and n=11 for *db*t10, c12. LnCTL = lean mice fed 0 % CLA diet, dbCTL = *db/db* mice fed 0 % CLA diet, *db*c9, t11 = *db/db* mice fed 0.4 % *c9, t11* CLA diet, *db*t10, c12 = *db/db* mice fed 0.4 % t10, *c12* CLA, *db*PW = *db/db* mice fed 0 % CLA in restricted amounts. Statistical differences among means ($p \leq 0.05$) are indicated by different lower case letters.

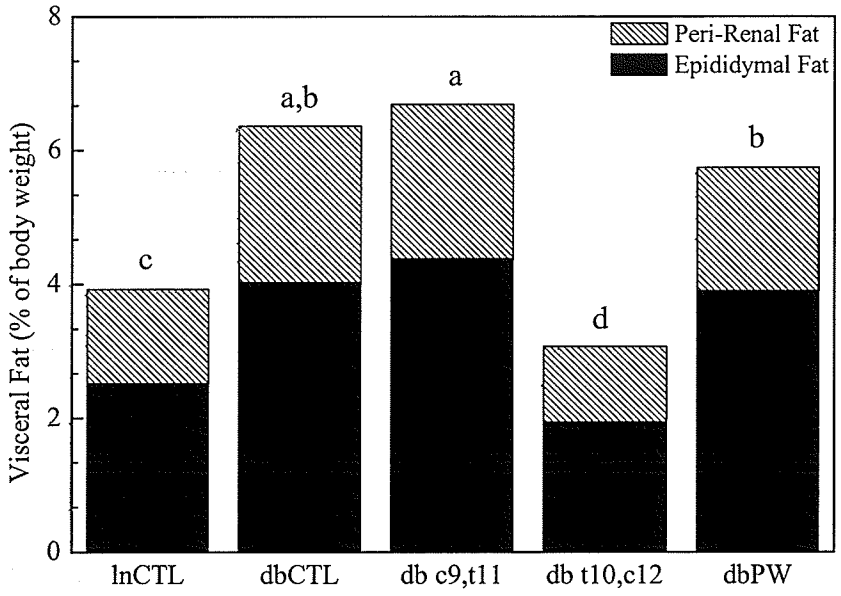

Figure 9: Visceral adipose tissue. Visceral adipose tissue = epididymal + peri-renal adipose tissue; n=9 for *db*CTL, n=10 for *db*c9, t11, *db*PW, lnCTL and n=11 for *db*t10, c12. LnCTL = lean mice fed 0 % CLA diet, *db*CTL = *db/db* mice fed 0 % CLA diet, *db*c9, t11 = *db/db* mice fed 0.4 % *c9, t11* CLA diet, *db*t10, c12 = *db/db* mice fed 0.4 % *t10, c12* CLA, *db*PW = *db/db* mice fed 0 % CLA in restricted amounts. Statistical differences among means ($p \leq 0.05$) for visceral fat are indicated by different lower case letters.

Serum biochemistry

Serum glucose

Fasting serum glucose of the lean and *db*/db mice was measured using a commercial spectrophotometric kit. There was no difference in fasting serum glucose levels among the *db/db* mice (Figure 10). Serum glucose of the lean mice was significantly lower than all of the *db/db* mice.

Serum insulin

Fasting serum insulin from the lean and *db*/db mice was measured using a commercial EIA kit. Serum insulin was highest in the *db*c9, t11 group although it did not differ from the *db*CTL group (Figure 11). Serum insulin was greater in the *db*c9, t11 group than the *db*t10, c12, *db*PW, and lnCTL groups although the serum insulin levels of the *db*PW and *db*t10, c12groups did not differ from the *db*CTL mice. The serum insulin level of the lnCTL group was lower than the *db*CTL group.

HOMA-IR

When fasting serum glucose and insulin was used to calculate the HOMA-IR, there were no difference in insulin sensitivity among any of the *db/db* mice (Figure 12). The HOMA-IR values of the *db/db* mice were ~6 fold greater than the lean mice.

Serum triacylglycerides

Fasting serum triacylglycerides from the lean and *db/db* mice were measured using a commercial spectrophotometric kit. Serum triacylglycerides were significantly higher in the *db*t10, c12group than the *db*c9, t11 group; however, neither group was significantly different from the *db*CTL or *db*PW mice (Figure 13). Serum

triacylglycerides were significantly lower in the lnCTL mice than all of the *db/db* mice groups.

Serum cholesterol

Serum total cholesterol of the lean and *db/db* mice was measured using a commercial spectrophotometric kit. No changes in total cholesterol levels were seen among the *db*CTL, *db*c9, t11 or the *db*t10, c12groups (Figure 14). The *db*PW group that was diet-restricted had a modest decrease in serum total cholesterol, as was to be expected. The lnCTL had lower total cholesterol levels than all of the *db/db* mouse groups.

Serum leptin

Fasting serum leptin concentrations from lean and *db/db* mice were measured using a commercial EIA kit. Serum leptin levels were significantly higher in the *db*c9, t11 group than all other groups (Figure 15). There were no differences in fasting serum leptin levels among the *db*CTL, *db*t10, c12 or *db*PW mice. Expectedly, the lnCTL group had the lowest fasting serum leptin concentrations.

When leptin levels were expressed relative to peri-renal or epididymal fat (Figure 16), the *db*t10, c12 had significantly higher leptin levels than all other groups. There was no difference seen among the *db*CTL, *db*c9, t11 or *db*PW groups. Leptin levels per mg of peri-renal or epididymal fat was still lowest in the lnCTL group.

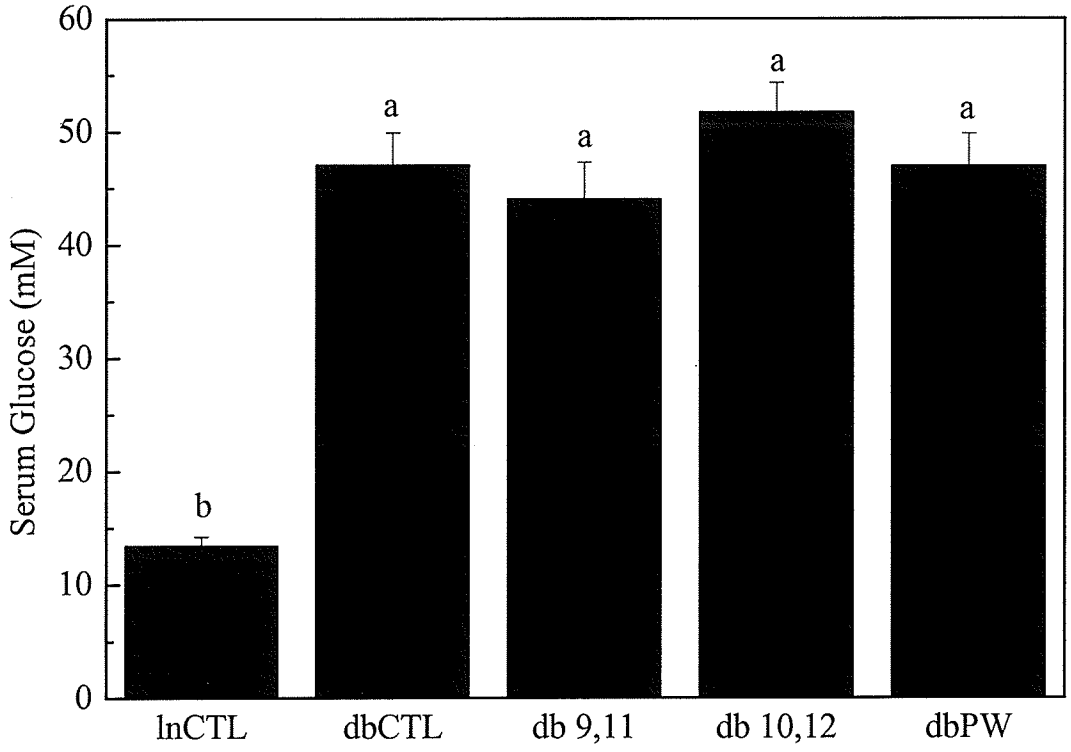

Figure 10: Serum glucose. Fasting serum glucose from lean and *db/db* mice was measured using a commercial spectrophotometric kit. Samples were assayed in duplicate. Data are presented as mean ± SEM; n = 10 for lnCTL and *db*t10, c12and n = 9 for *db*CTL, *db*c9, t11 and *db*PW. LnCTL = lean mice fed 0 % CLA diet, *db*CTL = *db/db* mice fed 0 % CLA diet, *db*c9, t11 = *db/db* mice fed 0.4 % c9, t11 CLA diet, *db*t10, c12 = *db/db* mice fed 0.4 % t10, c12 CLA, *db*PW = *db/db* mice fed 0 % CLA in restricted amounts. Statistical differences among means ($p \leq 0.05$) are indicated by different lower case letters.

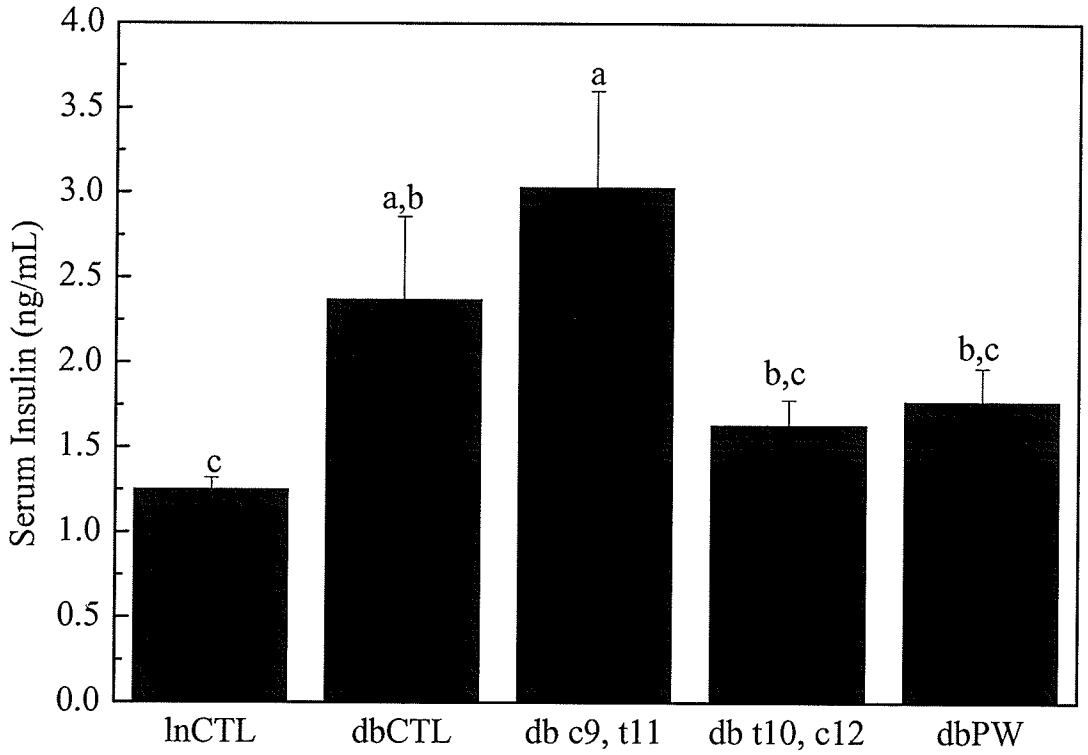

Figure 11: Serum insulin. Fasting serum insulin from lean and *db/db* mice was measured using a commercial EIA kit. Samples were assayed in duplicate. Data are presented as mean ± SEM; n = 11 for *db*t10, c12, n = 10 for lnCTL, *db*c9, t11 and dbPW and n = 9 for *db*CTL all groups. LnCTL = lean mice fed 0 % CLA diet, *db*CTL = *db/db* mice fed 0 % CLA diet, *db*c9, t11 = *db/db* mice fed 0.4 % c9, t11 CLA diet, *db*t10, c12 = *db/db* mice fed 0.4 % t10, c12 CLA, *db*PW = *db/db* mice fed 0 % CLA in restricted amounts. Statistical differences among means ($p \leq 0.05$) are indicated by different lower case letters.

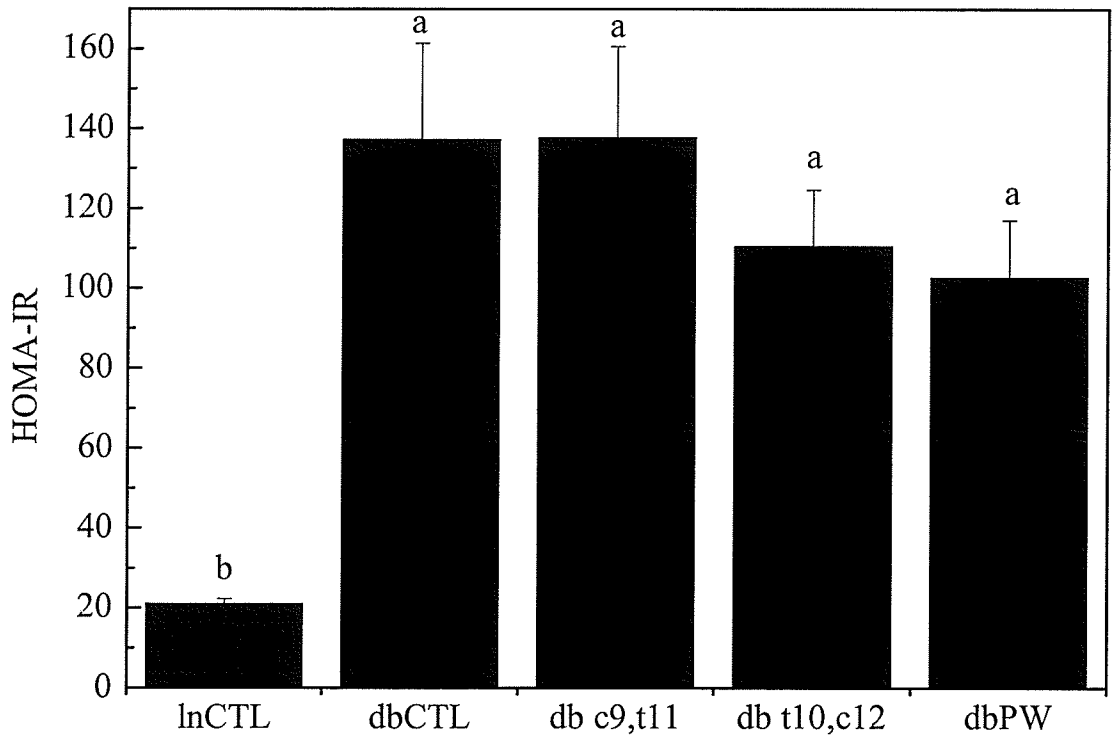

Figure 12: Homeostasis model assessment-insulin resistance. Homeostasis model assessment-insulin resistance (HOMA-IR) was calculated using fasting serum from lean and db/db mice measured for insulin using a commercial EIA kit and glucose using a commercial spectrophotometric kit. All samples were assayed in duplicate. Data are presented as mean ± SEM; n = 10 for *db*t10, c12, *db*CTL, lnCTL, n = 9 for *db*c9, t11 and *db*PW. LnCTL = lean mice fed 0 % CLA diet, *db*CTL = *db/db* mice fed 0 % CLA diet, *db*c9, t11 = *db/db* mice fed 0.4 % c9, t11 CLA diet, *db*t10, c12 = *db/db* mice fed 0.4 % t10, c12 CLA, *db*PW = *db/db* mice fed 0 % CLA in restricted amounts. Statistical differences among means ($p \leq 0.05$) are indicated by different lower case letters.

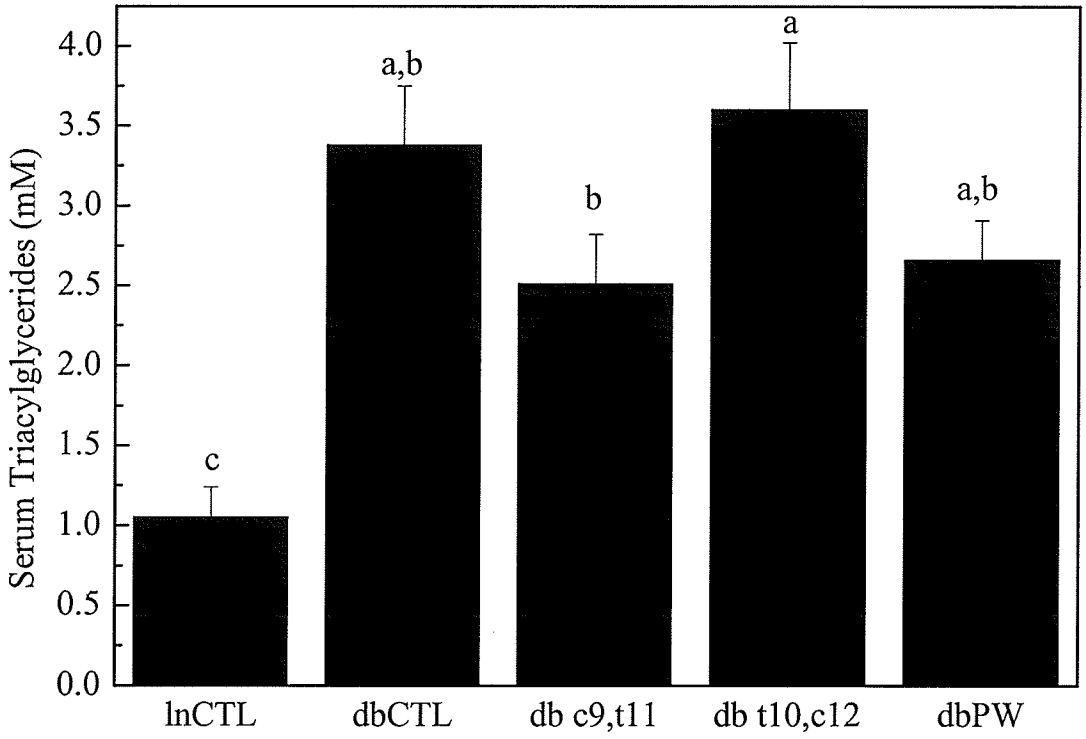

Figure 13: Serum triacylglycerides. Fasting serum triacylglycerides from lean and *db/db* mice was measured using a commercial spectrophotometric kit. Samples were assayed in duplicate. Data are presented as mean ± SEM; n = 10 for *db*t10, c12, n = 9 for *db*CTL, n = 8 for lnCTL and *db*c9, t11 and n = 7 for *db*PW. LnCTL = lean mice fed 0 % CLA diet, *db*CTL = *db/db* mice fed 0 % CLA diet, *db*c9, t11 = *db/db* mice fed 0.4 % c9, t11 CLA diet, *db*t10, c12 = *db/db* mice fed 0.4 % t10, c12 CLA, *db*PW = *db/db* mice fed 0 % CLA in restricted amounts. Statistical differences among means ($p \leq 0.05$) are indicated by different lower case letters.

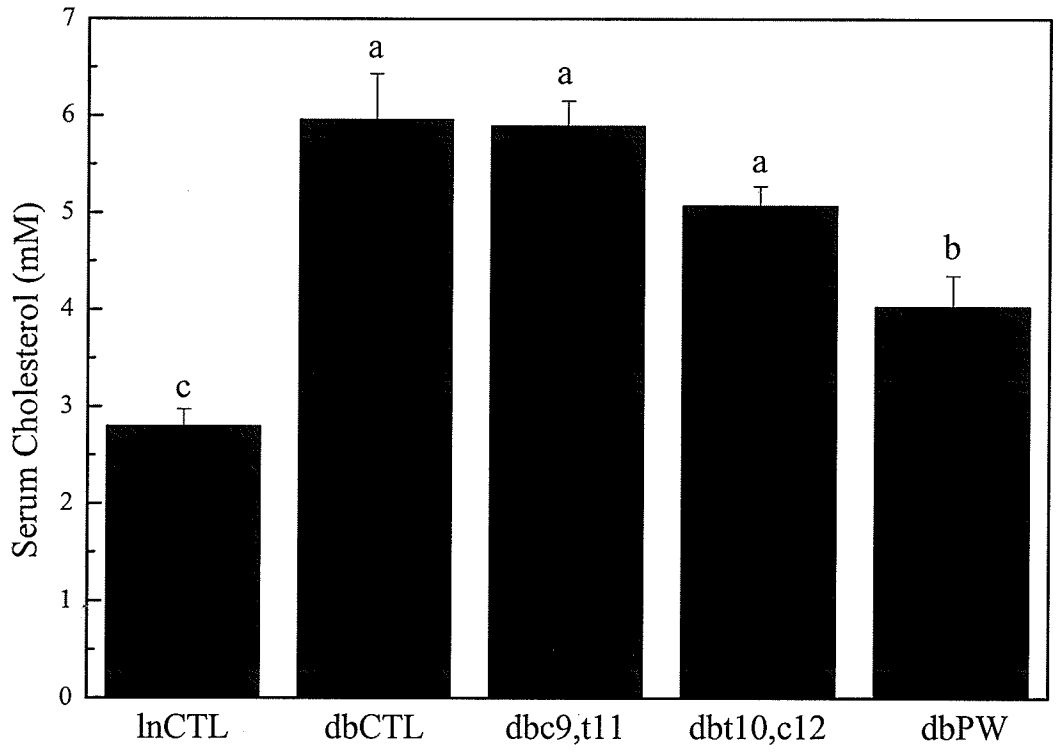

Figure 14: Serum cholesterol. Fasting serum total cholesterol from lean and db/db mice was measured using a commercial spectrophotometric kit. Samples were assayed in triplicate. Data are presented as mean ± SEM; n = 5 for all groups. LnCTL = lean mice fed 0 % CLA diet, *db*CTL = *db/db* mice fed 0 % CLA diet, *db*c9, t11 = *db/db* mice fed 0.4 % c9, t11 CLA diet, *db*t10, c12 = *db/db* mice fed 0.4 % t10, c12 CLA, *db*PW = *db/db* mice fed 0 % CLA in restricted amounts. Statistical differences among means ($p \leq 0.05$) are indicated by different lower case letters.

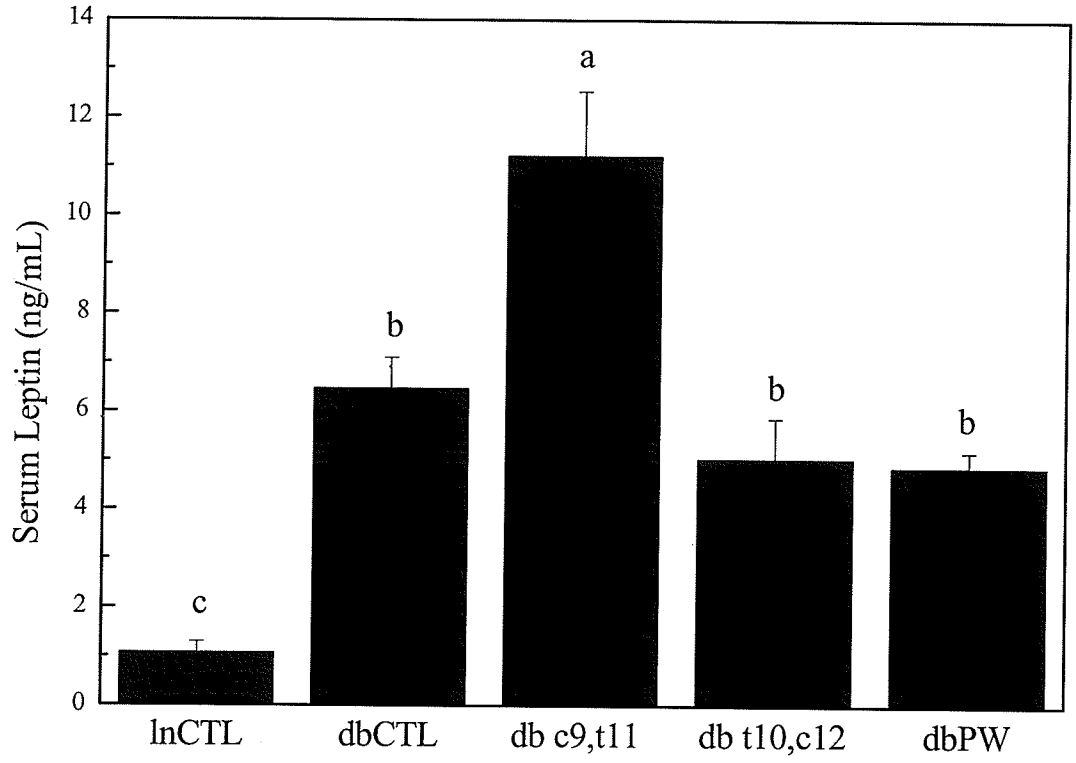

Figure 15: Serum leptin. Fasting serum leptin from lean and db/db mice was measured using a commercial EIA kit. Samples were assayed in duplicate. Data are presented as mean ± SEM; n = 11 for *db*t10, c12, n = 10 for lnCTL and *db*PW, n = 9 for *db*CTL and n = 8 for *db*c9, t11. LnCTL = lean mice fed 0 % CLA diet, *db*CTL = *db/db* mice fed 0 % CLA diet, *db*c9, t11 = *db/db* mice fed 0.4 % c9, t11 CLA diet, *db*t10, c12 = *db/db* mice fed 0.4 % t10, c12 CLA, *db*PW = *db/db* mice fed 0 % CLA in restricted amounts. Statistical differences among means ($p \leq 0.05$) are indicated by different lower case letters.

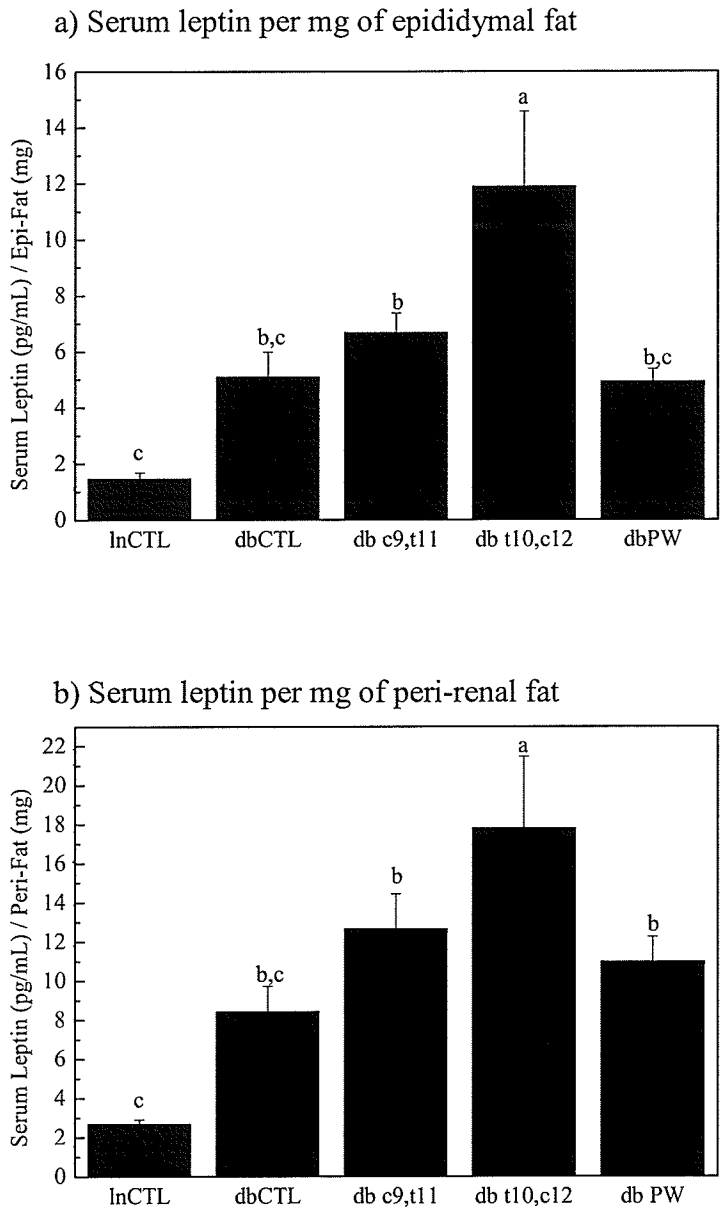

Figure 16: Serum leptin per mg adipose tissue. a) Fasting serum leptin per mg epididymal adipose tissue and b) fasting serum leptin per mg peri-renal adipose tissue are presented as mean ± SEM; n = 11 for *db*t10,c12, n = 10 for lnCTL and *db*PW, n = 9 for *db*CTL and n = 8 for *db*c9,t11. LnCTL = lean mice fed 0 % CLA diet, *db*CTL = *db/db* mice fed 0 % CLA diet, *db*c9, t11 = *db/db* mice fed 0.4 % c9, t11 CLA diet, *db*t10, c12 = *db/db* mice fed 0.4 % t10, c12 CLA, *db*PW = *db/db* mice fed 0 % CLA in restricted amounts. Statistical differences among means ($p \leq 0.05$) are indicated by different lower case letters.

Adipose tissue adipokines

The levels of the adipose-derived hormones leptin and adiponectin were measured by Western blotting in the adipose tissue to compare with the serum levels of leptin that were measured by a commercial kit.

Leptin

Leptin protein levels in epididymal adipose were measured by Western blotting of tissue samples from the lean and *db/db* mice (Figure 17). There was no difference between epididymal leptin levels of the lean and *db/db mice* except for the *db*t10, c12 group that had highly elevated leptin levels in epididymal fat.

Adiponectin (ACRP 30)

Adiponectin levels were measure in epididymal adipose tissue samples from lean and *db/db* mice. The lnCTL group had the highest levels of adiponectin; however, they were not significantly higher than the *db*CTL, *db*c9, t11 or *db*PW groups (Figure 18). The *db*t10, c12 group had significantly lower adiponectin tissue levels than the lnCTL group. There was, however, a trend of lower adiponectin levels in the *db/db* mice compared to the lnCTL group.

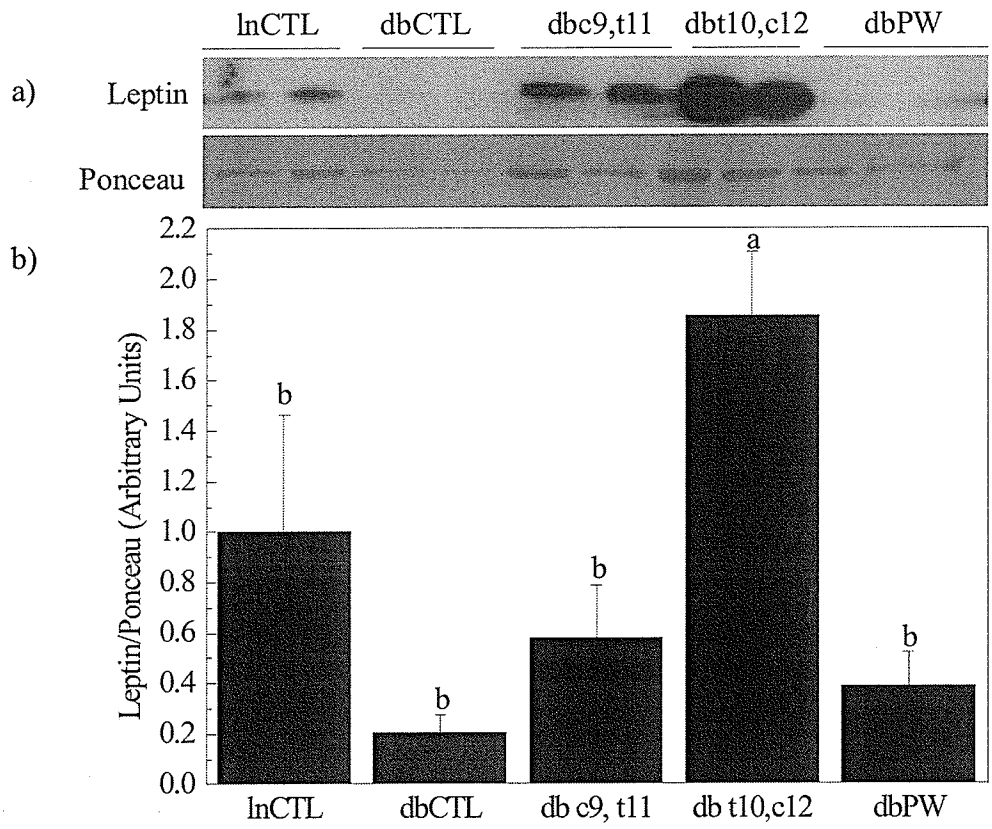

Figure 17: Leptin protein levels in epididymal adipose tissue. Leptin protein levels were measured in epididymal adipose tissue samples from lean and *db/db* mice by Western blot analysis. A) Representative Western blot and b) corresponding graph obtained by scanning densitometry of the bands in arbitrary units. Data were derived by calculating the ratio of Leptin to Ponceau S staining and are expressed as mean ± SEM, with the mean of the lnCTL group set to 1; n=6 for all groups. LnCTL = lean mice fed 0 % CLA diet, *db*CTL = *db/db* mice fed 0 % CLA diet, *db*c9, t11 = *db/db* mice fed 0.4 % c9, t11 CLA diet, *db*t10, c12 = *db/db* mice fed 0.4 % t10, c12 CLA, *db*PW = *db/db* mice fed 0 % CLA in restricted amounts. Statistical differences among means ($p \leq 0.05$) are indicated by different lowercase letters.

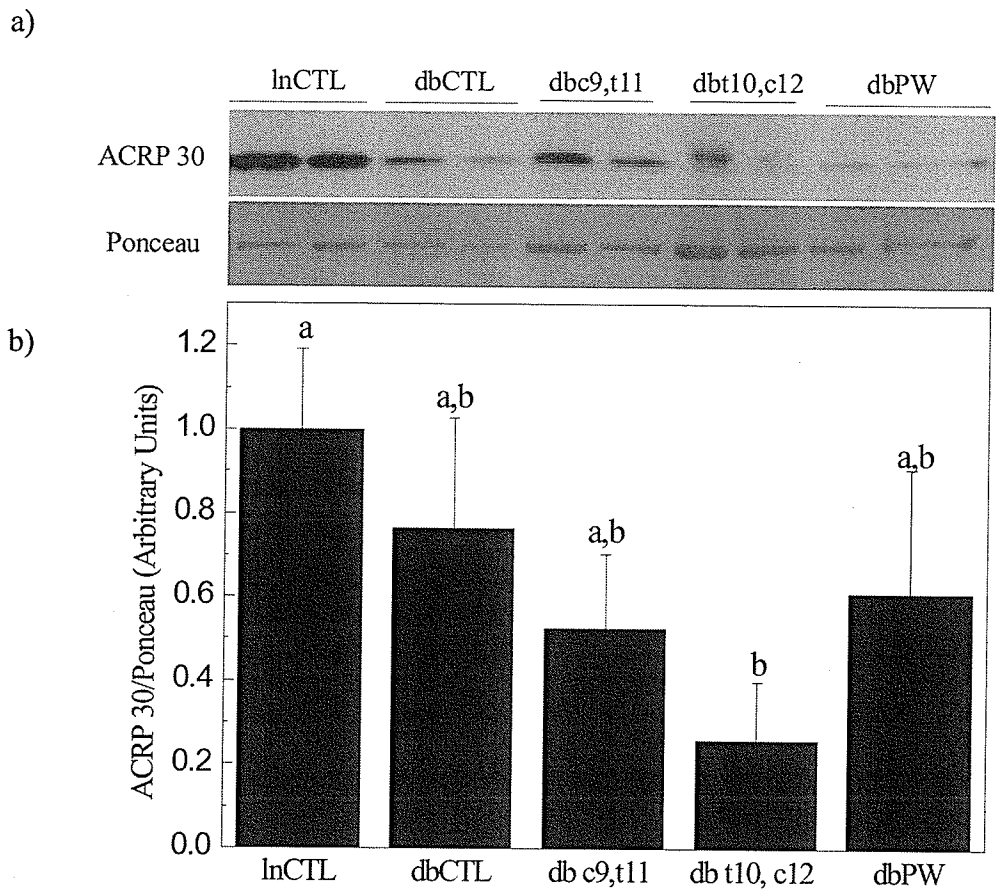

Figure 18: ACRP30 protein levels in epididymal adipose tissue. Adiponectin (ACRP30) protein levels were measured in epididymal adipose tissue samples from lean and *db/db* mice by Western blot analysis. a) Representative Western blot and b) corresponding graph obtained by scanning densitometry of the bands in arbitrary units. Data were derived by calculating the ratio of ACRP 30 to Ponceau S staining and are expressed as mean ± SEM, with the mean of the lnCTL group set to 1; n=6 for all groups. LnCTL = lean mice fed 0 % CLA diet, *db*CTL = *db/db* mice fed 0 % CLA diet, *db*c9, t11 = *db/db* mice fed 0.4 % c9, t11 CLA diet, *db*t10, c12 = *db/db* mice fed 0.4 % t10, c12 CLA, *db*PW = *db/db* mice fed 0 % CLA in restricted amounts. Statistical differences among means ($p \leq 0.05$) are indicated by different lowercase letters.

Phospho-signal transducers and activators of transcription

The ability of leptin to regulate food intake is dependent on signalling through the signal transducers and activators of transcription (STAT-3) in the hypothalamus. In peripheral tissues, the levels of phospho-STAT-3 (p-STAT-3) can be used to determine the level of activation of STAT-3 by leptin. Levels of p-STAT-3 that had been phosphorylated at Tyrosine705 were measured in epididymal adipose tissue samples from lean and *db/db* mice (Figure 19). The *db*c9, t11 mice had significantly higher levels of p-STAT-3 than the *db*t10, c12mice, although neither group differed from the *db*CTL group. The lnCTL, *db*PW and *db*t10, c12 groups had the lowest levels of p-STAT-3.

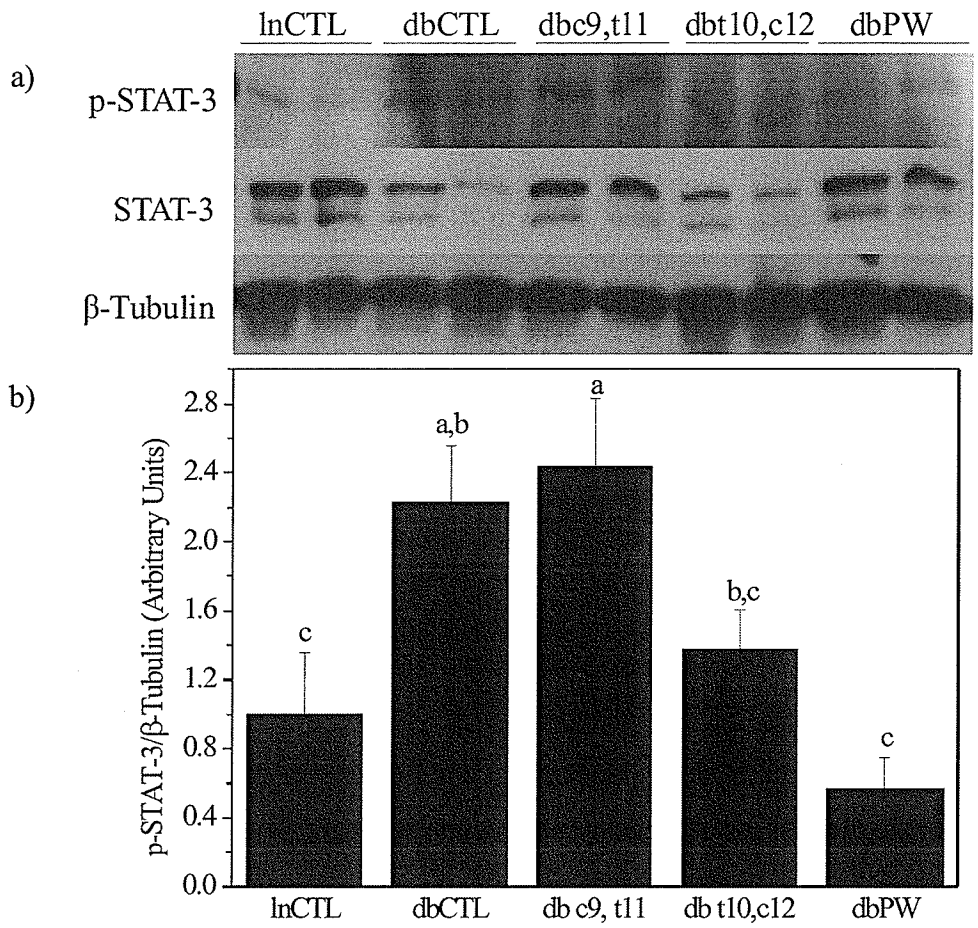

Figure 19: Signal transducers and activators of transcription phosphorylation at Tyr705 in epididymal adipose tissue. Signal transducers and activators of transcription (p-STAT-3) phosphorylation at Tyr705 protein levels were measured in epididymal adipose tissue samples from lean and *db/db* mice by Western blot analysis. a) Representative Western blot and b) corresponding graph obtained by scanning densitometry of the bands in arbitrary units. Data were derived by calculating the ratio of p-STAT-3 to β-Tubulin and are expressed as mean ± SEM, with the mean of the lnCTL group set to 1; n=4 for all groups. LnCTL = lean mice fed 0 % CLA diet, *db*CTL = *db/db* mice fed 0 % CLA diet, *db*c9, t11 = *db/db* mice fed 0.4 % c9, t11 CLA diet, *db*t10, c12 = *db/db* mice fed 0.4 % t10, c12 CLA, *db*PW = *db/db* mice fed 0 % CLA in restricted amounts. Statistical differences among means ($p \leq 0.05$) are indicated by different lowercase letters.

Insulin signalling

In the fasting state, the levels of key-mediators of insulin signalling, Akt/Protein kinase B, p85α-PI3K and PDK-1, are phosphorylated in the epididymal adipose tissue of the lean and *db/db* mice as measured by Western blotting. These enzymes can be activated downstream of the insulin receptor as well as ObRb and can be key contributors to cross-talk between insulin and leptin signalling.

Phospho-Akt (Serine 473)

Levels of Phospho-Akt that had been phosphorylated at Serine 473 were measured in the epididymal adipose tissue of lean and *db/db* mice. No significant changes in the level of phospho-Akt were observed among any of the groups (Figure 20).

Phospho- p85α-phosphatidylinositol 3-kinase (Tyrosine 508)

Levels of phosphatidylinositol 3-kinase that had been phosphorylated at Tyrosine508 on the p85α regulatory sub-unit (p-p85α PI3K) were measured in epididymal adipose tissue samples from lean and *db/db* mice. The levels of p-p85α PI3K were highly elevated in the *db*CTL, *db*c9, t11 and *db*t10, c12 compared to the lnCTL mice (Figure 21). Levels of p-p85α PI3K were significantly higher in the epididymal adipose tissue of *db*t10, c12 than the *db*CTL and *db*PW groups.

Phospho-phosphoinositide dependent protein kinase-1 (Serine 241)

Levels of phospho-phosphoinositide dependent protein kinase-1 (p-PDK-1) phosphorylated at Serine 241 were measured in the epididymal adipose tissue of lean and *db/db* mice. The lnCTL group had the highest levels of p-PDK-1 although they were not significantly higher than the *db*CTL group (Figure 22). The *db*c9, t11, *db*t10, c12, and

the *db*PW had lower levels of p-PDK-1 than the *db*CTL group, although only the levels measured in the *db*t10, c12 and *db*PW groups differed significantly from lnCTL and *db*CTL.

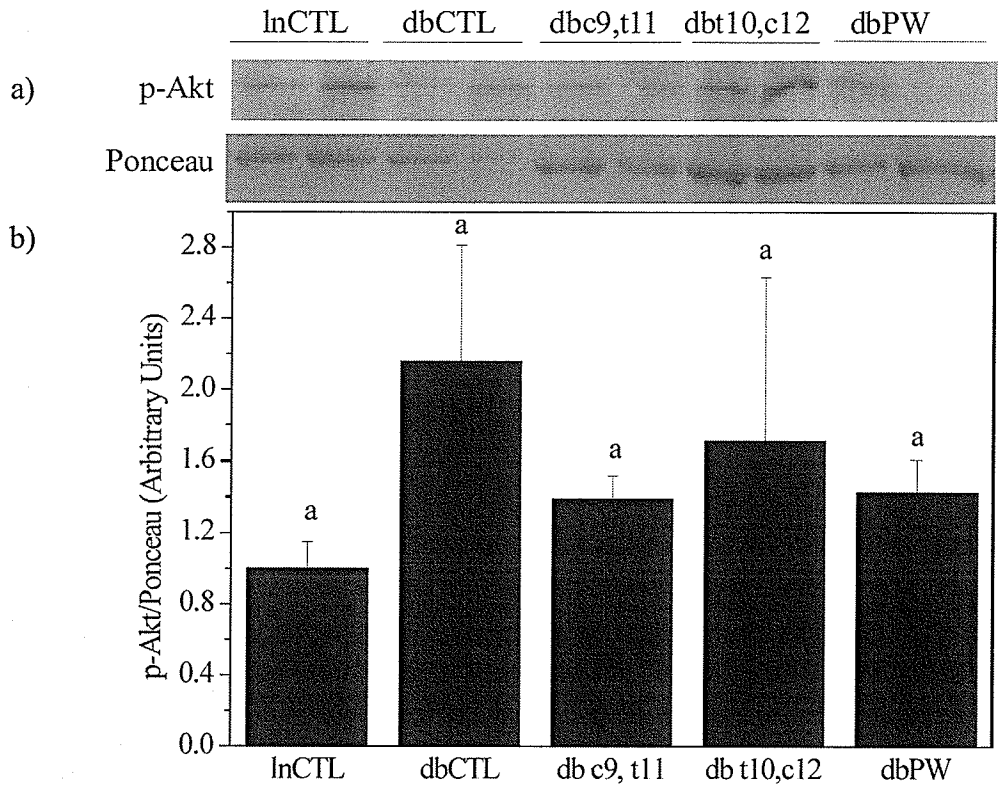

Figure 20: Akt phosphorylation at Ser473 in epididymal adipose tissue. Phospho-Akt (Ser473) (p-Akt) levels were measured in epididymal adipose tissue samples from lean and *db/db* mice by Western blot analysis. a) Representative Western blot and b) corresponding graph obtained by scanning densitometry of the bands in arbitrary units. Data were derived by calculating the ratio of p-Akt to Ponceau S staining and are expressed as mean ± SEM, with the mean of the lnCTL group set to 1; n=4 for all groups. LnCTL = lean mice fed 0 % CLA diet, *db*CTL = *db/db* mice fed 0 % CLA diet, *db*c9, t11 = *db/db* mice fed 0.4 % c9, t11 CLA diet, *db*t10, c12 = *db/db* mice fed 0.4 % t10, c12 CLA, *db*PW = *db/db* mice fed 0 % CLA in restricted amounts. Statistical differences among means ($p \leq 0.05$) are indicated by different lowercase letters.

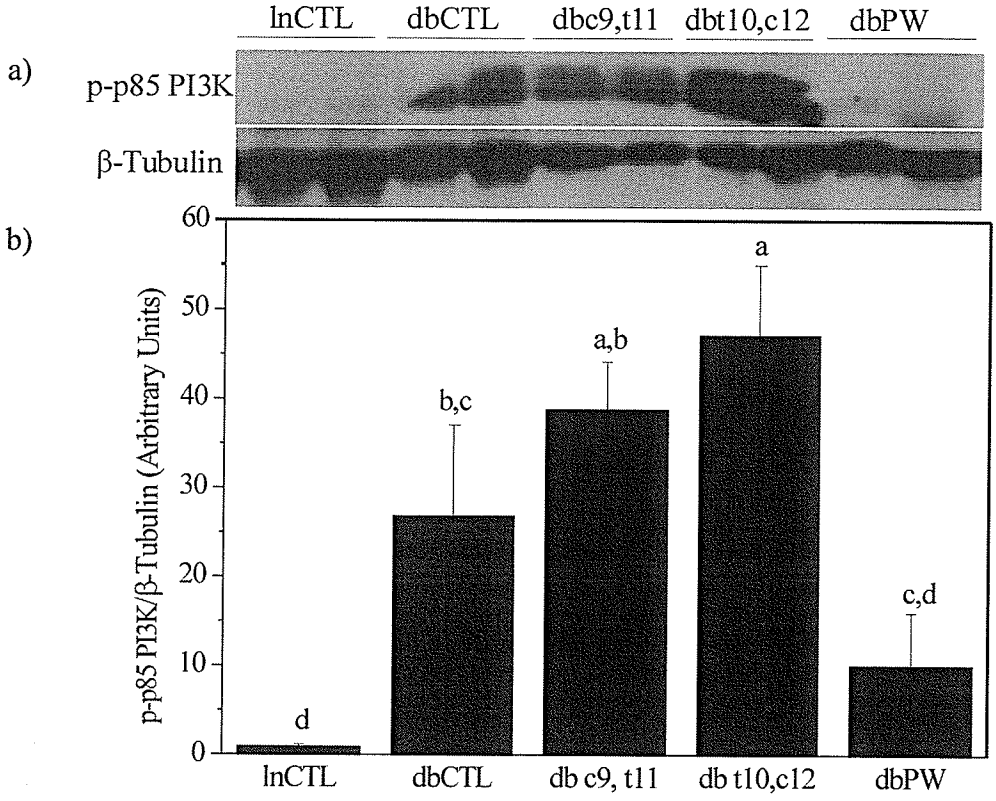

Figure 21: (p85α) Phosphatidylinositol 3-kinase phosphorylation at Tyr508 in epididymal adipose tissue. Levels of phosphatidylinositol 3-kinase (p-p85 PI3K) that are phosphorylated at the tyrosine 508 residue on the 85 kDa regulatory subunit were measured in epididymal adipose tissue samples from lean and *db/db* mice by Western blot analysis. a) Representative Western blot and b) corresponding graph obtained by scanning densitometry of the bands in arbitrary units. Data were derived by calculating the ratio of PI3-K to β-Tubulin and are expressed as mean ± SEM, with the mean of the lnCTL group set to 1; n=4 for dbCTL and n=6 for all other groups. LnCTL = lean mice fed 0 % CLA diet, *db*CTL = *db/db* mice fed 0 % CLA diet, *db*c9, t11 = *db/db* mice fed 0.4 % c9, t11 CLA diet, *db*t10, c12 = *db/db* mice fed 0.4 % t10, c12 CLA, *db*PW = *db/db* mice fed 0 % CLA in restricted amounts. Statistical differences among means ($p \leq 0.05$) are indicated by different lowercase letters.

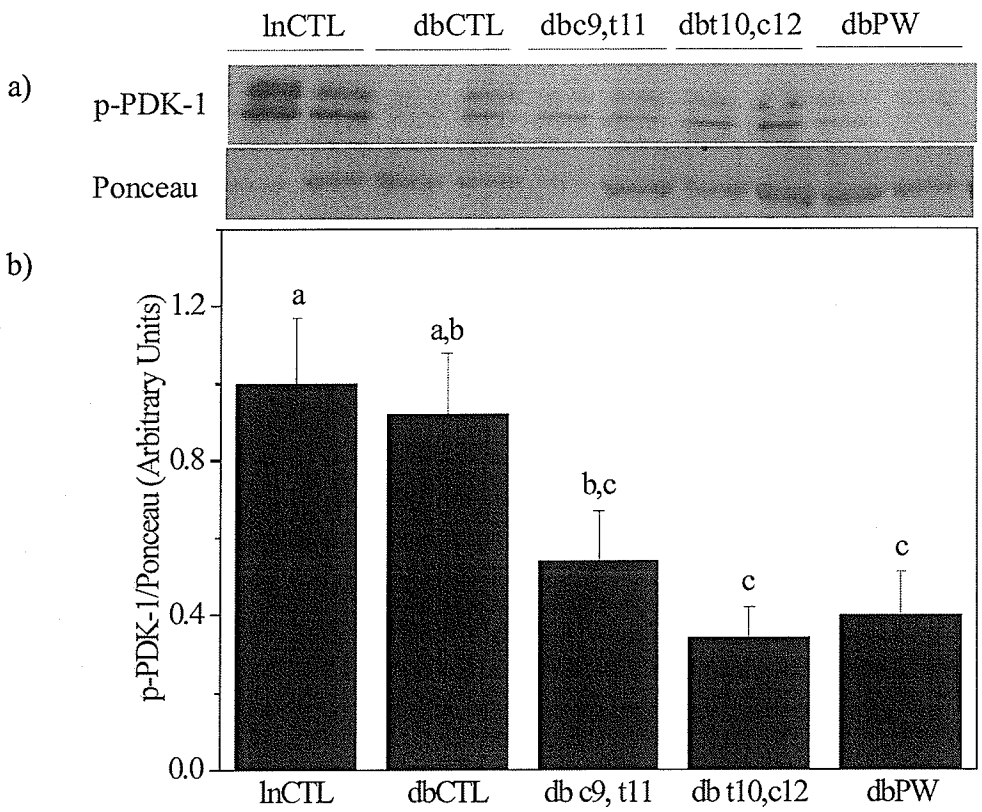

Figure 22: Phosphoinositide dependent protein kinase 1 phosphorylation at Ser241 in epididymal adipose tissue. Phosphoinositide dependent protein kinase (p-PDK-1) phosphorylated at Ser241 protein levels were measured in epididymal adipose tissue samples from lean and *db/db* mice by Western blot analysis. a) Representative Western blot and b) corresponding graph obtained by scanning densitometry of the bands in arbitrary units. Data were derived by calculating the ratio of p-PDK-1 to Ponceau S staining and are expressed as mean ± SEM, with the mean of the lnCTL group set to 1; n=4 for all groups. LnCTL = lean mice fed 0 % CLA diet, *db*CTL = *db/db* mice fed 0 % CLA diet, *db*c9, t11 = *db/db* mice fed 0.4 % c9, t11 CLA diet, *db*t10, c12 = *db/db* mice fed 0.4 % t10, c12 CLA, *db*PW = *db/db* mice fed 0 % CLA in restricted amounts. Statistical differences among means ($p \leq 0.05$) are indicated by different lowercase letters.

Isoforms of protein kinase C in epididymal adipose tissue

An increase in lipid availability can lead to the chronic activation of a variety of PKCs which can lead to unregulated phosphorylation of a number of mediators of insulin signalling. This study is one of the first to demonstrate that all three classes (conventional, novel, and atypical) of PKC are indeed present in whole and subcellular fractions of epididymal adipose tissue of *db/db* mice (see Table 4) as well as their lean counterparts. It is also one of the first to show that both the levels of PKC and their subcellular distribution can be changed by both isomers of CLA.

Table 4. Protein kinase C isoforms detected in epididymal fat of *db/db* mice

PKC Isoform	Present in adipose tissue	Epi-fat levels in *db*c9,t11[1]	Epi-fat levels in *db*t10,c12[1]	Detected in subcellular fractions
PKCα	YES	No difference	No difference	NO[2]
PKCβI	YES	No difference	No difference	YES
p-PKCα/βII	YES	No difference	↓	Not Tested
PKCγ	NO	NO	NO	NO
PKCδ	YES	No difference	No difference	Not Tested
PKCη	Not Tested	Not Tested	Not Tested	Not Tested
PKCθ	YES	No difference	No difference	YES
PKCε	YES	No difference	↑	Not Tested
PKCμ	YES	No difference	No difference	YES
PKCζ/λ	NO	NO	NO	NO
p-PKCζ/λ	YES	No difference	No difference	Not Tested

1. PKC levels compared to *db*CTL group. 2. Isoform undetected.

Conventional protein kinase C isoforms

Protein kinase C-alpha

Levels of protein kinase C-alpha (PKCα) were measured in the epididymal adipose tissue samples from lean and *db/db* mice. There was no difference in the levels of PKCα between the lean and *db/db* mice (Figure 23). However, the *db*PW group had significantly higher levels of PKCα than the *db*CTL and *db*t10, c12groups.

Protein kinase C-beta$_I$

Levels of protein kinase C-beta$_I$ (PKCβ$_I$) were measured in epididymal adipose tissue samples from lean and *db/db* mice. Levels of PKCβ$_I$ were significantly higher in the lnCTL group than all of *db/db* mice except for the *db*c9, t11 group (Figure 24). There were no significant differences in PKCβ$_I$ levels among any of the *db/db* mice. When epididymal adipose tissue samples were subjected to subcellular fractionation, levels of PKCβ$_I$ in the cytosolic fraction of the *db*CTL mice were greater than in all other groups (Figure 25). All other groups had a greater level of PKCβ$_I$ in the microsomal fraction of the epididymal adipose tissue.

Phospho-protein kinase C-alpha/beta$_{II}$

Levels of phospho-protein kinase C-alpha/beta$_{II}$ (Thr638/641) (p-PKCα/β$_{II}$) were measured in epididymal adipose tissue samples obtained from lean and *db/db* mice. Levels of p-PKCα/β$_{II}$ were significantly higher in the lnCTL group vs. all of the *db/db* mice (Figure 26). The *db*c9, t11 had significantly higher levels of p-PKCα/β$_{II}$ than the *db*PW and the *db*t10, c12groups. Although higher, the p-PKCα/β$_{II}$ levels of the *db*c9, t11 group were not significantly higher than the *db*CTL group.

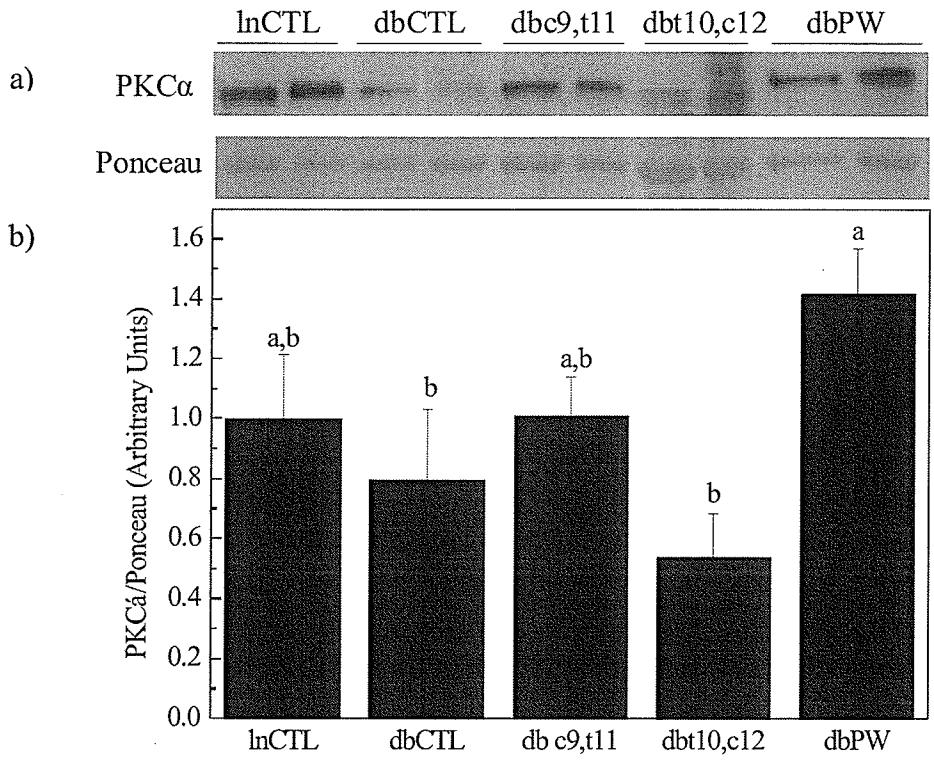

Figure 23: Protein kinase C-alpha protein levels in epididymal adipose tissue. Protein kinase C-alpha (PKCα) protein levels were measured in epididymal adipose tissue samples from lean and *db/db* mice by Western blot analysis. a) Representative Western blot and b) corresponding graph obtained by scanning densitometry of the bands in arbitrary units. Data were derived by calculating the ratio of PKCα to Ponceau S staining and are expressed as mean ± SEM, with the mean of the lnCTL group set to 1; n=4 for all groups. LnCTL = lean mice fed 0 % CLA diet, *db*CTL = *db/db* mice fed 0 % CLA diet, *db*c9, t11 = *db/db* mice fed 0.4 % c9, t11 CLA diet, *db*t10, c12 = *db/db* mice fed 0.4 % t10, c12 CLA, *db*PW = *db/db* mice fed 0 % CLA in restricted amounts. Statistical differences among means ($p \leq 0.05$) are indicated by different lowercase letters.

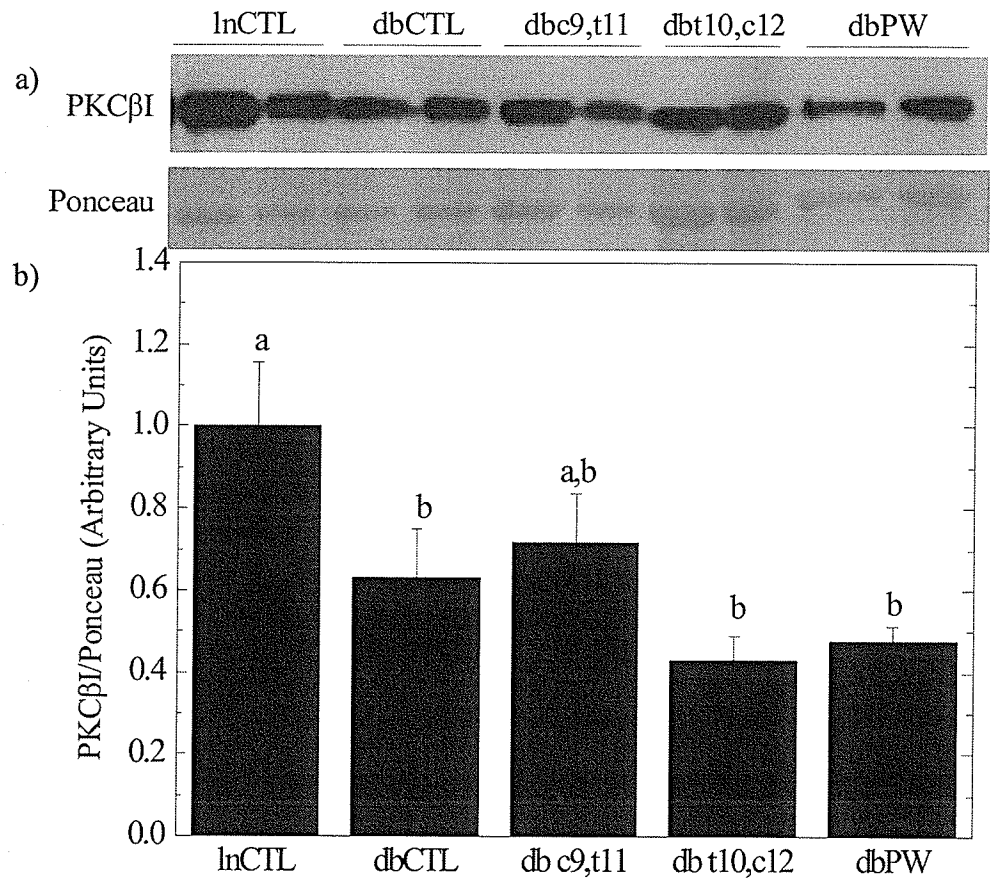

Figure 24: Protein kinase C-BetaI protein levels in epididymal adipose tissue. Protein kinase C-Beta$_I$ (PKCβ_I) protein levels were measured in epididymal adipose tissue samples from lean and *db/db* mice by Western blot analysis. a) Representative Western blot and b) corresponding graph obtained by scanning densitometry of the bands in arbitrary units. Data were derived by calculating the ratio of PKCβ_I to Ponceau S staining and are expressed as mean ± SEM, with the mean of the lnCTL group set to 1; n=4 for all groups. LnCTL = lean mice fed 0 % CLA diet, *db*CTL = *db/db* mice fed 0 % CLA diet, *db*c9, t11 = *db/db* mice fed 0.4 % c9, t11 CLA diet, *db*t10, c12 = *db/db* mice fed 0.4 % t10, c12 CLA, *db*PW = *db/db* mice fed 0 % CLA in restricted amounts. Statistical differences among means ($p \leq 0.05$) are indicated by different lowercase letters.

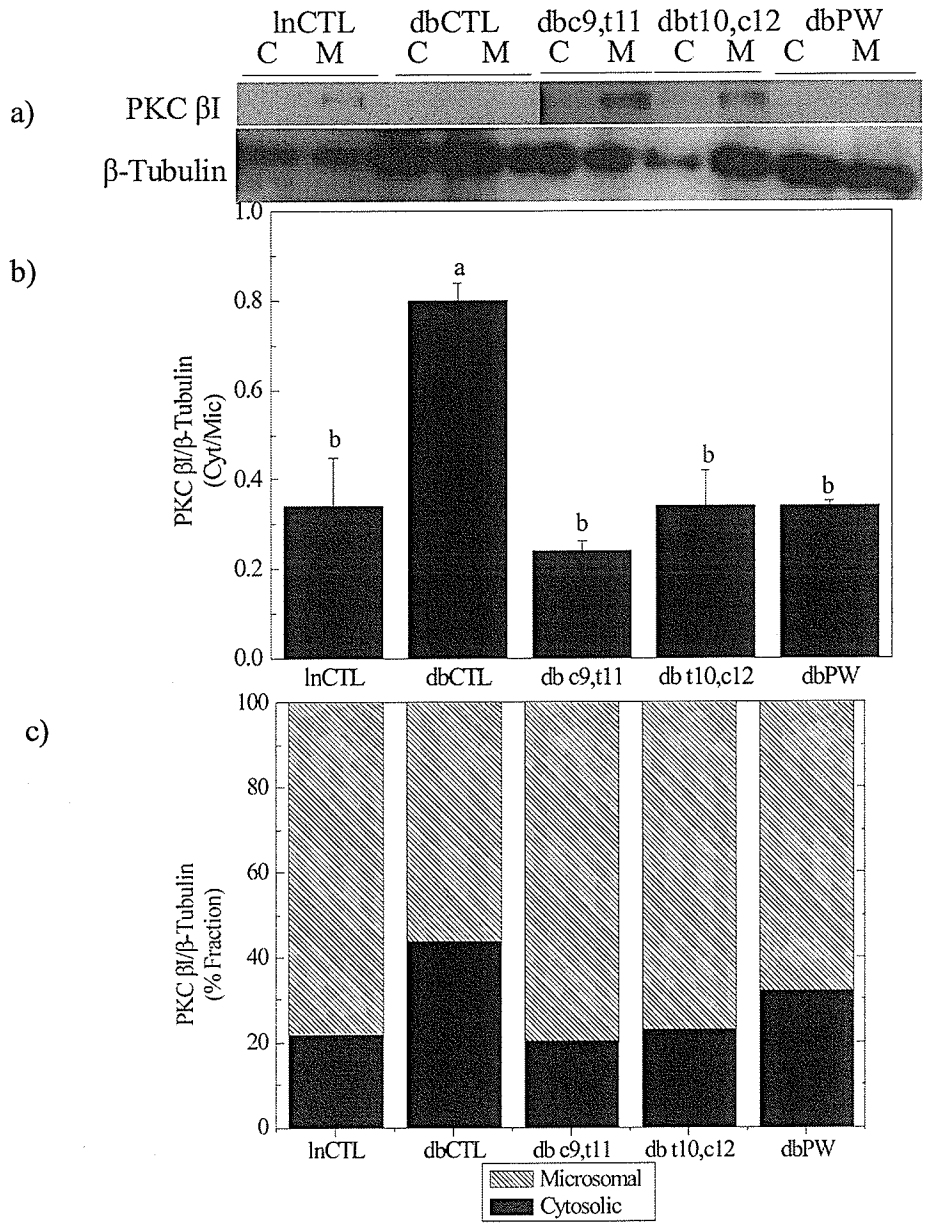

Figure 25: Protein kinase C-betaI levels in subcellular fractions of epididymal adipose tissue. Protein kinase C-beta$_I$ (PKCβ_I) protein levels were measured in epididymal adipose tissue samples from lean and *db/db* mice that underwent subcellular fractionation to yield cytosolic and microsomal fractions which were analyzed by Western blotting. a) Representative Western blot, C=cytosolic fraction M=microsomal fraction, b) corresponding graph obtained by scanning densitometry of the bands in arbitrary units expressed as a ratio of cytosolic to microsomal fractions and c) corresponding graph representing the levels of PKCβ_I in each fraction expressed as a percentage. Data were derived by calculating the ratio of PKCβ_I in each fraction to β-Tubulin and are expressed as mean ± SEM, n=3 for all groups. LnCTL = lean mice fed 0 % CLA diet, *db*CTL = *db/db* mice fed 0 % CLA diet, *db*c9, t11 = *db/db* mice fed 0.4 %

c9, t11 CLA diet, *db*t10, c12 = *db/db* mice fed 0.4 % t10, c12 CLA, *db*PW = *db/db* mice fed 0 % CLA in restricted amounts. Statistical differences among means ($p \leq 0.05$) are indicated by different lowercase letters.

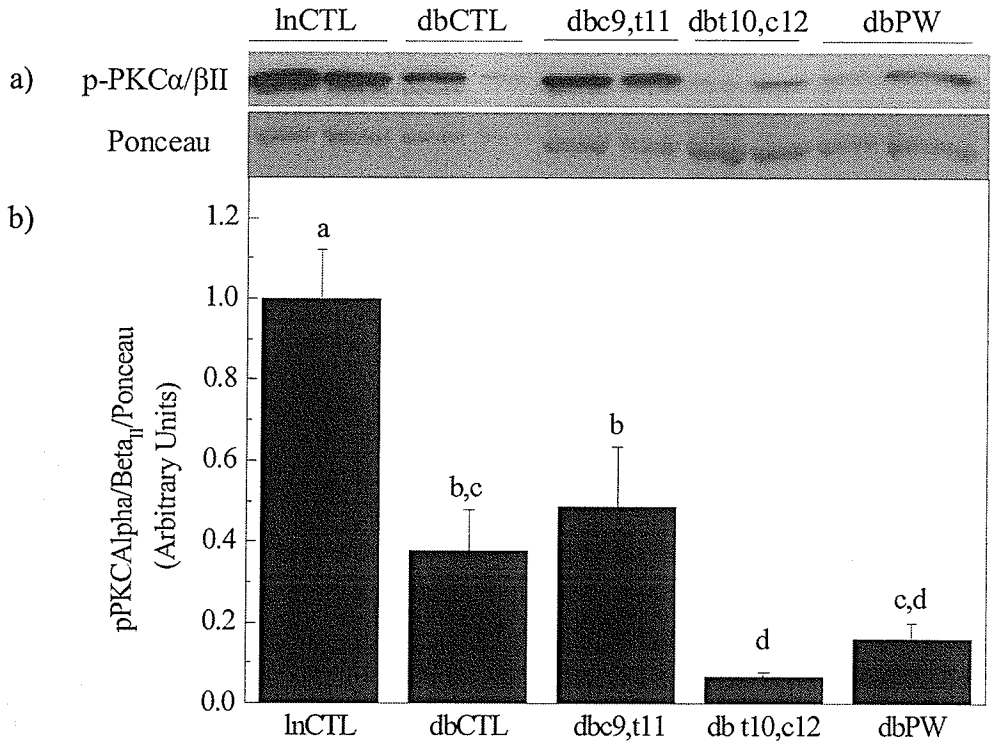

Figure 26: Protein kinase C-alpha/betaII phosphorylation at Thr638/641 in epididymal adipose tissue. Protein kinase C-alpha/beta$_{II}$ (p-PKCα/β_{II}) phosphorylated at Thr638.641 levels were measured in epididymal adipose tissue samples from lean and *db/db* mice by Western blot analysis. a) Representative Western blot and b) corresponding graph obtained by scanning densitometry of the bands in arbitrary units. Data were derived by calculating the ratio of p-PKCα/β_{II} to Ponceau S staining and are expressed as mean ± SEM, with the mean of the lnCTL group set to 1; n=4 for all groups. LnCTL = lean mice fed 0 % CLA diet, *db*CTL = *db/db* mice fed 0 % CLA diet, *db*c9, t11 = *db/db* mice fed 0.4 % c9, t11 CLA diet, *db*t10, c12 = *db/db* mice fed 0.4 % t10, c12 CLA, *db*PW = *db/db* mice fed 0 % CLA in restricted amounts. Statistical differences among means ($p \leq 0.05$) are indicated by different lowercase letters.

Novel protein kinase C isoforms

Protein kinase C-delta

Levels of protein kinase C-delta (PKCδ) were measured in the epididymal adipose tissue samples from lean and *db/db* mice. No differences were seen between the lnCTL and the *db/db* mice or among any of the *db/db* mice (Figure 27).

Protein kinase C-epsilon

Levels of protein kinase C-epsilon (PKCε) were measured in the epididymal adipose tissue samples from lean and *db/db* mice. There was no difference between the lnCTL and *db*CTL groups (Figure 28). The *db*t10, c12 group was significantly higher than all of the other *db/db* mice as well as the lean mice.

Protein kinase C-theta

Levels of protein kinase C-theta (PKCθ) were measured in the epididymal adipose tissue samples from lean and *db/db* mice. The levels of PKCθ were greater in the *db*c9, t11 group than the lnCTL, *db*t10, c12 and *db*PW groups (Figure 29). The *db*c9, t11 group was not significantly higher than the *db*CTL mice. Subcellular fractions of the epididymal adipose tissue revealed no differences in microsomal PKCθ levels among any of the *db/db* mice (Figure 30). The only group that differed from the lnCTL group was the *db*t10, c12 mice which had significantly higher microsomal PKCθ levels.

Protein kinase C-mu/protein kinase D

Levels of protein kinase C-mu (PKCμ) were measured in the epididymal adipose tissue samples from lean and *db/db* mice. No differences were seen between the lnCTL and the *db/db* mice or among any of the *db/db* mice (Figure 31). However, when

epididymal adipose tissue samples underwent subcellular fractionation, levels of PKCμ were highest in the cytosolic fraction of the *db*PW mice (Figure 32). Microsomal levels of PKCμ were higher in the *db*CTL and *db*t10, c12 mice, compared to *db*CTL but none of these groups were different from the lnCTL group.

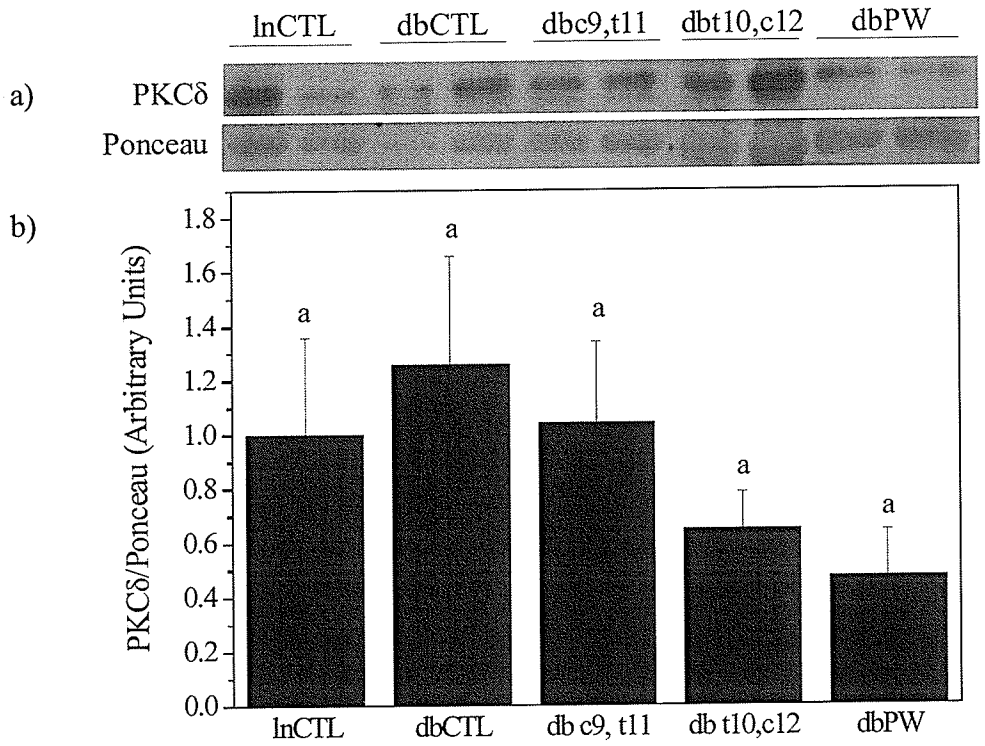

Figure 27: Protein kinase C-delta protein levels in epididymal adipose tissue. Protein kinase C-delta (PKCδ) protein levels were measured in epididymal adipose tissue samples from lean and *db/db* mice by Western blot analysis. a) Representative Western blot and b) corresponding graph obtained by scanning densitometry of the bands in arbitrary units. Data were derived by calculating the ratio of PKCδ to Ponceau S staining and are expressed as mean ± SEM, with the mean of the lnCTL group set to 1; n=6 for all groups. LnCTL = lean mice fed 0 % CLA diet, *db*CTL = *db/db* mice fed 0 % CLA diet, *db*c9, t11 = *db/db* mice fed 0.4 % c9, t11 CLA diet, *db*t10, c12 = *db/db* mice fed 0.4 % t10, c12 CLA, *db*PW = *db/db* mice fed 0 % CLA in restricted amounts. Statistical differences among means ($p \leq 0.05$) are indicated by different lowercase letters.

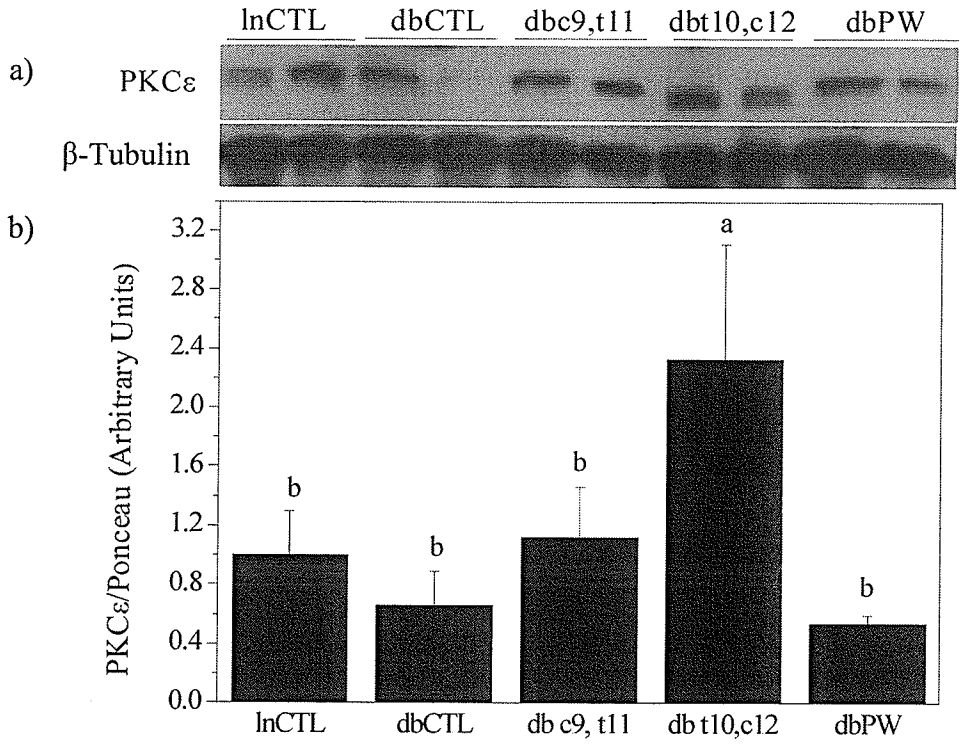

Figure 28: Protein kinase C-epsilon protein levels in epididymal adipose tissue. Protein kinase C-epsilon (PKCε) protein levels were measured in epididymal adipose tissue samples from lean and *db/db* mice by Western blot analysis. a) Representative Western blot and b) corresponding graph obtained by scanning densitometry of the bands in arbitrary units. Data were derived by calculating the ratio of PKCε to β-Tubulin and are expressed as mean ± SEM, with the mean of the lnCTL group set to 1; n=4 for all groups. LnCTL = lean mice fed 0 % CLA diet, *db*CTL = *db/db* mice fed 0 % CLA diet, *db*c9, t11 = *db/db* mice fed 0.4 % c9, t11 CLA diet, *db*t10, c12 = *db/db* mice fed 0.4 % t10, c12 CLA, *db*PW = *db/db* mice fed 0 % CLA in restricted amounts. Statistical differences among means ($p \leq 0.05$) are indicated by different lowercase letters.

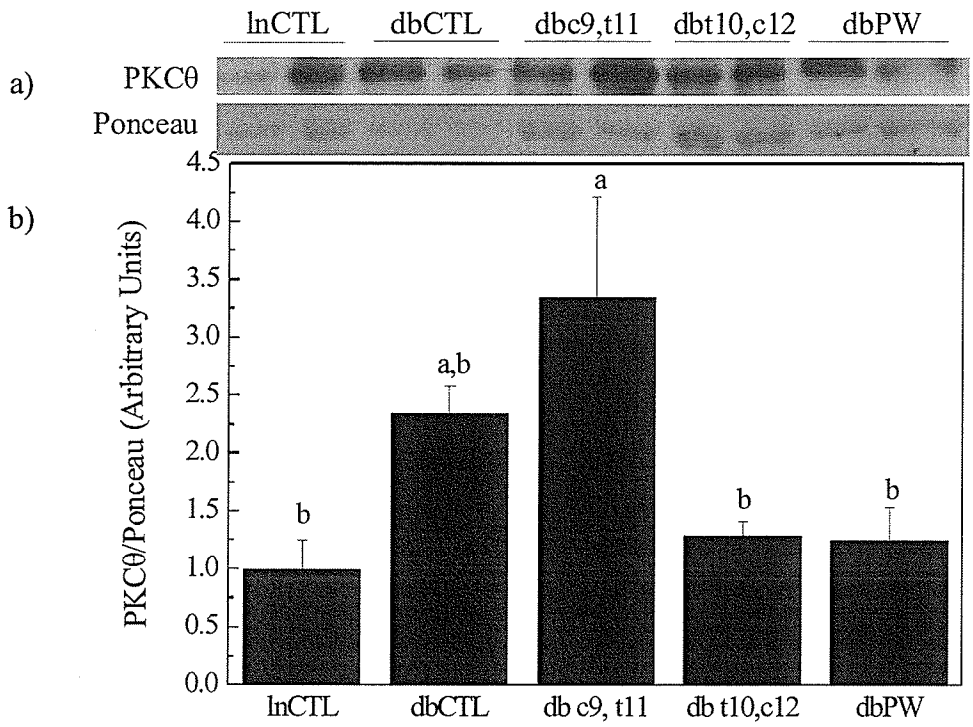

Figure 29: Protein kinase C-theta protein levels in epididymal adipose tissue. Protein kinase C-theta (PKCθ) protein levels were measured in epididymal adipose tissue samples from lean and *db/db* mice by Western blot analysis. a) Representative Western blot and b) corresponding graph obtained by scanning densitometry of the bands in arbitrary units. Data were derived by calculating the ratio of PKCθ to Ponceau S staining and are expressed as mean ± SEM, with the mean of the lnCTL group set to 1; n=6 for all groups. LnCTL = lean mice fed 0 % CLA diet, *db*CTL = *db/db* mice fed 0 % CLA diet, *db*c9, t11 = *db/db* mice fed 0.4 % c9, t11 CLA diet, *db*t10, c12 = *db/db* mice fed 0.4 % t10, c12 CLA, *db*PW = *db/db* mice fed 0 % CLA in restricted amounts. Statistical differences among means ($p \leq 0.05$) are indicated by different lowercase letters.

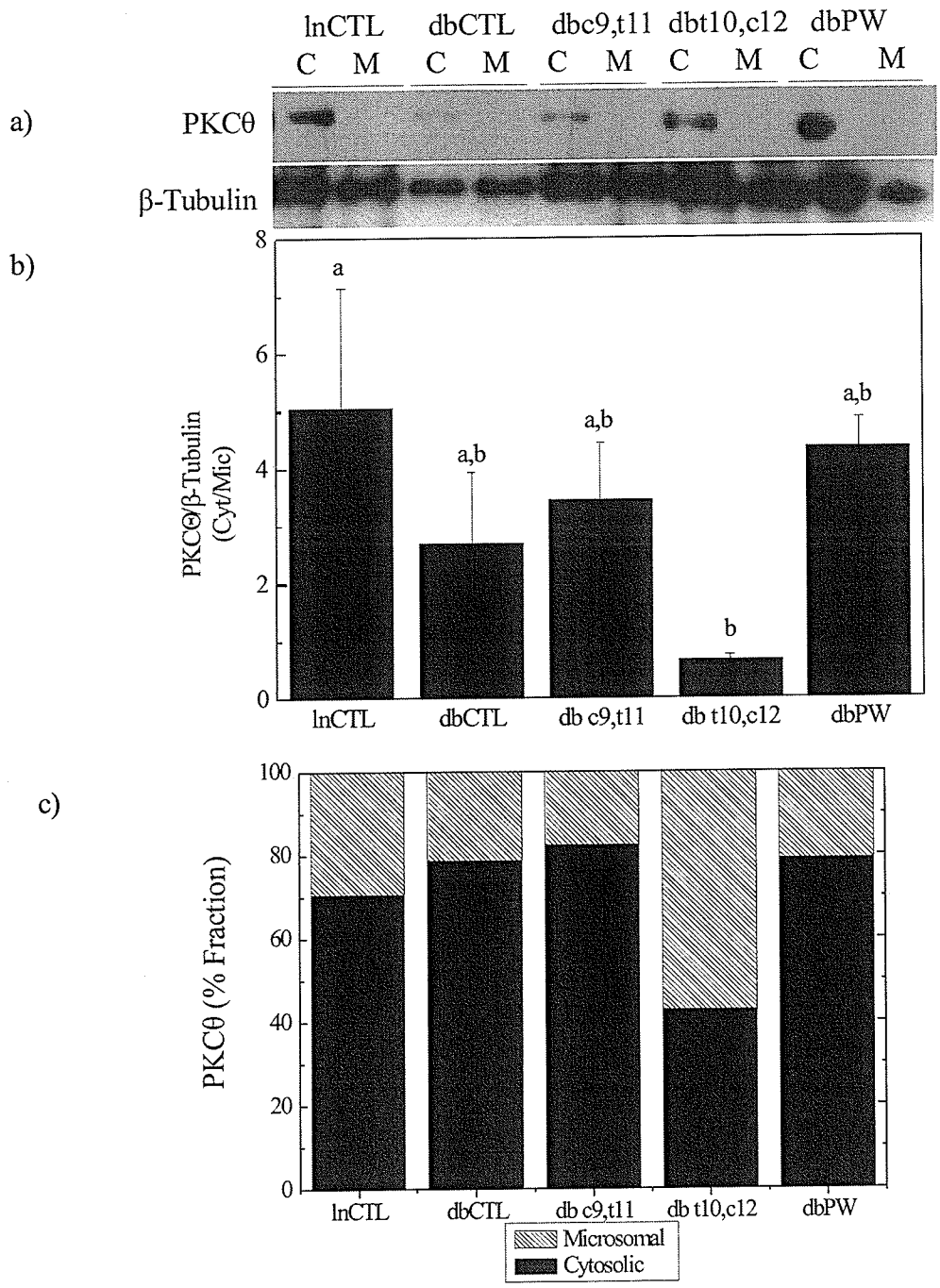

Figure 30: Protein kinase C-theta levels in subcellular fractions of epididymal adipose tissue. Protein kinase C-theta (PKCθ) protein levels were measured in epididymal adipose tissue samples from lean and *db/db* mice that underwent subcellular fractionation to yield cytosolic and microsomal fractions which were analyzed by Western blotting. a) Representative Western blot, C=cytosolic fraction M=microsomal fraction, b) corresponding graph obtained by scanning densitometry of the bands in arbitrary units expressed as a ratio of cytosolic to microsomal fractions and c) corresponding graph representing the levels of PKCθ in each fraction expressed as a

percentage. Data were derived by calculating the ratio of PKCθ in each fraction to β-Tubulin and are expressed as mean ± SEM; n=3 for all groups. LnCTL = lean mice fed 0 % CLA diet, *db*CTL = *db/db* mice fed 0 % CLA diet, *db*c9, t11 = *db/db* mice fed 0.4 % c9, t11 CLA diet, *db*t10, c12 = *db/db* mice fed 0.4 % t10, c12 CLA, *db*PW = *db/db* mice fed 0 % CLA in restricted amounts. Statistical differences among means ($p \leq 0.05$) are indicated by different lowercase letters.

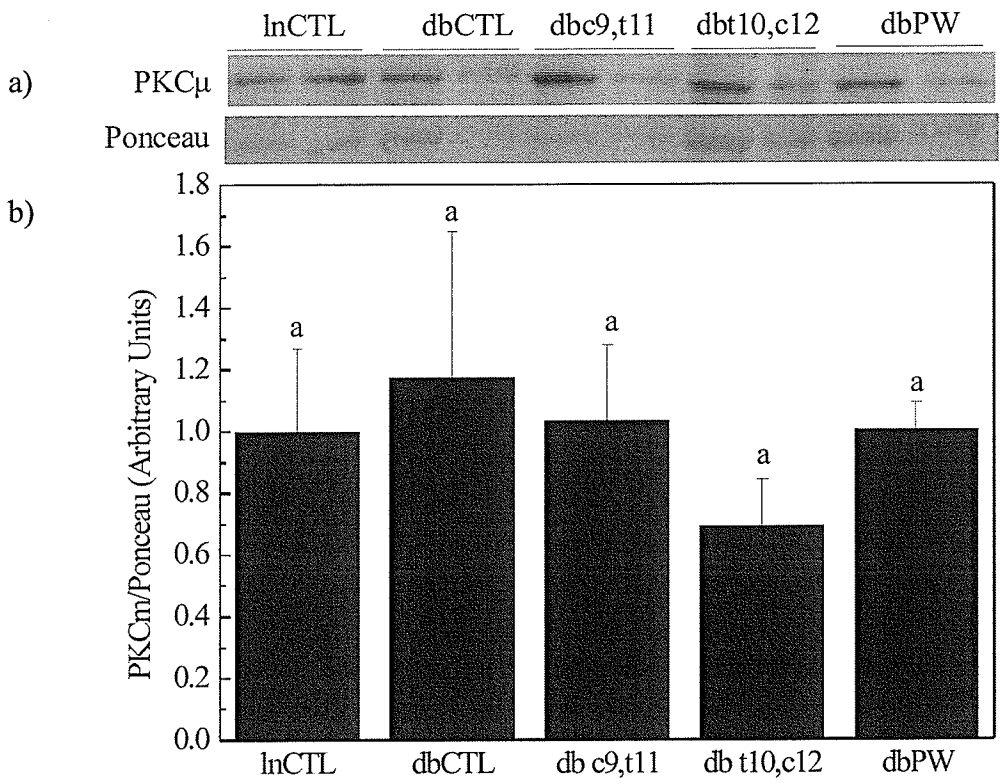

Figure 31: Protein kinase C-mu protein levels in epididymal adipose tissue. Protein kinase C-mu (PKCμ) protein levels were measured in epididymal adipose tissue samples from lean and *db/db* mice by Western blot analysis. a) Representative Western blot and b) corresponding graph obtained by scanning densitometry of the bands in arbitrary units. Data were derived by calculating the ratio of PKCμ to Ponceau S staining and are expressed as mean ± SEM, with the mean of the lnCTL group set to 1; n=6 for all groups. LnCTL = lean mice fed 0 % CLA diet, *db*CTL = *db/db* mice fed 0 % CLA diet, *db*c9, t11 = *db/db* mice fed 0.4 % c9, t11 CLA diet, *db*t10, c12 = *db/db* mice fed 0.4 % t10, c12 CLA, *db*PW = *db/db* mice fed 0 % CLA in restricted amounts. Statistical differences among means ($p \leq 0.05$) are indicated by different lowercase letters.

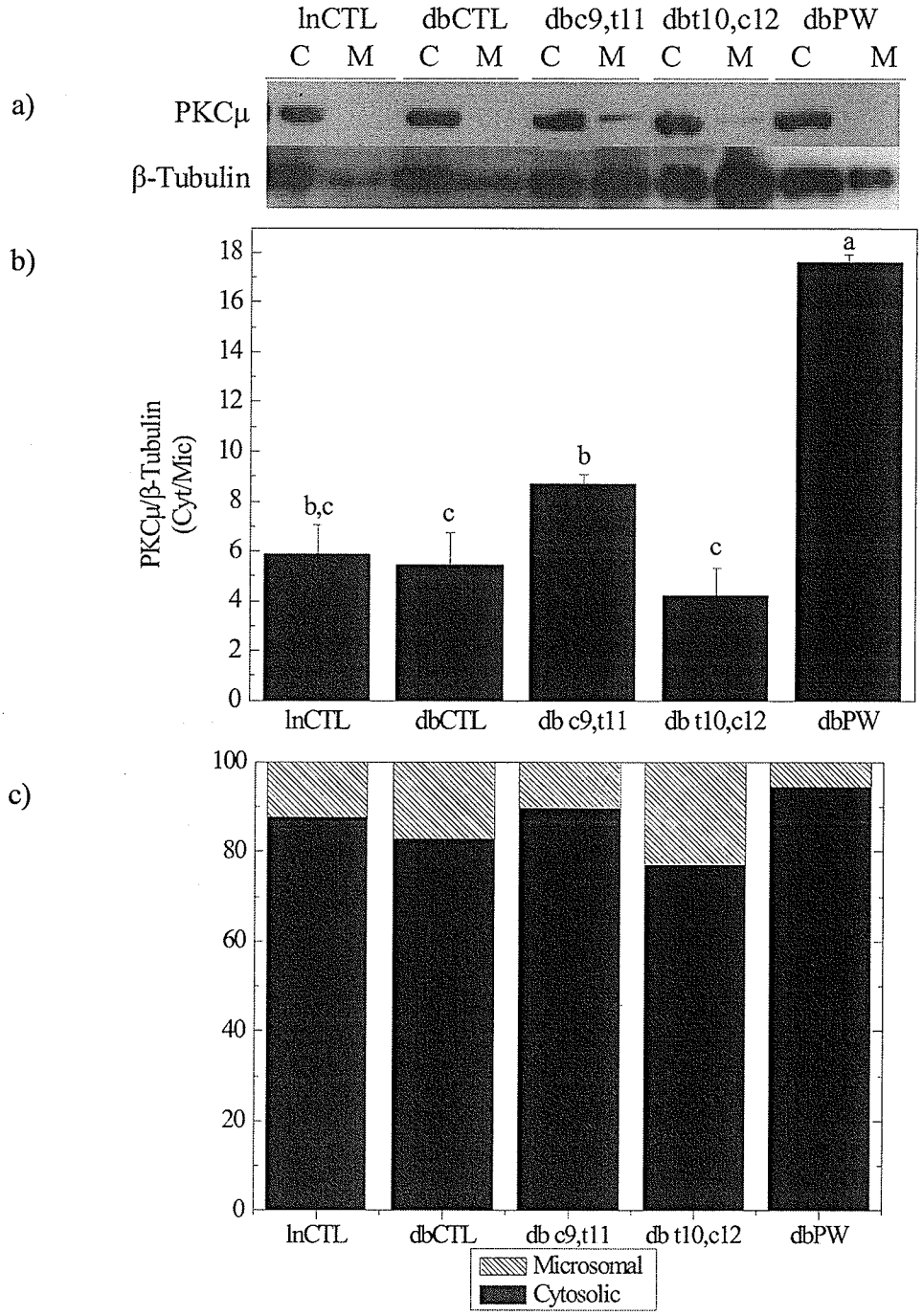

Figure 32: Protein kinase C-mu levels in subcellular fractions of epididymal adipose tissue. Protein kinase C-mu (PKCμ) protein levels were measured in epididymal adipose tissue samples from lean and *db/db* mice that underwent subcellular fractionation to yield cytosolic and microsomal fractions which were analyzed by Western blotting. a) Representative Western blot, C=cytosolic fraction M=microsomal fraction, b) corresponding graph obtained by scanning densitometry of the bands in arbitrary units expressed as a ratio of cytosolic to microsomal fractions and c) corresponding graph

representing the levels of PKCμ in each fraction expressed as a percentage. Data were derived by calculating the ratio of PKCμ in each fraction to β-Tubulin and are expressed as mean ± SEM, n=3 for all groups. LnCTL = lean mice fed 0 % CLA diet, *db*CTL = *db/db* mice fed 0 % CLA diet, *db*c9, t11 = *db/db* mice fed 0.4 % c9, t11 CLA diet, *db*t10, c12 = *db/db* mice fed 0.4 % t10, c12 CLA, *db*PW = *db/db* mice fed 0 % CLA in restricted amounts. Statistical differences among means ($p \leq 0.05$) are indicated by different lowercase letters.

Atypical protein kinase C isoforms

Phospho-protein kinase C-zeta/lambda

Levels of phospho-protein kinase C-zeta/lambda (p-PKCζ/λ) were measured in the epididymal adipose tissue samples from lean and *db/db* mice. The levels of p-PKCζ/λ were greater in the dbc9, t11 group than the lnCTL mice but they were not significantly higher than any of the *db/db* mice groups (Figure 33).

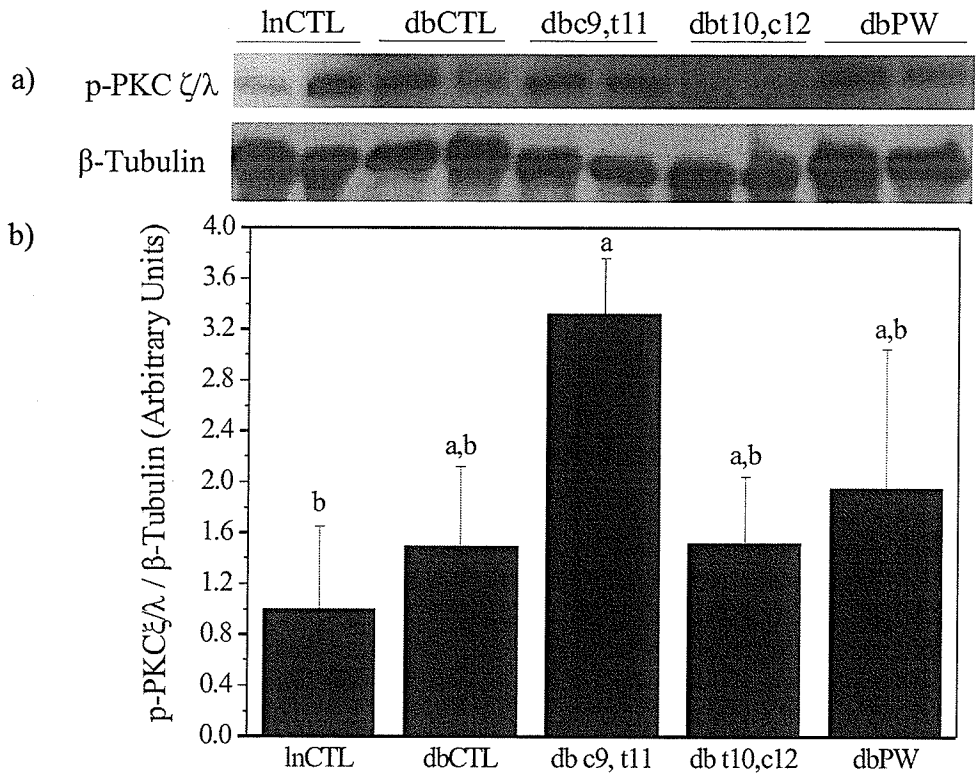

Figure 33: Protein kinase C-zeta/lambda phosphorylation at Thr410/403 in epididymal adipose tissue. Protein kinase C-zeta/lambda (p-PKCζ/λ) phosphorylated at Thr410/403 protein levels were measured in epididymal adipose tissue samples from lean and *db/db* mice by Western blot analysis. a) Representative Western blot and b) corresponding graph obtained by scanning densitometry of the bands in arbitrary units. Data were derived by calculating the ratio of p-PKCζ/λ to β-Tubulin and are expressed as mean ± SEM, with the mean of the lnCTL group set to 1; n=4 for all groups. LnCTL = lean mice fed 0 % CLA diet, *db*CTL = *db/db* mice fed 0 % CLA diet, *db*c9, t11 = *db/db* mice fed 0.4 % c9, t11 CLA diet, *db*t10, c12 = *db/db* mice fed 0.4 % t10, c12 CLA, *db*PW = *db/db* mice fed 0 % CLA in restricted amounts. Statistical differences among means ($p \leq 0.05$) are indicated by different lowercase letters.

STUDY 2 – CELL CULTURE MODEL

CLA treated 3T3-L1 adipocytes

In order to investigate how CLA affects the levels of leptin, p-STAT-3 and PKC in adipose tissue and how these actions may be mediated through ObRb, mouse-derived, mature 3T3-L1 adipocytes that do have a functional leptin receptor were treated with leptin and the individual isomers of CLA, mixed isomers, as well as linoleic acid and linoleic acid mixed with the two isomers of CLA.

Leptin

Levels of leptin were measured at 0, 1, 2, 4, 8 and 24 hours after treatment of mature 3T3-L1 adipocytes with 6.25 nM leptin, 60 μM *c9, t11* CLA, 60 μM *t10, c12 CLA*, 60 μM linoleic acid, 60 μM (50:50) mixture of *c9, t11* CLA and *t10, c12* CLA (MIX), 60 μM (50:50) mixture of linoleic acid and *t10, c12* CLA (LA + t10, c12) or linoleic acid and *c9, t11* CLA (LA + c9, t11) with ethanol serving as the vehicle control. After two hours of treatment with LA + *t10, c12* CLA, leptin protein levels increased significantly higher (4-fold) than all other groups (Figure 34).

Phospho-signal transducers and activators of transcription

Levels of signal transducers and activators of transcription phosphorylation at Tyrosine705 (p-STAT-3) were measured after a one hour treatment with leptin, 60 μM *c9, t11* CLA, 60 μM *t10, c12 CLA*, 60 μM linoleic acid, 60 μM (50:50) mixture of *c9, t11* CLA and *t10, c12* CLA (MIX), 60 μM (50:50) mixture of linoleic acid and *t10, c12* CLA (LA + t10, c12) or linoleic acid and *c9, t11* CLA (LA + c9, t11) with ethanol being used as a vehicle control. Changes in p-STAT-3 were all relative to the vehicle control which

was set as the baseline. The *c9, t11* CLA treated cells had a significantly higher increase in the level of p-STAT-3 than the MIX and the LA + *c9, t11* CLA treated cells when compared to ethanol treated cells (Figure 35).

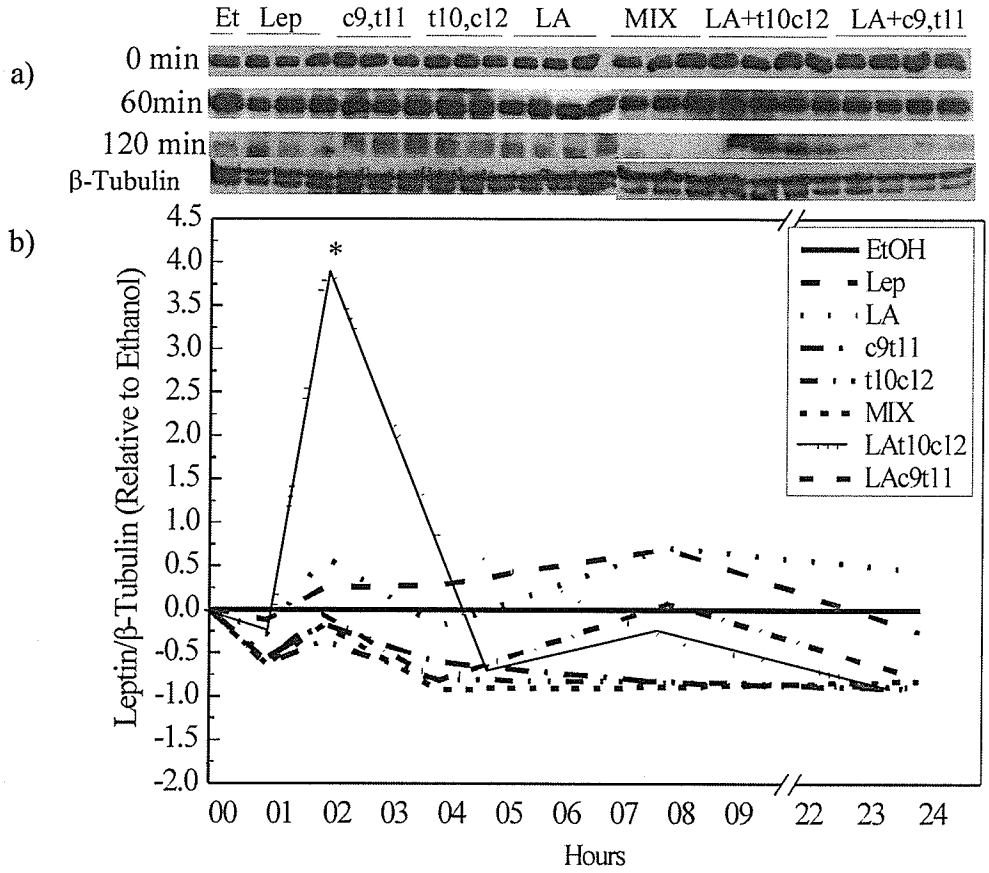

Figure 34: Leptin protein levels of mature 3T3-L1 adipocytes at 0, 1, 2, 4, 8 and 24 hours after CLA treatment. Leptin protein levels were measured in 3T3-L1 adipocytes at time points of 0, 1, 2, 4, 8 and 24 hours by Western blot analysis. a) Representative Western blots for time-points of 0, 1 and 2 hours. b) Corresponding graph obtained by scanning densitometry of the bands in arbitrary units. Data were derived by calculating the ratio of leptin to β-tubulin. All time-points are expressed relative to the 0 hour time-point and all groups are expressed relative to ethanol, which was used as a vehicle control. Et = Ethanol (n=1), Lep = 6.25 nM leptin (n=3), LA = 60 μM linoleic acid (n=3), c9,t11 = 60 μM *c9, t11* CLA (n=3), t10,c12 = 60 μM *t10, c12* CLA (n=3), MIX = 60 μM of a 50:50 mixture of *c9, t11* CLA and *t10, c12* CLA (n=3), LA + t10c12 = 60 μM of 50:50 mixture of linoleic acid and *t10, c12* CLA (n=4) and LA+c9,t11 = 60 μM mixture of a 50:50 mixture of linoleic acid and *c9, t11* CLA (n=4). * denotes significant difference between LA + *t10, c12* CLA and all other treatments at 2 hours.

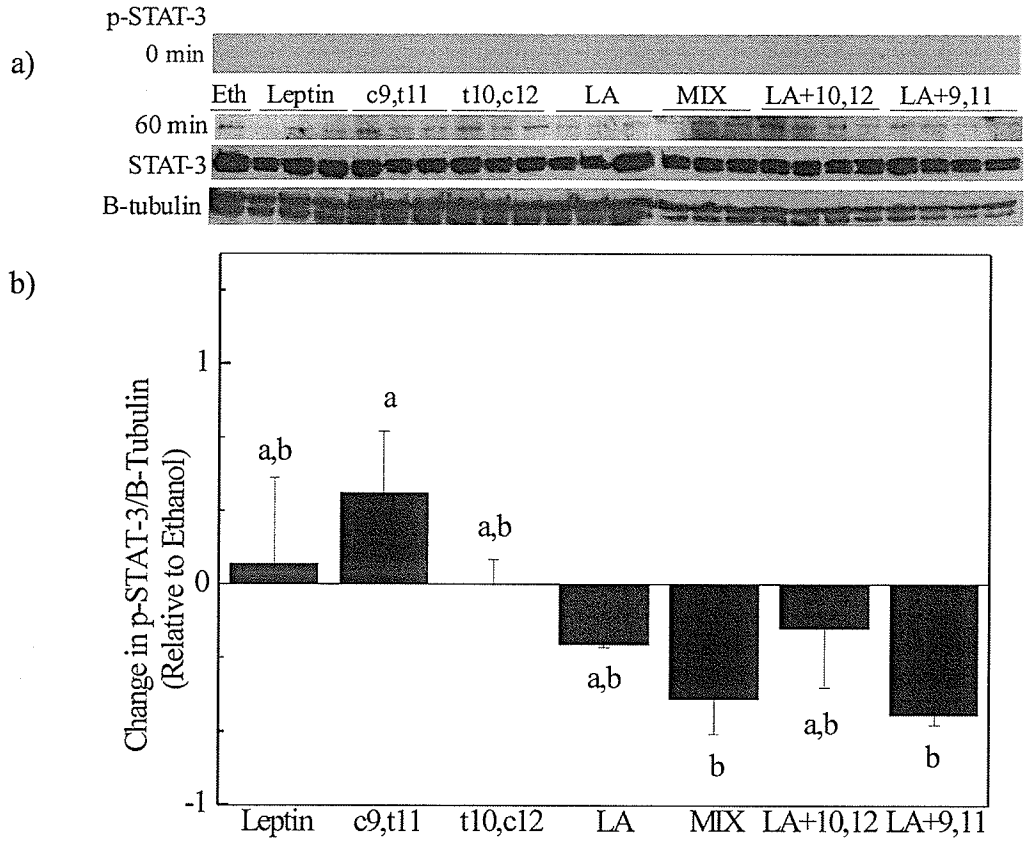

Figure 35: Change in signal transducers and activators of transcription phosphorylation at Tyr705 in mature 3T3-L1 adipocytes after 60 minutes of CLA treatment. Signal transducers and activators of transcription (p-STAT-3) phosphorylated at Tyr705 protein levels were measured from 3T3-L1 adipocytes at time points of 0 and 60 minutes by Western blot analysis. a) Representative Western blot at 1 hour b) Corresponding graph obtained by scanning densitometry of the bands in arbitrary units. Data were derived by calculating the ratio of p-STAT-3 to β-tubulin which was expressed relative to the 0 hour time-point while all groups are expressed relative to ethanol, which was used as a vehicle control. Et = Ethanol (n=1), Lep = 6.25 nM leptin (n=3), LA = 60 μM linoleic acid (n=3), c9,t11 = 60 μM *c9, t11* CLA (n=3), t10,c12 = 60 μM *t10, c12* CLA (n=3), MIX = 60 μM of a 50:50 mixture of *c9, t11* CLA and *t10, c12* CLA (n=3), LA + t10c12 = 60 μM of 50:50 mixture of linoleic acid and *t10, c12* CLA (n=4) and LA+c9,t11 = 60 μM mixture of a 50:50 mixture of linoleic acid and *c9, t11* CLA (n=4). Statistical differences among means ($p \leq 0.05$) are indicated by different lowercase letters.

Isoforms of protein kinase C found in 3T3-L1 adipocytes

An increase in lipid availability can lead to the chronic activation of a variety of PKCs which can lead to unregulated phosphorylation of a number of mediators of insulin signalling. This study is one of the first to demonstrate that all three classes (conventional, novel, and atypical) of PKC are indeed present in whole cell fractions of 3T3-L1 adipocytes (Table 5). It is also one of the first to show that the levels of PKC change over one hour in response to treatments of CLA

Table 5. Protein kinase C isoforms detected in 3T3-L1 adipocytes

PKC Isoform	PKC isoforms detected	60 μM treatment of *c9, t11* CLA[1]	60 μM treatment of *t10, c12* CLA[1]
PKCα	YES	No difference	No difference
PKCβI	YES	No difference	No difference
p-PKCα/βII	YES	YES	No difference
PKCγ	NO[2]	NO	NO
PKCδ	NO	NO	NO
PKCη	Not Tested	Not Tested	Not Tested
PKCθ	NO	NO	NO
PKCε	YES	No difference	↑
PKCμ	YES	No difference	↑
PKCζ/λ	NO	NO	NO
p-PKCζ/λ	YES	↓	No difference

1. Change in PKC levels after one hour, relative to 60 μM treatment of linoleic acid. 2. PKC isoform undetected.

Conventional protein kinase C isoforms

Protein kinase C-alpha

Levels of protein kinase C-alpha (PKCα) were measured after treating the mature 3T3-L1 adipocytes for one hour with leptin, 60 μM *c9, t11* CLA, 60 μM *t10, c12 CLA*, 60 μM linoleic acid, 60 μM (50:50) mixture of *c9, t11* CLA and *t10, c12* CLA (MIX), 60 μM (50:50) mixture of linoleic acid and *t10, c12* CLA (LA + t10, c12) or linoleic acid and *c9, t11* CLA (LA + c9, t11) with ethanol being used as a vehicle control. Changes in PKCα over one hour were measured relative to the vehicle control. The cells treated with *c9, t11* CLA, *t10, c12* CLA and linoleic acid all showed a significant increase PKCα levels while the other treatment groups did not (Figure 36).

Protein kinase C-beta I

Levels of protein kinase C-beta I (PKCβI) were measured after a one hour treatment of the mature 3T3-L1 adipocytes with leptin, 60 μM *c9, t11* CLA, 60 μM *t10, c12 CLA*, 60 μM linoleic acid, 60 μM (50:50) mixture of *c9, t11* CLA and *t10, c12* CLA (MIX), 60 μM (50:50) mixture of linoleic acid and *t10, c12* CLA (LA + t10, c12) or linoleic acid and *c9, t11* CLA (LA + c9, t11) with ethanol being used as a vehicle control. Changes in PKCβI over one hour were measured relative to the vehicle control. The cells treated with *c9, t11* CLA, *t10, c12* CLA and leptin all showed higher levels of PKCβI compared to the MIX, LA + c9, t11 or LA + t10, c12 treated groups (Figure 37).

Phospho-protein kinase C-alpha/beta$_{II}$

Levels of phospho-protein kinase C-alpha/beta$_{II}$ (Thr638/641) (p-PKCα/β_{II}) were measured after a one hour treatment of the mature 3T3-L1 adipocytes with leptin, 60 μM

c9, t11 CLA, 60 μM *t10, c12 CLA*, 60 μM linoleic acid, 60 μM (50:50) mixture of *c9, t11* CLA and *t10, c12* CLA (MIX), 60 μM (50:50) mixture of linoleic acid and *t10, c12* CLA (LA + t10, c12) or linoleic acid and *c9, t11* CLA (LA + c9, t11) with ethanol being used as a vehicle control. All groups showed lower levels of p-PKCα/β_{II}, with the leptin and *c9, t11* CLA treated groups having the smallest decrease in p-PKCα/β_{II} (Figure 38).

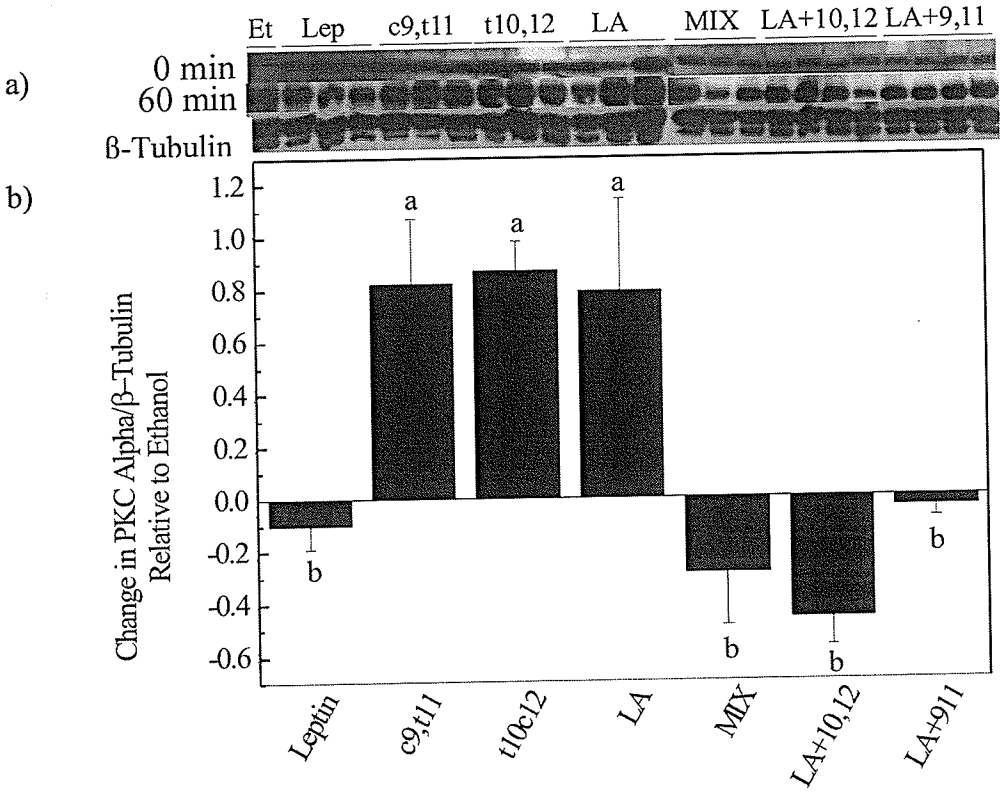

Figure 36: Change in protein kinase C-alpha protein levels in mature 3T3-L1 adipocytes after 60 minutes of CLA treatment. Protein kinase C-alpha (PKCα) protein levels were measured from 3T3-L1 adipocytes at time points of 0 and 60 minutes by Western blot analysis. a) Representative Western blot at 1 hour b) Corresponding graph obtained by scanning densitometry of the bands in arbitrary units. Data were derived by calculating the ratio of PKCα to β-tubulin which was expressed relative to the 0 hour time-point while all groups are expressed relative to ethanol, which was used as a vehicle control. Et = Ethanol (n=1), Lep = 6.25 nM leptin (n=3), LA = 60 μM linoleic acid (n=3), c9,t11 = 60 μM *c9, t11* CLA (n=3), t10,c12 = 60 μM *t10, c12* CLA (n=3), MIX = 60 μM of a 50:50 mixture of *c9, t11* CLA and *t10, c12* CLA (n=3), LA + t10c12 = 60 μM of 50:50 mixture of linoleic acid and *t10, c12* CLA (n=4) and LA+c9,t11 = 60 μM mixture of a 50:50 mixture of linoleic acid and *c9, t11* CLA (n=4). Statistical differences among means ($p \leq 0.05$) are indicated by different lowercase letters.

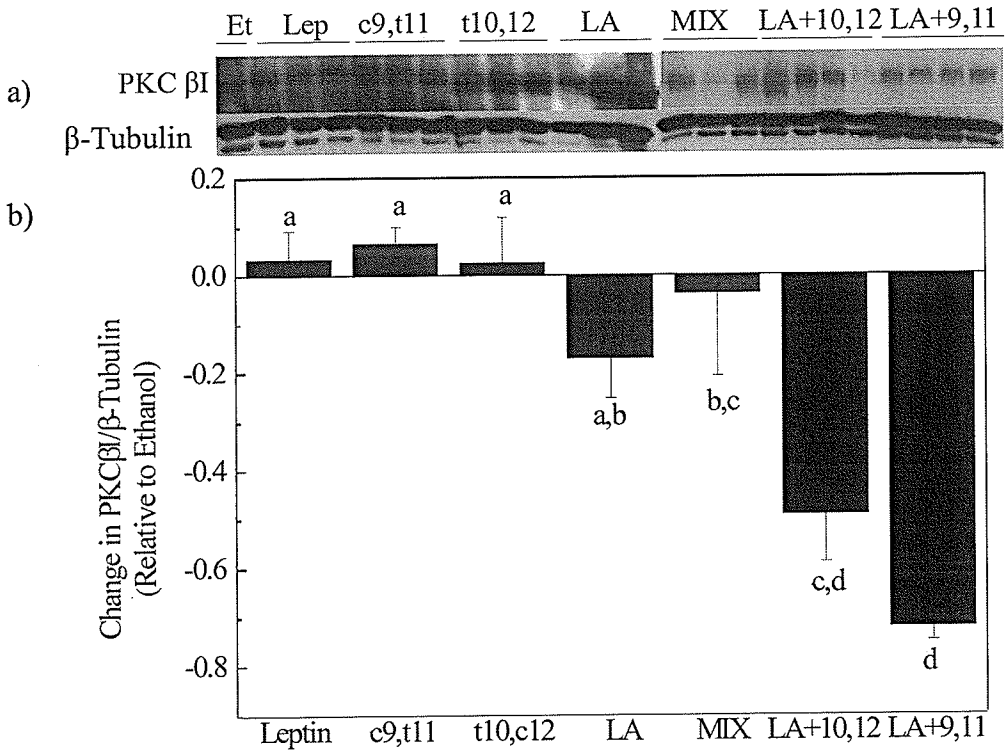

Figure 37: Change in protein kinase C-betaI protein levels in mature 3T3-L1 adipocytes after 60 minutes of CLA treatment. Protein kinase C-beta$_I$ (PKCβI) protein levels were measured from 3T3-L1 adipocytes at time points of 0 and 60 minutes by Western blot analysis. a) Representative Western blot at 1 hour b) Corresponding graph obtained by scanning densitometry of the bands in arbitrary units. Data were derived by calculating the ratio of PKCβI to β-tubulin which was expressed relative to the 0 hour time-point while all groups are expressed relative to ethanol, which was used as a vehicle control. Et = Ethanol (n=1), Lep = 6.25 nM leptin (n=3), LA = 60 μM linoleic acid (n=3), c9,t11 = 60 μM *c9, t11* CLA (n=3), t10,c12 = 60 μM *t10, c12* CLA (n=3), MIX = 60 μM of a 50:50 mixture of *c9, t11* CLA and *t10, c12* CLA (n=3), LA + t10c12 = 60 μM of 50:50 mixture of linoleic acid and *t10, c12* CLA (n=4) and LA+c9,t11 = 60 μM mixture of a 50:50 mixture of linoleic acid and *c9, t11* CLA (n=4). Statistical differences among means ($p \leq 0.05$) are indicated by different lowercase letters.

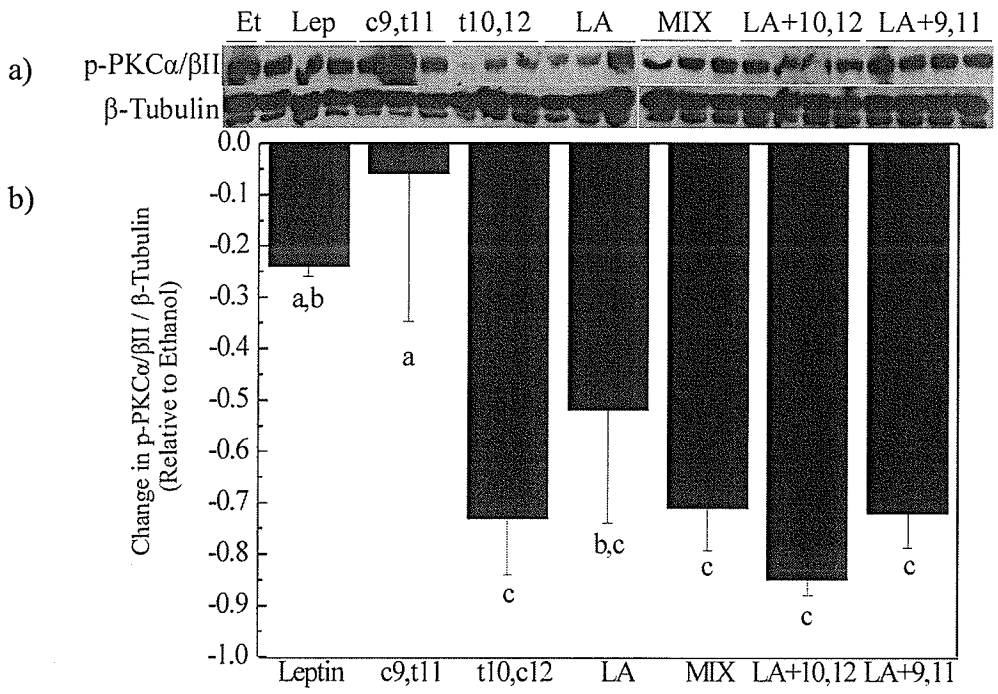

Figure 38: Change in protein kinase C-alpha/betaII phosphorylation at Thr638/641 in mature 3T3-L1 adipocytes after 60 minutes of CLA treatment. Protein kinase C-alpha/beta$_{II}$ (p-PKCα/β_{II}) phosphorylated at Thr638/641 protein levels were measured from 3T3-L1 adipocytes at time points of 0 and 60 minutes by Western blot analysis. a) Representative Western blot at 1 hour b) Corresponding graph obtained by scanning densitometry of the bands in arbitrary units. Data were derived by calculating the ratio of p-PKCα/β_{II} to β-tubulin which was expressed relative to the 0 hour time-point while all groups are expressed relative to ethanol, which was used as a vehicle control. Et = Ethanol (n=1), Lep = 6.25 nM leptin (n=3), LA = 60 μM linoleic acid (n=3), c9,t11 = 60 μM *c9, t11* CLA (n=3), t10,c12 = 60 μM *t10, c12* CLA (n=3), MIX = 60 μM of a 50:50 mixture of *c9, t11* CLA and *t10, c12* CLA (n=3), LA + t10c12 = 60 μM of 50:50 mixture of linoleic acid and *t10, c12* CLA (n=4) and LA+c9,t11 = 60 μM mixture of a 50:50 mixture of linoleic acid and *c9, t11* CLA (n=4). Statistical differences among means ($p \leq 0.05$) are indicated by different lowercase letters.

Novel protein kinase C isoforms

Protein kinase C-epsilon

Levels of protein kinase C-epsilon (PKCε) were measured after a one hour treatment of the mature 3T3-L1 adipocytes with leptin, 60 μM *c9, t11* CLA, 60 μM *t10, c12 CLA*, 60 μM linoleic acid, 60 μM (50:50) mixture of *c9, t11* CLA and *t10, c12* CLA (MIX), 60 μM (50:50) mixture of linoleic acid and *t10, c12* CLA (LA + t10, c12) or linoleic acid and *c9, t11* CLA (LA + c9, t11) with ethanol being used as a vehicle control. Changes in PKCε over one hour were measured relative to the vehicle control. After one hour, levels of PKCε were highest in cells treated with *t10, c12* CLA (Figure 39). There was no difference in PKCε levels between linoleic acid and any other treatment, except for *t10, c12* CLA. When in combination with either of the CLA isomers, linoleic acid also appeared to decrease protein levels of PKCε compared to the CLA isomers administered on their own. Leptin treated cells had significantly lower levels of PKCε than the *t10, c12* CLA treated cells.

Protein kinase C- mu

Levels of protein kinase C-mu (PKCμ) were measured after a one hour treatment of the mature 3T3-L1 adipocytes with leptin, 60 μM *c9, t11* CLA, 60 μM *t10, c12 CLA*, 60 μM linoleic acid, 60 μM (50:50) mixture of *c9, t11* CLA and *t10, c12* CLA (MIX), 60 μM (50:50) mixture of linoleic acid and *t10, c12* CLA (LA + t10, c12) or linoleic acid and *c9, t11* CLA (LA + c9, t11) with ethanol being used as a vehicle control. Changes in PKCμ over one hour were measured relative to the vehicle control. 3T3-L1 adipocytes treated with *t10, c12* CLA had significantly increased levels of PKCμ compared to all other groups (Figure 40). Linoleic acid and the *c9, t11* CLA treated cells had similar increases

in PKCμ protein levels, while leptin treated cells had a slight increase in PKCμ levels. Cells treated with MIX-CLA or when either isomer was mixed with linoleic saw a decrease in protein levels of PKCμ after one hour compared to CLA isomers or linoleic acid alone.

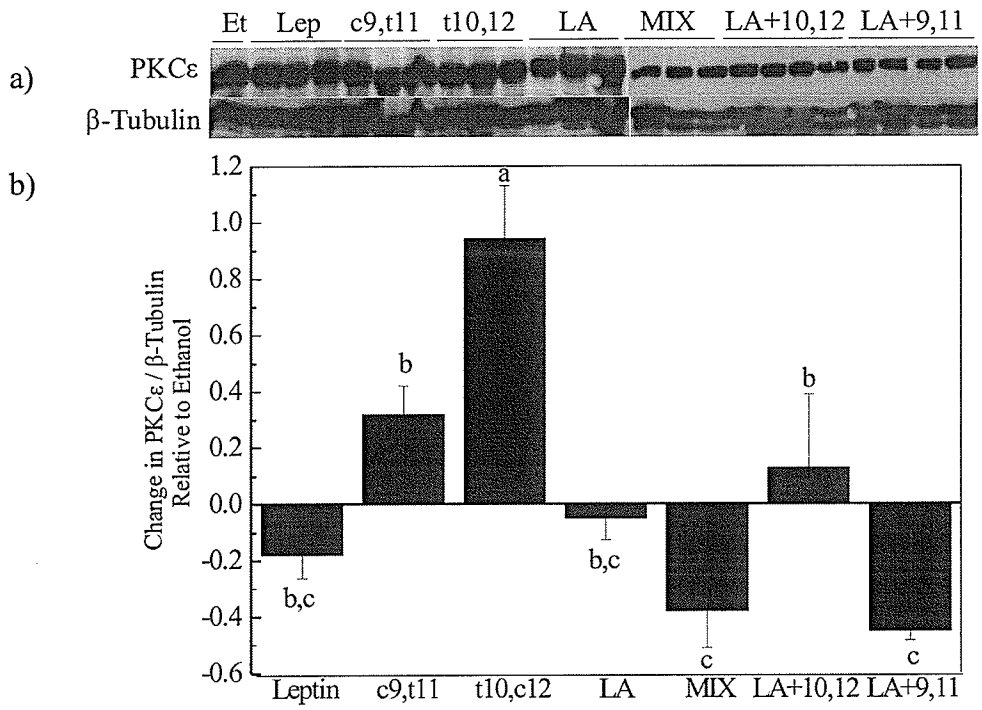

Figure 39: Change in protein kinase C-epsilon protein levels in mature 3T3-L1 adipocytes after 60 minutes of CLA treatment. Protein kinase C-epsilon (PKCε) protein levels were measured from 3T3-L1 adipocytes at time points of 0 and 60 minutes by Western blot analysis. a) Representative Western blot at 1 hour b) Corresponding graph obtained by scanning densitometry of the bands in arbitrary units. Data were derived by calculating the ratio of PKCε to β-tubulin which was expressed relative to the 0 hour time-point while all groups are expressed relative to ethanol, which was used as a vehicle control. Et = Ethanol (n=1), Lep = 6.25 nM leptin (n=3), LA = 60 μM linoleic acid (n=3), c9,t11 = 60 μM *c9, t11* CLA (n=3), t10,c12 = 60 μM *t10, c12* CLA (n=3), MIX = 60 μM of a 50:50 mixture of *c9, t11* CLA and *t10, c12* CLA (n=3), LA + t10c12 = 60 μM of 50:50 mixture of linoleic acid and *t10, c12* CLA (n=4) and LA+c9,t11 = 60 μM mixture of a 50:50 mixture of linoleic acid and *c9, t11* CLA (n=4). Statistical differences among means ($p \leq 0.05$) are indicated by different lowercase letters.

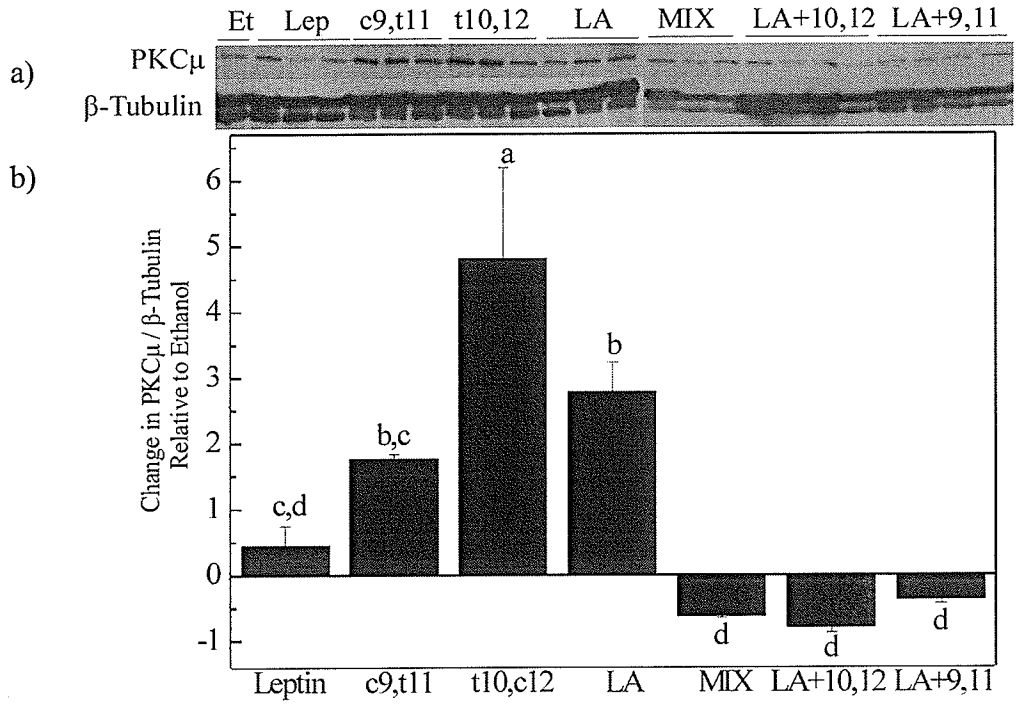

Figure 40: Change in protein kinase C-mu protein levels in mature 3T3-L1 adipocytes after 60 minutes of CLA treatment. Protein kinase C-mu (PKCμ) protein levels were measured from 3T3-L1 adipocytes at time points of 0 and 60 minutes by Western blot analysis. a) Representative Western blot at 1 hour b) Corresponding graph obtained by scanning densitometry of the bands in arbitrary units. Data were derived by calculating the ratio of PKCμ to β-tubulin which was expressed relative to the 0 hour time-point while all groups are expressed relative to ethanol, which was used as a vehicle control. Et = Ethanol (n=1), Lep = 6.25 nM leptin (n=3), LA = 60 μM linoleic acid (n=3), c9,t11 = 60 μM *c9, t11* CLA (n=3), t10,c12 = 60 μM *t10, c12* CLA (n=3), MIX = 60 μM of a 50:50 mixture of *c9, t11* CLA and *t10, c12* CLA (n=3), LA + t10c12 = 60 μM of 50:50 mixture of linoleic acid and *t10, c12* CLA (n=4) and LA+c9,t11 = 60 μM mixture of a 50:50 mixture of linoleic acid and *c9, t11* CLA (n=4). Statistical differences among means ($p \leq 0.05$) are indicated by different lowercase letters.

Atypical protein kinase C isoforms

Phospho-protein kinase C-zeta/lambda

Levels of phospho-protein kinase C-zeta/lambda (p-PKCζ/λ) were measured after a one hour treatment of the mature 3T3-L1 adipocytes with leptin, 60 μM *c9, t11* CLA, 60 μM *t10, c12 CLA*, 60 μM linoleic acid, 60 μM (50:50) mixture of *c9, t11* CLA and *t10, c12* CLA (MIX), 60 μM (50:50) mixture of linoleic acid and *t10, c12* CLA (LA + t10, c12) or linoleic acid and *c9, t11* CLA (LA + c9, t11) with ethanol being used as a vehicle control. Changes in p-PKCζ/λ over one hour were measured relative to the vehicle control. All treatment groups showed a decrease in the levels of p-PKCζ/λ after one hour (Figure 41). The leptin, *t10, c12* CLA or CLA-MIX treated cells had the smallest decrease in p-PKCζ/λ levels. The LA treatment relative to the vehicle control had a greater reduction in p-PKCζ/λ protein levels than CLA-MIX. The *c9, t11* CLA, LA + *c9, t11* CLA and LA + *t10, c12* CLA treated cells experienced the largest decrease in p-PKCζ/λ protein levels after one hour.

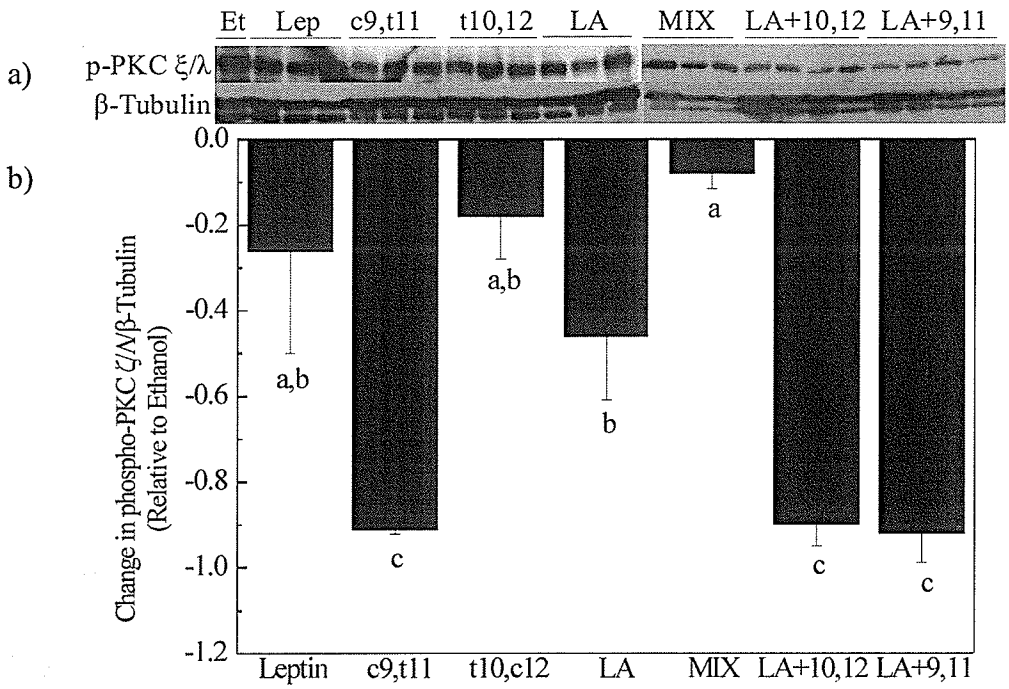

Figure 41: Change in protein kinase C-zeta/lambda phosphorylation at Thr410/403 in mature 3T3-L1 adipocytes after 60 minutes of CLA treatment. Protein kinase C-zeta/lambda (p-PKCζ/λ) phosphorylated at Thr410/403 protein levels were measured from 3T3-L1 adipocytes at time points of 0 and 60 minutes by Western blot analysis. a) Representative Western blot at 1 hour b) Corresponding graph obtained by scanning densitometry of the bands in arbitrary units. Data were derived by calculating the ratio of p-PKCζ/λ to β-tubulin which was expressed relative to the 0 hour time-point while all groups are expressed relative to ethanol, which was used as a vehicle control. Et = Ethanol (n=1), Lep = 6.25 nM leptin (n=3), LA = 60 μM linoleic acid (n=3), c9,t11 = 60 μM *c9, t11* CLA (n=3), t10,c12 = 60 μM *t10, c12* CLA (n=3), MIX = 60 μM of a 50:50 mixture of *c9, t11* CLA and *t10, c12* CLA (n=3), LA + t10c12 = 60 μM of 50:50 mixture of linoleic acid and *t10, c12* CLA (n=4) and LA+c9,t11 = 60 μM mixture of a 50:50 mixture of linoleic acid and *c9, t11* CLA (n=4). Statistical differences among means ($p \leq 0.05$) are indicated by different lowercase letters.

DISCUSSION

The goal of this thesis was to determine whether the depletion of adipose tissue and reduced insulin sensitivity that occurs from feeding *t10, c12* CLA is unique to mice or whether it is a genotype-specific effect that is dependent on having a functional leptin receptor. This was achieved by feeding *db/db* mice 0.4% *c9, t11* CLA or 0.4% *t10, c12* CLA and studying the effects on adiposity and insulin sensitivity. Mouse adipose tissue and 3T3-L1 adipocytes treated with CLA were also analyzed for levels of leptin, key mediators of insulin signalling and for the presence of various isoforms of protein kinase C that can be activated by fatty acids and alter lipid and glucose metabolism.

The main finding from this study was that *db/db* mice fed the *t10, c12* isomer of CLA stopped gaining weight immediately after starting the experimental diet (Figure 2). After six weeks, they had lost nearly all of their visceral adipose tissue (Figure 9) and weighed less than the lnCTL mice. The *db*PW mice, whose body weights were equivalent to the *db*t10, c12 mice had the same amount of visceral adipose tissue as the *db*CTL group. Despite the significant changes in body weight and adiposity, the weekly feed intake of the *db*t10, c12 group increased throughout the study and was significantly higher than the *db*c9, t11 mice but not the *db*CTL mice (Figure 4). Dietary intervention with the *c9, t11* CLA isomer did not lead to any changes in body weight or adiposity. HOMA-IR values were much higher in the *db/db* mice than the lean mice, although no changes in insulin resistance were seen between any of the *db/db* mice (Figure 12), despite changes in fasting insulin levels (Figure 11). Serum leptin levels were highest in the *db*c9, t11 group (Figure 15), but when corrected for amount of adipose tissue, leptin was significantly higher in the *db*t10, c12 mice (Figure 16). Leptin protein levels in

epididymal adipose tissue were analyzed by Western blotting and revealed highly elevated leptin protein levels in *t10, c12* CLA fed mice (Figure 17), despite a large reduction in adipose tissue. Likewise, reduced adiponectin protein levels in *db*t10,c12 (Figure 18) indicated adipocyte dysfunction.

This study is also one of the few to profile the PKC isoforms present in epididymal adipose tissue and to compare the levels between lean and *db/db* mice. It is also one of the first to show that CLA is able to change the levels of different PKC isoforms as well as their subcellular distribution in the epididymal adipose tissue of *db/db* mice (Table 4) and 3T3-L1 adipocytes (Table 5). These findings will be discussed in the following sections.

Effects on physical parameters of mice

The large decrease in body weight (Figure 4) and visceral adipose tissue (Figure 9) seen in the *db*t10, c12 mice was expected based on other mouse studies; how suddenly the changes in body weight occurred were, however, surprising. In the study by Hamura et al (2001), *db/db* mice fed mixed CLA-TGs showed similar changes in body weight to the mice in our study; however, feed intake was lower in the CLA-fed mice than the control *db/db* mice. In our study, the *db*t10, c12 group ate more as they lost weight. Unfortunately, the study by Hamura et al (2001) did not use a CLA-weight-matched group to determine if the changes in body composition and insulin sensitivity were due to the CLA-feeding or the decreased food intake and subsequent weight loss.

Visceral adipose tissue, which consists of the epididymal and peri-renal fat depots, is the rodent equivalent of omental fat in humans. An increase in the mass of this

tissue has been shown to correlate with the symptoms of the metabolic syndrome (3). The *db/db* mice had highly elevated visceral fat in both depots, however, the *t10, c12* CLA fed animals had amounts of peri-renal and epididymal fat that were equivalent to the fat depots of the lean mice when expressed as a percentage of body weight (Figure 8). Total visceral fat of the *db*t10, c12 mice was significantly lower than all of the other *db/db* mice as well as the lean mice. Because the visceral fat of the *db*PW mice, which had the same body weight as the *db*t10, c12 mice, did not differ from that of the *db*CTL group, it is reasonable to conclude that the *t10, c12* isomer of CLA specifically targets and reduces visceral adipose tissue in *db/db* mice.

Despite their decreased adiposity, the *db*t10, c12 mice also showed an increase in liver size and weight when expressed as a percentage of body weight, a change that was not seen in the *db*PW group (Figure 5). This is not a novel finding, as most CLA studies involving both lean and *ob/ob* mice have shown that feeding the *t10, c12* isomer or a 50:50 mixture of the *t10, c12* and *c9, t11* isomers results in an enlarged liver (9, 47, 48, 76). The livers of the mice remain to be tested to determine if the increase in liver mass of the *db*t10, c12 mice was due to increased lipid content. Other studies in mice have shown that the increase in liver mass is accompanied by an increase in liver triglyceride content (77). Alternatively, hepatomegaly could be induced if the *t10, c12* isomer is acting as a PPARα ligand which would also result in an increase in beta-oxidation in the liver (97). Hamsters fed an atherogenic diet with *t10, c12* CLA did not lose body fat, although they had increased liver weight without changes in liver composition. The livers of the *t10, c12* CLA fed hamsters showed increased expression and activity of acetyl-CoA carboxylase, the rate-limiting enzyme of fatty acid synthesis (96). The

authors hypothesized that the increase in liver size was due to hyperplasia and did not see any increase in any other lipogenic or target genes of PPARα in hamsters (96).

The *db*t10, c12 mice also exhibited an enlargement of the pancreas (Figure 6) when expressed as a percentage of body weight, an effect not seen when mice are fed a 50:50 mixture of CLA (77). Pancreatic β-cell hyperplasia in mice fed CLA has been suggested as a compensatory mechanism to increase insulin secretion if insulin sensitivity has been impaired (78). However, because *db/db* mice are already insulin-resistant, this compensatory mechanism is likely to have already taken place.

Effects on serum parameters

With the reduced adipose tissue of the *db*t10, c12 mice it would be reasonable to assume that they would have decreased serum triacylglycerides (TG); interestingly, the *db*c9, t11 mice had significantly lower TG levels than the *db*t10, c12 mice (Figure 13). Although neither group differed from the *db*CTL or *db*PW groups, all *db/db* mice had higher serum TGs than the lean mice. Mixed CLA triglycerides fed to *db/db* mice did not reduce serum TG levels in *db/db* mice as demonstrated by Hamura et al (2001). In *ob/ob* mice, feeding *t10, c12* CLA led to increased plasma triglycerides at various early time points. However, after 10 weeks, there were no significant differences in plasma triglycerides between control and CLA-fed *ob/ob* mice (47). Long-term studies where C57BL/6J mice were fed *t10, c12* CLA have shown a decrease in serum triglycerides, although this has also been accompanied by an increase in liver mass.

In order to study the degree of insulin resistance between the lean and *db/db* mice fed CLA, 6-hour fasting serum glucose and insulin levels were measured. Not

surprisingly, fasting glucose levels were significantly lower in the lean mice than the *db/db* mice; however, there were no differences between any of the *db/db* groups. The *db*c9, t 11 mice had higher fasting serum insulin levels than the lnCTL, *db*t10, c12 and *db*PW groups. When the glucose and insulin values for each group were employed to calculate the HOMA-IR, no difference was seen between any of the *db/db* mouse groups, indicating there was no improvement or worsening of insulin resistance (Figure 12).

Interestingly, the levels of the phosphorylated form of the p85α regulatory subunit of PI3- kinase was highly elevated in the adipose tissue of the *db/db* mice, especially in the CLA-fed mice (Figure 21). This has not been shown previously. Mice that lack p85α-PI3K are hypoglycaemic, have lower insulin levels and show increased glucose tolerance, which is thought to be due to upregulation of the catalytic subunits p50 and p55 (79). It has been previously demonstrated that increased PI3K activity does not necessarily result in an increase in Akt activity (80), which was confirmed by measuring the p-Akt levels of the epididymal fat of the *db/db* mice (Figure 19). This is because minimal activation of PI3K is required to activate Akt normally which leads to glucose transport in insulin-sensitive tissues. The highly elevated levels of p-p85α PI3K in the *db*CTL, *db*c9, t11 and *db*t10, c12 groups' adipose tissue and no change in p-Akt levels may be due to chronically high insulin levels, thereby hindering PI3K activation capability (32). The downstream target of PI3K, PDK-1 was also reduced in the epididymal adipose tissue of *db/db* mice (Figure 22); this is also indicative of reduced PI3K activity. An increase in p-p85α PI3K may reduce PI3K activity, making it incapable of generating the membrane bound lipid second messenger PI (3,4,5) P_3 which leads to the activation of Akt. The activation of Akt by insulin is essential for the proper storage of triglycerides and

production of adipokines by adipocytes, an ability which can be perturbed in conditions like T2DM (81).

Based on our results, the fasting epididymal adipose of *db/db* mice may not be efficiently signalling through PI3K – Akt and may be signalling through an alternative pathway, like PKCζ/λ which may promote the translocation of GLUT-4 to the cell membrane in order to enhance glucose uptake. Because the PI3K – PKCζ/λ – GLUT-4 pathway signals in parallel with PI3K – Akt in muscle and adipose tissue (81), it is reasonable to assume that the adipocytes are signalling in response to insulin through alternate pathways in *db/db* mice due to their altered glucose homeostasis and adipokine production.

Serum levels of the fat-derived hormone leptin are highly elevated in *db/db* mice compared to lean mice due to their lack of a functional leptin receptor and high levels of adipose tissue. Even with the severe ablation of adipose tissue, *db*t10, c12 mice still had serum leptin levels equivalent to both the *db*CTL and *db*PW mice (Figure 15). Interestingly, the *db*c9, t11 group had significantly higher serum leptin levels than all other groups. An increase in leptin production is usually indicative of increased adipose tissue mass, however, no differences were seen between the *db*c9, t11 or *db*CTL groups in adipose tissue mass (Figure 8a-d). The *c9, t11* CLA isomer may be able to signal to the adipose tissue to secrete leptin at a higher level. Unfortunately we did not analyze the subcutaneous fat depot, because leptin is produced at a higher level from subcutaneous adipose at a greater rate than visceral fat (85). Further investigation into the ability of *c9, t11* CLA to elevate serum leptin levels, even in a state of hyperleptinemia is required

to help understand the reason for this adaptation. Perhaps it is indicative of an improved ability of the adipose tissue to secrete leptin more efficiently.

When the serum leptin levels were divided by the mass of epididymal or peri-renal fat depots, leptin levels of the *db*t10, c12 were higher than all other groups (Figure 16). After this adjustment there was no difference between the *db*CTL, *db*PW or *db*c9, t11 groups. Because of the decrease in adipose tissue that occurs from feeding mice CLA, most studies have a reported a decrease in serum leptin levels (78). However, because leptin is secreted primarily from adipose tissue it is important to consider the amount of adipose tissue present.

The lipoatrophy and increased liver mass seen in the *db*t10, c12 mice resembles a condition known as lipodystrophy, where fat is redistributed to the liver, muscle or other organs resulting in insulin resistance. The depletion of adipose tissue is accompanied by a reduction in serum leptin; fortunately, many of the symptoms associated with lipodystrophy can usually be reversed with leptin therapy (82). The *db*t10, c12 group lost the majority of their white adipose tissue, however they were still able to preserve serum leptin levels equivalent to the *db*CTL and *db*PW (Figure 15) which may have prevented the level of insulin sensitivity from worsening. Even though *ob/ob* mice and *db/db* mice have similar phenotypes, *db/db* mice already have high circulating levels of leptin whereas *ob/ob* mice cannot produce leptin at all. In *ob/ob* mice, leptin infusion is able to prevent CLA induced insulin resistance; however, the added leptin does lead to hepatic steatosis (46). Because the fat content of the livers of the *db*t10, c12 group were not analyzed, we cannot conclude whether the *db*t10, c12 mice suffered from hepatic steatosis or hepatomegaly.

Leptin administration in streptozotocin-induced diabetic and non-obese diabetic (NOD) mice has been shown to reduce the symptoms of type 1 diabetes (T1DM) and allow these mouse models to survive, even without being able to produce insulin (83). In the same model of T1DM, streptozotocin-induced diabetic mice, which are characterized by insufficient insulin production, high serum TGs and low liver glycogen and TG storage, *t10, c12* CLA reversed these symptoms in the absence of insulin (98). There appears to be a strong relationship between *t10, c12* CLA and adequate adipokine and leptin production that may help to further explain the role that adipose tissue plays in influencing insulin sensitivity, glucose and lipid metabolism.

Effects on adipose tissue parameters

Levels of proteins present in the epididymal adipose tissue of lean and *db/db* mice were identified by Western blotting. Similar to the high levels of serum leptin seen in the *db*t10, c12 group (when adjusted for body weight); leptin levels in the epididymal adipose tissue of the *db*t10, c12 were significantly higher than that of the lean and *db/db* mice (Figure 17). This is the first study to show that in *db/db* mice, *t10, c12* CLA increases leptin levels in epididymal adipose tissue, despite significant decreases in the size of the fat depots and an overnight fast, both of which decrease leptin biosynthesis by adipose tissue. This is the opposite of what would be expected, as a decrease in fat pad mass should lead to decreased leptin production as an indicator of decreased energy intake and fat loss and a signal to increase feeding. Because the *db/db* mice fed *t10,* c12 CLA were increasing their feed intake as they lost weight, CLA may be acting as a signalling molecule that can alter both the secretion and synthesis of leptin by adipose tissue. The increase in epididymal fat leptin protein levels (Figure 17) may be an attempt

to keep the serum levels of leptin constant as the primary leptin secretory organs are being depleted. Pigs fed CLA had decreased expression of the leptin gene as well as a decrease in leptin protein levels in the subcutaneous adipose tissue (84). Although a CLA mixture was used, subcutaneous adipose tissue has been shown to secrete more leptin than the other adipose tissue depots (85); it is also likely that there are differences in leptin production and secretion between adipose depots in response to CLA.

Leptin is secreted from adipocytes in a pulsatile fashion; over a period of 24 hours, leptin levels tended to build up in the cells and then decrease (59). For the cell culture work, it could be assumed that leptin is being secreted into the media by the adipocytes after which, leptin levels would build up again in the adipocytes before being secreted again. After one hour, the leptin levels of mature 3T3-L1 adipocytes decreased slightly with all treatments compared to the vehicle treated (ethanol) control adipocytes (Figure 34). After two hours, the cells treated with 60 μM of a 50:50 mixture of linoleic acid and the *t10, c12* isomer of CLA had a 4-fold increase in cellular leptin levels compared to the 60 μM *c9, t11* CLA treated cells; all other treatments were lower than the vehicle control treated cells. Leptin treated cells did not show any difference in cellular leptin levels at any of the other time points (Figure 34). The increased levels of leptin seen in the *t10, c12* CLA treated 3T3-L1 adipocytes was similar to what was seen in the epididymal adipose tissue of the *db*t10, c12 mice. By 24 hours, cells treated with *t10,* c12 CLA contained less leptin compared to the zero time point. Treatment of primary rat adipocytes with 50 μM CLA for 96 hours decreased leptin mRNA expression and attenuated both basal and insulin-stimulated leptin secretion (59). This is interesting as insulin increases leptin expression in 3T3-L1 adipocytes while leptin secretion

increases throughout differentiation (86). Secretion of leptin from 3T3-L1 adipocytes has also been shown to be decreased after a 24-hour treatment with 100 μM of *t10, c12* CLA; this study also showed a decrease in leptin mRNA expression in peri-renal fat and serum leptin of mice fed the same isomer (56). These differences when compared to our study could be due to the fat depot analyzed or the concentration of CLA used. Although these studies did not analyze leptin protein levels, there may be a difference between the levels of protein and mRNA, or even an impairment of the secretion of leptin from adipocytes that are treated with *t10, c12* CLA. The resulting leptin accumulation could occur because exogenous leptin is required for down-regulation of leptin production (87). The study by Kang et al (2001), however, did not show any changes in feed intake with the *t10, c12* CLA fed mice after 4 weeks of feeding whereas the *db/db* mice were continually increasing their feed intake as their adipose tissue was depleted (Figure 3).

After one hour, phosphorylation of STAT-3 at Tyr705 was the same in leptin, LA or *t10, c12* CLA treated 3T3-L1 adipocytes; whereas p-STAT-3 levels were significantly decreased in the 3T3-L1 adipocytes treated with *c9, t11* CLA (Figure 35). Levels of p-STAT-3 in the adipose tissue of the *db/db* mice were significantly higher in the epididymal adipose tissue of *db*c9, t11 mice than in *db*t10, c12 mice (Figure 19), a difference which could be explained by the higher levels of serum leptin in the *db*CTL and *db*c9, t11 mice. To our knowledge, this is the first study to look at the activation of STAT-3, an important component of ObRb signalling that could potentially be modified by CLA in adipose tissue and adipocytes, even in the absence of a fully functional leptin receptor, as is seen in the *db/db* mice.

Activation of protein kinase C in adipose tissue and 3T3-L1 adipocytes

With an increase in lipid availability, activation of PKC can result in dysregulated phosphorylation of cell surface receptors and key mediators of insulin signalling, which in turn can lead to the impaired insulin response commonly seen in obesity and T2DM. Levels of the lipid regulated PKCs, epsilon and mu, were both increased in mature 3T3-L1 adipocytes after the 1-hour incubation with 60 μM of *t10, c12* CLA (Figure 39, 40). In contrast, levels of phosphorylated PKCα/β_{II} decreased significantly due to *t10, c12* CLA, in both 3T3-L1 adipocytes as well as in the *db/db* mice (Figure 26 + 38), despite an increase in PKCα and PKCβ_I after a one hour CLA treatment in the 3T3-L1 adipocytes (Figure 36 + 37). Levels of phospho-PKC ζ/λ were higher after a 1-hour treatment with *t10, c12 CLA* than the *c9, t11* CLA treated cells (Figure 41).

Not only do the levels of PKC differ between mouse genotypes and dietary treatments (CLA) in adipose tissue and in the 3T3-L1 adipocytes, but the subcellular distribution of PKCs also varies according to genotype, dietary treatment and metabolic state (fasting). It has been well-documented that the activation of PKC (ratio of membrane to cytosolic form) varies between tissues (88). This is the first study to examine both the levels of PKC in epididymal fat and their subcellular distribution in a 6 hour fasting state as well as in 3T3-L1 adipocytes treated with leptin, CLA or linoleic acid.

The cytosolic to particulate ratio of PKCβ_I, PKCβ_{II} and PKCε has been shown to decrease in the adipose tissue of aging Sprague-Dawley rats (6-weeks vs. 6-months) (89). Despite their elevated serum TGs, obese *fa/fa* Zucker rats do not show any difference in epididymal fat PKC when compared to their lean counterparts (*fa/+*). However, in the

fed-state, PKCθ and PKCε membrane fraction levels are significantly increased in the muscle tissue of *fa/fa* Zucker rats (90). Recent studies using PKCε -/- mice, which lack PKCε in all tissues, have revealed that a challenge with a high fat diet show improved glucose homeostasis during intraperitoneal glucose tolerance tests. Similarly, a PKCε inhibitory peptide (εV1-2) injected for 5 days into *db/db* mice improved glucose control during intraperitoneal glucose tolerance tests (91). This may be due to increased pancreatic TG lipolysis resulting in improved insulin secretion. Interestingly, PKCε protein levels were elevated in the epididymal adipose tissue of *db/db* mice fed *t10, c12* CLA (Figure 28) as well as 3T3-L1 adipocytes treated with 60 μM *t10, c12* CLA for one hour (Figure 39). As an extracellularly regulated kinase that can be activated by lipids, PKCε could be activated by *t10, c12* CLA resulting in a worsening of glucose and lipid homeostasis and reduced ability to store TGs properly in adipocytes or it could be a side-effect that occurs as a result of these conditions. Further studies involving PKCε inhibitors and identification of the phosphorylation targets of PKCε in adipose, liver, muscle and pancreatic tissue will be important in elucidating the role that PKCε plays in influencing glucose and lipid metabolism.

PKCθ is another PKC isoform that is activated by increased lipid availability. In short-term studies, PKCθ knock-out mice are resistant to the impaired insulin signalling in muscle tissue that would normally accompany a high-fat diet challenge. Long-term, high-fat feeding studies involving PKCθ knock-out mice fail to show the same protective effect on insulin signalling, likely indicating that there is a threshold to the protective-effect offered by limiting PKCθ activity (99). The *db/db* mice fed *t10, c12* CLA had a significantly lower cytosolic-membrane ratio of PKCθ (Figure 30) indicating increased

activity compared to the lnCTL. The whole cell adipose tissue fractions of *c9, t11* CLA fed mice had higher levels of PKCθ compared to the *t10, c12* CLA fed mice. The observed changes and the diversity of results coupled with the dynamic nature of PKC add to the complexity in interpreting how these enzymes influence glucose and lipid metabolism. Very little research has gone into exploring the levels of PKC specifically in adipose tissue, despite being an insulin-sensitive tissue that play a large role in the progression of T2DM. CLA could be modulating the different classes of PKC isoforms in opposing ways.

The significance of these findings is unknown at the moment; however, the knowledge that these kinases can be modulated in their levels as well as their subcellular distribution due to genotype or from dietary manipulation should be further explored. The activation of various PKCs in adipocytes in response to insulin after being incubated with CLA as well as exploring their targets of phosphorylation will be important steps to fully elucidate the mechanisms and role that PKCs and CLA play in adipose tissue metabolism.

CONCLUSION

The ability of CLA to reduce adipose tissue in mice is well documented in a variety of genotypes. While it has been shown to reduce adipose tissue slightly in rats and humans, the changes are nowhere near as profound as those seen in mice. This study further confirms that there is a species-specific effect given that the *db/db* mice fed CLA as part of a low fat diet had increased liver, kidney and pancreatic mass along with the ablation of adipose tissue. Although there was no worsening of insulin resistance in *db/db* mice fed *t10, c12* CLA, there is evidence that the normal activation of a variety of PKC isoforms in the epididymal adipose tissue of *db/db* mice may be altered by CLA. Because there is limited data on how PKC from adipose tissue can influence, or be influenced by diet and metabolism, the role that PKC plays in preventing insulin resistance in an obesogenic environment remains to be elucidated. Our unique results indicate that leptin protein levels are elevated the epididymal adipose tissue of *db/db* mice that have undergone significant weight loss as a result of feeding *t10, c12* CLA. Clarification of the cellular signalling mechanisms that influence the production and secretion of leptin in adipose tissue may be a key to understanding the mechanism of how CLA is altering adipose tissue metabolism in mice.

SUMMARY OF MAIN FINDINGS

Genotype effect

Differences observed between lean mice and *db/db* mice fed a 0% CLA diet

- greater body weight and feed intake in *db/db* mice
- greater peri-renal, epididymal and total visceral mass in *db/db* mice
- total liver mass and liver weight as a percentage of body weight in *db/db* mice
- kidney mass is greater in *db/db* mice
- higher fasting glucose and insulin concentrations and HOMA-IR values in *db/db* mice
- higher serum triacyglyceride and total cholesterol concentrations in *db/db* mice
- higher serum leptin concentration in *db/db* mice
- higher protein levels of p-STAT-3 in epididymal adipose tissue in *db/db* mice.
- greater protein levels of p-p85 PI3K levels in epididymal adipose tissue of *db/db* mice.
- reduced protein levels of PKCβI and p-PKCα/βII in epididymal adipose tissue of *db/db* mice

No effect. No genotype differences in pancreas mass or leptin, ACRP30, p-Akt, p-PDK-1 protein levels in epididymal adipose tissue. No difference in PKCα, PKCδ, PKCε, PKCθ, PKCμ or p-PKCζ/λ protein levels in epididymal adipose tissue.

Diet effect

Differences observed among *db*c9, t11; *db*t10, c12 and *db*CTL mice:

- lower body weight, epididymal and peri-renal adipose tissue as a percentage of body weight in *t10, c12* CLA fed *db/db* mice compared to the *db*CTL and *db*c9,t11 groups
- higher serum leptin concentrations in *c9, t11* CLA fed *db/db* mice than all other *db/db* mice
- greater serum leptin concentrations per mg of peri-renal and epididymal adipose tissue in *t10, c12* CLA fed *db/db* mice than all other groups
- higher levels of leptin protein in epididymal adipose tissue of *db/db* mice fed *t10, c12* CLA
- higher levels of p-p85 PI3K in epididymal adipose tissue of *db/db* mice fed *t10, c12* CLA than all other *db/db* mice
- lower p-PDK-1 protein levels in epididymal adipose tissue of *db/db* mice fed *t10, c12* CLA and *db*PW group compared to all other *db/db* mice
- lower protein levels of p-PKCα/βII in epididymal adipose tissue in *db/db* mice fed *t10, c12* CLA although no difference compared to *db*PW. Mice fed *c9, t11* CLA have significantly higher levels of p-PKCα/βII compared to *db*t10, c12 and *db*PW groups.
- greater protein levels of PKCε in epididymal adipose tissue of *db/db* mice fed *t10, c12* CLA than all other groups

Effect of CLA on 3T3-L1 adipocytes

- increased leptin levels of 3T3-L1 adipocytes treated with 60 μM of linoleic acid + *t10, c12* CLA after 120 minutes

- PKCα, PKCβI, p-PKCα/βII, PKCε, PKCμ and p-PKCζ/λ are present in 3T3-L1 adipocytes
- after one hour, 3T3-L1 adipocytes treated with 60 μM of *c9, t11* CLA, *t10, c12* CLA or LA had higher PKCα levels compared to leptin, MIX-CLA, LA + *t10, c12* CLA or LA + *c9, t11* CLA
- after one hour, 3T3-L1 adipocytes treated with leptin, 60 μM of *c9, t11* CLA, *t10, c12* CLA had higher PKCβI levels compared to 60 μM of LA + *c9, t11* CLA or LA + *t10, c12* CLA
- after one hour, 3T3-L1 adipocytes treated with 60 μM of *c9, t11* CLA had higher levels of p-PKCα/βII levels compared to 60 μM of *t10, c12* CLA, MIX-CLA, LA + *t10, c12* CLA or LA + *c9, t11* CLA
- after one hour, 3T3-L1 adipocytes treated with 60 μM of *t10, c12* CLA had higher PKCε levels than those treated with leptin, 60 μM *c9, t11* CLA, LA, MIX-CLA, LA + *t10, c12* CLA or LA + *c9, t11* CLA
- after one hour, 3T3-L1 adipocytes treated with 60 μM of *t10, c12* CLA had higher PKCμ levels than those treated with leptin, 60 μM *c9, t11* CLA, LA, MIX-CLA, LA + *t10, c12* CLA or LA + *c9, t11* CLA
- after one hour, 3T3-L1 adipocytes treated with 60 μM of MIX- CLA had higher levels of p-PKCζ/λ levels compared to 60 μM of *c9, t11* CLA, LA, LA + *t10, c12* CLA or LA + *c9, t11* CLA

STRENGTHS AND LIMITATIONS

- Animal model. *Strength.* The *db/db* mouse has been shown to be a suitable model for T2DM and obesity and at 7 weeks of age the mice used in this study were already obese and by the end of the study were insulin resistant (HOMA-IR) with elevated serum triacylglycerides, cholesterol and leptin concentrations compared to the lean C57BLKS/J mice (*db/+*). Even though both *fa/fa* Zucker rats and *db/db* mice display a similar phenotype that is the result of a faulty ObRb, the effects of CLA on these two animal models are quite different. This is important as it further confirms the varied results between species fed CLA by using different species with the same mutation. *Limitation.* The mutation of the *diabetes* gene that leads to a dysfunctional leptin receptor in mice is very rare in humans, which makes it difficult to extrapolate the findings of this study for application in humans. However, many of the metabolic and physiological changes that occur in T2DM and obesity, including hyperleptinemia, which can occur in a leptin resistant state, are present in the *db/db* mouse.
- Gender. *Strength.* Since the analysis of leptin levels was fundamental to this study, male mice were used because their leptin production does not vary due to a menstrual cycle. Female humans have been shown to have higher fasting plasma leptin levels that do not correlate with the hypertension or insulin resistance when corrected for BMI, while they do with men (92, 93). Leptin levels also vary with the menstrual cycle and increase with the rise in progesterone during the luteal phase (94), which would make it difficult to interpret changes in serum leptin concentrations as being solely from the diet. *Limitations.* It is more difficult to

extrapolate the results of this study to female mice as the effects of CLA on leptin levels and adipose tissue metabolism may be different due to increased leptin concentrations.

- Use of weight-matched and lean control groups. *Strength.* The use of a weight-matched group was useful for confirming that the changes in white adipose tissue, liver, pancreas, kidneys and the serum parameters were due to CLA and not simply from the weight loss incurred by restricting the food intake of the *db*PW group. The use of a lean control group from the same background strain was important for comparing the differences between lean and obese/diabetic mice. *Limitations.* It was difficult to restrict the feed intake of the weight-matched group fast enough to parallel the body weight loss of the *db*t10,c12 group. The *db*PW group would eat their feed allotment in one meal as opposed to spreading out their feed intake throughout the day. At the end of the study, this could have resulted in an altered metabolic state for the *db*PW group after fasting for more than 20 hours, as opposed to 6 hours for the other groups. The *db*PW group did not have the same body composition as *db*t10,c12 even though they have similar body weights.
- Use of single isomers. *Strength.* This allowed us to differentiate the effects of *c9, t11* and *t10, c12* CLA on *db/db* mice. *Limitations.* An additional group with a 50:50 mixture of the *c9, t11* and the *t10, c12* CLA isomers would have been useful because most commercially available CLA supplements contain equal amounts of each of these isomers.

- HOMA-IR. *Strength.* The homeostasis model assessment for insulin resistance (HOMA-IR), which uses fasting serum glucose and insulin concentrations, has been shown to correlate with both euglycemic and hyperglycemic clamp studies which are considered to be the "gold standard" for measuring insulin sensitivity (74). This makes HOMA-IR a suitable model calculation for assessing the level of insulin resistance between the lean and *db/db* mice and effects of diet interventions such as CLA. *Limitations.* The HOMA-IR has only been validated for humans and its applicability to mouse studies may not be ideal. Having measurements of fasting insulin or glucose levels of the mice prior to beginning the study or any other time points prior to termination would be helpful to determine if there were any changes in insulin sensitivity throughout the study from the dietary treatments.
- PKC activation and isoforms. *Strength.* This is the first study to do comprehensive analyses of PKC isoforms in adipose tissue in relation to obesity and insulin resistance. Isoforms of PKC from all three classes (conventional, novel and atypical) were found in both adipose tissue and in 3T3-L1 adipocytes. While not all isoforms were found or investigated, all three classes of isoforms, which all require different cellular conditions for activation, were indeed present in adipocytes at varying levels between genotypes and treatment groups. *Limitations.* The one-hour time point of the 3T3-L1 adipocytes treated with CLA is likely not the key time point for peak activation of these PKCs and further investigation examining subcellular distribution at various time points after treatment with CLA should be explored.

- Cell culture model. *Strength.* 3T3-L1 adipocytes are a mouse derived adipocyte cell line that offers much flexibility for exploring the effects of CLA on leptin and PKC in a variety of conditions. This cell model allowed us to compare the effects of CLA on adipocytes with a functional leptin receptor to the adipose tissue with a dysfunctional leptin receptor of the *db/db* mice. *Limitations.* The 3T3-L1 adipocytes are not from *db/db* mice, which means that there may be a different response to CLA than what might occur in primary adipocytes. CLA that is ingested by *db/db* mice for 6 weeks has to be digested, absorbed and metabolized before reaching adipose tissue which may result in a much different response than when adipocytes are treated with CLA for 24 hours or less.

FUTURE DIRECTIONS

- Investigate the effects of CLA on *db/db* and lean mice fed a higher fat diet to see if the higher fat can help prevent excess depletion of adipose tissue
- Increase the length of time of the dietary treatment to see whether or not the weight loss observed in *t10, c12* CLA fed mice persists longer than 6 weeks
- Explore PKC isoform distribution in adipose tissue of mice in both the fed and fasted states
- Investigate leptin, ACRP30, insulin signalling mediators or PKC mRNA levels for comparison with protein levels detected in adipose tissue and adipocytes
- Compare the effects of CLA feeding in lean and *db/db* mice on protein levels and mRNA levels in various adipose tissue depots including peri-renal and subcutaneous
- Instead of 3T3-L1 adipocytes which have a functional long-form leptin receptor, treat primary adipocytes from *db/db* mice with CLA and compare to adipocytes from lean mice
- Treat primary adipocytes from *db/db* and *ob/ob* mice and *fa/fa* Zucker rats with CLA in order to compare treatments on leptin protein levels, mRNA expression and PKC activation between different species with functional and non-functional leptin receptors.
- Investigate the potential PKC phosphorylation substrates in epididymal adipose tissue of CLA fed mice and adipocytes treated with CLA
- Analyze activation of insulin signalling mediators in response to insulin in primary mouse adipocytes and 3T3-L1 adipocytes incubated with CLA

- Analyze triglyceride content of adipose and liver tissue as well as serum free fatty acids of *db/db* and lean mice
- Utilize PKC knock-out models to determine the significance of PKC on the mechanism whereby CLA effects body fat in mice
- Treat adipocytes with CLA as well as PKC inhibitors to determine the direct effect of CLA on adipocyte size, function and leptin levels due to PKC activity

IMPLICATIONS

Our research has shown that dietary intervention with *t10, c12* CLA for six weeks results in a great reduction of white adipose tissue in obese *db/db* mice lacking a functional leptin receptor, however, the usual worsening of insulin resistance seen in other mouse genotypes fed CLA did not occur. Interestingly, liver, pancreas and kidney mass when expressed as a percentage of body weight is higher in *db/db* mice fed *t10, c12* CLA. Our data further suggest that with a low fat diet, mice respond differently to CLA than rats with a similar genotype. This study is also the first to show that PKC isoforms from all three classes are present in the epididymal adipose tissue of lean and obese mice and that their activity can potentially be modulated by dietary intervention with CLA. Our data suggest that further research is required to fully elucidate the mechanism of action of CLA on adipose tissue metabolism and its subsequent effects on insulin sensitivity so that its safety can be fully confirmed.

REFERENCES

1. Anis AH, Zhang W, Bansback N, Guh DP, Amarsi Z, Birmingham CL. Obesity and overweight in canada: An updated cost-of-illness study. Obes Rev. 2009 Apr 1.

2. Bloomgarden ZT. Type 2 diabetes in the young: The evolving epidemic. Diabetes Care. 2004 Apr;27(4):998-1010.

3. Despres JP, Arsenault BJ, Cote M, Cartier A, Lemieux I. Abdominal obesity: The cholesterol of the 21st century? Can J Cardiol. 2008 Sep;24 Suppl D:7D-12D.

4. Thamer C, Machann J, Stefan N, Haap M, Schafer S, Brenner S, et al. High visceral fat mass and high liver fat are associated with resistance to lifestyle intervention. Obesity (Silver Spring). 2007 Feb;15(2):531-8.

5. Gabriely I, Ma XH, Yang XM, Atzmon G, Rajala MW, Berg AH, et al. Removal of visceral fat prevents insulin resistance and glucose intolerance of aging: An adipokine-mediated process? Diabetes. 2002 Oct;51(10):2951-8.

6. Riserus U, Arner P, Brismar K, Vessby B. Treatment with dietary trans10cis12 conjugated linoleic acid causes isomer-specific insulin resistance in obese men with the metabolic syndrome. Diabetes Care. 2002 Sep;25(9):1516-21.

7. Noto A, Zahradka P, Ryz NR, Yurkova N, Xie X, Taylor CG. Dietary conjugated linoleic acid preserves pancreatic function and reduces inflammatory markers in obese, insulin-resistant rats. Metabolism. 2007 Jan;56(1):142-51.

8. Roche HM, Noone E, Sewter C, Mc Bennett S, Savage D, Gibney MJ, et al. Isomer-dependent metabolic effects of conjugated linoleic acid: Insights from molecular markers sterol regulatory element-binding protein-1c and LXR alpha. Diabetes. 2002 Jul;51(7):2037-44.

9. Tsuboyama-Kasaoka N, Takahashi M, Tanemura K, Kim HJ, Tange T, Okuyama H, et al. Conjugated linoleic acid supplementation reduces adipose tissue by apoptosis and develops lipodystrophy in mice. Diabetes. 2000 Sep;49(9):1534-42.

10. Wang P, Mariman E, Renes J, Keijer J. The secretory function of adipocytes in the physiology of white adipose tissue. J Cell Physiol. 2008 Jul;216(1):3-13.

11. Waki H, Tontonoz P. Endocrine functions of adipose tissue. Annu Rev Pathol. 2007;2:31-56.

12. Ahima RS. Adipose tissue as an endocrine organ. Obesity (Silver Spring). 2006 Aug;14 Suppl 5:242S-9S.

13. Hajer GR, van Haeften TW, Visseren FL. Adipose tissue dysfunction in obesity, diabetes, and vascular diseases. Eur Heart J. 2008 Sep 5.

14. Zhang Y, Proenca R, Maffei M, Barone M, Leopold L, Friedman JM. Positional cloning of the mouse obese gene and its human homologue. Nature. 1994 Dec 1;372(6505):425-32.

15. Harris RB, Mitchell TD, Yan X, Simpson JS, Redmann SM,Jr. Metabolic responses to leptin in obese db/db mice are strain dependent. Am J Physiol Regul Integr Comp Physiol. 2001 Jul;281(1):R115-32.

16. van Dielen FM, van 't Veer C, Buurman WA, Greve JW. Leptin and soluble leptin receptor levels in obese and weight-losing individuals. J Clin Endocrinol Metab. 2002 Apr;87(4):1708-16.

17. Lahlou N, Clement K, Carel JC, Vaisse C, Lotton C, Le Bihan Y, et al. Soluble leptin receptor in serum of subjects with complete resistance to leptin: Relation to fat mass. Diabetes. 2000 Aug;49(8):1347-52.

18. Eiras S, Camina JP, Diaz-Rodriguez E, Gualillo O, Casanueva FF. Leptin inhibits lysophosphatidic acid-induced intracellular calcium rise by a protein kinase C-dependent mechanism. J Cell Physiol. 2004 Nov;201(2):214-26.

19. Lafontan M. Fat cells: Afferent and efferent messages define new approaches to treat obesity. Annu Rev Pharmacol Toxicol. 2005;45:119-46.

20. Fruhbeck G. Intracellular signalling pathways activated by leptin. Biochem J. 2006 Jan 1;393(Pt 1):7-20.

21. Zhang F, Chen Y, Heiman M, Dimarchi R. Leptin: Structure, function and biology. Vitam Horm. 2005;71:345-72.

22. Emilsson V, Arch JR, de Groot RP, Lister CA, Cawthorne MA. Leptin treatment increases suppressors of cytokine signalling in central and peripheral tissues. FEBS Lett. 1999 Jul 16;455(1-2):170-4.

23. Ueki K, Kondo T, Tseng YH, Kahn CR. Central role of suppressors of cytokine signalling proteins in hepatic steatosis, insulin resistance, and the metabolic syndrome in the mouse. Proc Natl Acad Sci U S A. 2004 Jul 13;101(28):10422-7.

24. Myers Jr MG, White MF. The molecular basis of insulin action. In: Insulin Signalling From Cultured Cells to Animal Models. Taylor & Francis; 2002.

25. Capeau J. Insulin signalling: Mechanisms altered in insulin resistance. Med Sci (Paris). 2003 Aug-Sep;19(8-9):834-9.

26. Welsh N, Makeeva N, Welsh M. Overexpression of the shb SH2 domain-protein in insulin-producing cells leads to altered signalling through the IRS-1 and IRS-2 proteins. Mol Med. 2002 Nov;8(11):695-704.

27. Yamada T, Katagiri H, Asano T, Tsuru M, Inukai K, Ono H, et al. Role of PDK1 in insulin-signalling pathway for glucose metabolism in 3T3-L1 adipocytes. Am J Physiol Endocrinol Metab. 2002 Jun;282(6):E1385-94.

28. Dokken BB, Sloniger JA, Henriksen EJ. Acute selective glycogen synthase kinase-3 inhibition enhances insulin signalling in prediabetic insulin-resistant rat skeletal muscle. Am J Physiol Endocrinol Metab. 2005 Jun;288(6):E1188-94.

29. Eldar-Finkelman H, Schreyer SA, Shinohara MM, LeBoeuf RC, Krebs EG. Increased glycogen synthase kinase-3 activity in diabetes- and obesity-prone C57BL/6J mice. Diabetes. 1999 Aug;48(8):1662-6.

30. Kandror KV, Pilch PF. Isolation of GLUT4 storage vesicles. Curr Protoc Cell Biol. 2006 Apr;Chapter 3:Unit 3.20.

31. Lizcano JM, Alessi DR. The insulin signalling pathway. Curr Biol. 2002 Apr 2;12(7):R236-8.

32. Pessin JE, Saltiel AR. Signalling pathways in insulin action: Molecular targets of insulin resistance. J Clin Invest. 2000 Jul;106(2):165-9.

33. Hennige AM, Stefan N, Kapp K, Lehmann R, Weigert C, Beck A, et al. Leptin down-regulates insulin action through phosphorylation of serine-318 in insulin receptor substrate 1. FASEB J. 2006 Jun;20(8):1206-8.

34. Grunberger G, Zick Y. Insulin signalling : From cultured cells to animal models. London ; New York: Taylor & Francis; 2002.

35. Silveira MB, Carraro R, Monereo S, Tebar J. Conjugated linoleic acid (CLA) and obesity. Public Health Nutr. 2007 Oct;10(10A):1181-6.

36. Dhiman TR, Nam SH, Ure AL. Factors affecting conjugated linoleic acid content in milk and meat. Crit Rev Food Sci Nutr. 2005;45(6):463-82.

37. Hamura M, Yamatoya H, Kudo S. Glycerides rich in conjugated linoleic acid (CLA) improve blood glucose control in diabetic C57BLKS-Leprdb/leprdb mice. Journal of Oleo Science. 2001;50(11):889-894.

38. Pariza MW, Ashoor SH, Chu FS, Lund DB. Effects of temperature and time on mutagen formation in pan-fried hamburger. Cancer Lett. 1979 Jul;7(2-3):63-9.

39. Pariza MW. Perspective on the safety and effectiveness of conjugated linoleic acid. Am J Clin Nutr. 2004 Jun;79(6 Suppl):1132S-6S.

40. Whigham LD, Watras AC, Schoeller DA. Efficacy of conjugated linoleic acid for reducing fat mass: A meta-analysis in humans. Am J Clin Nutr. 2007 May;85(5):1203-11.

41. Kamphuis MM, Lejeune MP, Saris WH, Westerterp-Plantenga MS. Effect of conjugated linoleic acid supplementation after weight loss on appetite and food intake in overweight subjects. Eur J Clin Nutr. 2003 Oct;57(10):1268-74.

42. Ryder JW, Portocarrero CP, Song XM, Cui L, Yu M, Combatsiaris T, et al. Isomer-specific antidiabetic properties of conjugated linoleic acid. improved

glucose tolerance, skeletal muscle insulin action, and UCP-2 gene expression. Diabetes. 2001 May;50(5):1149-57.

43. Noto A, Zahradka P, Yurkova N, Xie X, Truong H, Nitschmann E, et al. Dietary conjugated linoleic acid decreases adipocyte size and favorably modifies adipokine status and insulin sensitivity in obese, insulin-resistant rats. Metabolism. 2007 Dec;56(12):1601-11.

44. Moloney F, Yeow TP, Mullen A, Nolan JJ, Roche HM. Conjugated linoleic acid supplementation, insulin sensitivity, and lipoprotein metabolism in patients with type 2 diabetes mellitus. Am J Clin Nutr. 2004 Oct;80(4):887-95.

45. Moloney F, Toomey S, Noone E, Nugent A, Allan B, Loscher CE, et al. Antidiabetic effects of cis-9, trans-11-conjugated linoleic acid may be mediated via anti-inflammatory effects in white adipose tissue. Diabetes. 2007 Mar;56(3):574-82.

46. Wendel AA, Purushotham A, Liu LF, Belury MA. Conjugated linoleic acid fails to worsen insulin resistance but induces hepatic steatosis in the presence of leptin in *ob/ob* mice. J Lipid Res. 2008 Jan;49(1):98-106.

47. Wargent E, Sennitt MV, Stocker C, Mayes AE, Brown L, O'Dowd J, et al. Prolonged treatment of genetically obese mice with conjugated linoleic acid improves glucose tolerance and lowers plasma insulin concentration: Possible involvement of PPAR activation. Lipids Health Dis. 2005 Jan 10;4:3.

48. Purushotham A, Wendel AA, Liu LF, Belury MA. Maintenance of adiponectin attenuates insulin resistance induced by dietary conjugated linoleic acid in mice. J Lipid Res. 2007 Feb;48(2):444-52.

49. White BD, Martin RJ. Evidence for a central mechanism of obesity in the zucker rat: Role of neuropeptide Y and leptin. Proc Soc Exp Biol Med. 1997 Mar;214(3):222-32.

50. Henriksen EJ, Teachey MK, Taylor ZC, Jacob S, Ptock A, Kramer K, et al. Isomer-specific actions of conjugated linoleic acid on muscle glucose transport in the obese zucker rat. Am J Physiol Endocrinol Metab. 2003 Jul;285(1):E98-E105.

51. Roberts R, Hodson L, Dennis AL, Neville MJ, Humphreys SM, Harnden KE, et al. Markers of de novo lipogenesis in adipose tissue: Associations with small adipocytes and insulin sensitivity in humans. Diabetologia. 2009 May;52(5):882-90.

52. de Souza CJ, Eckhardt M, Gagen K, Dong M, Chen W, Laurent D, et al. Effects of pioglitazone on adipose tissue remodeling within the setting of obesity and insulin resistance. Diabetes. 2001 Aug;50(8):1863-71.

53. Hafstad AD, Solevag GH, Severson DL, Larsen TS, Aasum E. Perfused hearts from type 2 diabetic (db/db) mice show metabolic responsiveness to insulin. Am J Physiol Heart Circ Physiol. 2006 May;290(5):H1763-9.

54. Ip C, Banni S, Angioni E, Carta G, McGinley J, Thompson HJ, et al. Conjugated linoleic acid-enriched butter fat alters mammary gland morphogenesis and reduces cancer risk in rats. J Nutr. 1999 Dec;129(12):2135-42.

55. Mehra A, Macdonald I, Pillay TS. Variability in 3T3-L1 adipocyte differentiation depending on cell culture dish. Anal Biochem. 2007 Mar 15;362(2):281-3.

56. Kang K, Pariza MW. Trans-10,cis-12-conjugated linoleic acid reduces leptin secretion from 3T3-L1 adipocytes. Biochem Biophys Res Commun. 2001 Sep 21;287(2):377-82.

57. Brown JM, Boysen MS, Chung S, Fabiyi O, Morrison RF, Mandrup S, et al. Conjugated linoleic acid induces human adipocyte delipidation: Autocrine/paracrine regulation of MEK/ERK signalling by adipocytokines. J Biol Chem. 2004 Jun 18;279(25):26735-47.

58. Kang K, Liu W, Albright KJ, Park Y, Pariza MW. Trans-10,cis-12 CLA inhibits differentiation of 3T3-L1 adipocytes and decreases PPAR gamma expression. Biochem Biophys Res Commun. 2003 Apr 11;303(3):795-9.

59. Perez-Matute P, Marti A, Martinez JA, Fernandez-Otero MP, Stanhope KL, Havel PJ, et al. Conjugated linoleic acid inhibits glucose metabolism, leptin and adiponectin secretion in primary cultured rat adipocytes. Mol Cell Endocrinol. 2007 Mar 30;268(1-2):50-8.

60. Bensinger SJ, Tontonoz P. Integration of metabolism and inflammation by lipid-activated nuclear receptors. Nature. 2008 Jul 24;454(7203):470-7.

61. Lemberger T, Braissant O, Juge-Aubry C, Keller H, Saladin R, Staels B, et al. PPAR tissue distribution and interactions with other hormone-signalling pathways. Ann N Y Acad Sci. 1996 Dec 27;804:231-51.

62. Aminot-Gilchrist DV, Anderson HD. Insulin resistance-associated cardiovascular disease: Potential benefits of conjugated linoleic acid. Am J Clin Nutr. 2004 Jun;79(6 Suppl):1159S-63S.

63. Ferre P, Foufelle F. SREBP-1c transcription factor and lipid homeostasis: Clinical perspective. Horm Res. 2007;68(2):72-82.

64. Stringer DM. Investigating the isomer-specific effects of conjugated linoleic acid on metabolic syndrome, hepatic steatosis and selected mediators of hepatic lipid metabolism in the fafa zucker rat; 2006.

65. Sampson SR, Cooper DR. Specific protein kinase C isoforms as transducers and modulators of insulin signalling. Mol Genet Metab. 2006 Sep-Oct;89(1-2):32-47.

66. Idris I, Gray S, Donnelly R. Protein kinase C activation: Isozyme-specific effects on metabolism and cardiovascular complications in diabetes. Diabetologia. 2001 Jun;44(6):659-73.

67. Song HJ, Sneddon AA, Barker PA, Bestwick C, Choe SN, McClinton S, et al. Conjugated linoleic acid inhibits proliferation and modulates protein kinase C isoforms in human prostate cancer cells. Nutr Cancer. 2004;49(1):100-8.

68. Parker PJ, Murray-Rust J. PKC at a glance. J Cell Sci. 2004 Jan 15;117(Pt 2):131-2.

69. Ip MM, Masso-Welch PA, Shoemaker SF, Shea-Eaton WK, Ip C. Conjugated linoleic acid inhibits proliferation and induces apoptosis of normal rat mammary epithelial cells in primary culture. Exp Cell Res. 1999 Jul 10;250(1):22-34.

70. Olfert ED, Cross BM, McWilliam AA, Canadian Council on Animal Care. Guide to the care and use of experimental animals. 2nd ed. Ottawa: Canadian Council on Animal Care; 1993.

71. Trinder P. Determination of blood glucose using an oxidase-peroxidase system with a non-carcinogenic chromogen. J Clin Pathol. 1969 Mar;22(2):158-61.

72. Allain CC, Poon LS, Chan CS, Richmond W, Fu PC. Enzymatic determination of total serum cholesterol. Clin Chem. 1974 Apr;20(4):470-5.

73. Roschlau P, Bernt E, Gruber W. Enzymatic determination of total cholesterol in serum (author's transl). Z Klin Chem Klin Biochem. 1974 Sep;12(9):403-7.

74. Matthews DR, Hosker JP, Rudenski AS, Naylor BA, Treacher DF, Turner RC. Homeostasis model assessment: Insulin resistance and beta-cell function from fasting plasma glucose and insulin concentrations in man. Diabetologia. 1985 Jul;28(7):412-9.

75. Gallagher S, Winston SE, Fuller SA, Hurrell JG. Immunoblotting and immunodetection. Curr Protoc Immunol. 2008 Nov;Chapter 8:Unit 8.10.

76. de Roos B, Rucklidge G, Reid M, Ross K, Duncan G, Navarro MA, et al. Divergent mechanisms of cis9, trans11-and trans10, cis12-conjugated linoleic acid affecting insulin resistance and inflammation in apolipoprotein E knockout mice: A proteomics approach. FASEB J. 2005 Oct;19(12):1746-8.

77. Poirier H, Rouault C, Clement L, Niot I, Monnot MC, Guerre-Millo M, et al. Hyperinsulinaemia triggered by dietary conjugated linoleic acid is associated with a decrease in leptin and adiponectin plasma levels and pancreatic beta cell hyperplasia in the mouse. Diabetologia. 2005 Jun;48(6):1059-65.

78. Poirier H, Niot I, Clement L, Guerre-Millo M, Besnard P. Development of conjugated linoleic acid (CLA)-mediated lipoatrophic syndrome in the mouse. Biochimie. 2005 Jan;87(1):73-9.

79. Terauchi Y, Tsuji Y, Satoh S, Minoura H, Murakami K, Okuno A, et al. Increased insulin sensitivity and hypoglycaemia in mice lacking the p85 alpha subunit of phosphoinositide 3-kinase. Nat Genet. 1999 Feb;21(2):230-5.

80. Fruman DA, Mauvais-Jarvis F, Pollard DA, Yballe CM, Brazil D, Bronson RT, et al. Hypoglycaemia, liver necrosis and perinatal death in mice lacking all isoforms of phosphoinositide 3-kinase p85 alpha. Nat Genet. 2000 Nov;26(3):379-82.

81. Berggreen C, Gormand A, Omar B, Degerman E, Goransson O. Protein kinase B activity is required for the effects of insulin on lipid metabolism in adipocytes. Am J Physiol Endocrinol Metab. 2009 Apr;296(4):E635-46.

82. Oral EA, Simha V, Ruiz E, Andewelt A, Premkumar A, Snell P, et al. Leptin-replacement therapy for lipodystrophy. N Engl J Med. 2002 February 21;346(8):570-8.

83. Yu X, Park BH, Wang MY, Wang ZV, Unger RH. Making insulin-deficient type 1 diabetic rodents thrive without insulin. Proc Natl Acad Sci U S A. 2008 Sep 16;105(37):14070-5.

84. Di Giancamillo A, Rossi R, Vitari F, Pastorelli G, Corino C, Domeneghini C. Dietary conjugated linoleic acids decrease leptin in porcine adipose tissue. J Nutr. 2009 Aug 26.

85. Zha JM, DI WJ, Zhu T, Xie Y, Yu J, Liu J, et al. Comparison of gene transcription between subcutaneous and visceral adipose tissue in chinese adults. Endocr J. 2009 Jun 30.

86. Slieker LJ, Sloop KW, Surface PL. Differentiation method-dependent expression of leptin in adipocyte cell lines. Biochem Biophys Res Commun. 1998 Oct 9;251(1):225-9.

87. MacDougald OA, Hwang CS, Fan H, Lane MD. Regulated expression of the obese gene product (leptin) in white adipose tissue and 3T3-L1 adipocytes. Proc Natl Acad Sci U S A. 1995 Sep 26;92(20):9034-7.

88. Frevert EU, Kahn BB. Protein kinase C isoforms epsilon, eta, delta and zeta in murine adipocytes: Expression, subcellular localization and tissue-specific regulation in insulin-resistant states. Biochem J. 1996 Jun 15;316 (Pt 3):865-71.

89. Qu X, Seale JP, Donnelly R. Tissue- and isoform-specific effects of aging in rats on protein kinase C in insulin-sensitive tissues. Clin Sci (Lond). 1999 Sep;97(3):355-61.

90. Qu X, Seale JP, Donnelly R. Tissue and isoform-selective activation of protein kinase C in insulin-resistant obese zucker rats - effects of feeding. J Endocrinol. 1999 Aug;162(2):207-14.

91. Schmitz-Peiffer C, Laybutt DR, Burchfield JG, Gurisik E, Narasimhan S, Mitchell CJ, et al. Inhibition of PKC epsilon improves glucose-stimulated insulin secretion and reduces insulin clearance. Cell Metab. 2007 Oct;6(4):320-8.

92. Sheu WH, Lee WJ, Chen YT. High plasma leptin concentrations in hypertensive men but not in hypertensive women. J Hypertens. 1999 Sep;17(9):1289-95.

93. Sheu WH, Lee WJ, Chen YT. Gender differences in relation to leptin concentration and insulin sensitivity in nondiabetic chinese subjects. Int J Obes Relat Metab Disord. 1999 Jul;23(7):754-9.

94. Hardie L, Trayhurn P, Abramovich D, Fowler P. Circulating leptin in women: A longitudinal study in the menstrual cycle and during pregnancy. Clin Endocrinol (Oxf). 1997 Jul;47(1):101-6.

95. Toker A, Meyer M, Reddy KK, Falck JR, Aneja R, Aneja S, Parra A,Burns DJ, Ballas LM, Cantley LC. Activation of protein kinase C family members by the novel polyphosphoinositides PtdIns-3, 4-P2 and PtdIns-3, 4, 5-P3. 1994. J Biol Chem 269:32358–67.

96. Miranda J, Fernandez-Quintela A, Churruca I, Rodriguez VM, Simon E, Portillo MP. Hepatomegaly induced by trans-10,cis-12 conjugated linoleic acid in adult hamsters fed an atherogenic diet is not associated with steatosis. J Am Coll Nutr. 2009 Feb;28(1):43-9.

97. Zahradka P. Cardiovascular actions of the peroxisome proliferator-activated receptor-alpha (PPARalpha) agonist Wy14,643. Cardiovasc Drug Rev. 2007 Summer;25(2):99-122.

98. Jourdan T, Djaouti L, Demizieux L, Gresti J, Verges B, Degrace P. Liver carbohydrate and lipid metabolism of insulin-deficient mice is altered by trans-10, cis-12 conjugated linoleic acid. J Nutr. 2009 Aug 19.

99. Schmitz-Peiffer C, Biden TJ. Protein kinase C function in muscle, liver, and beta-cells and its therapeutic implications for type 2 diabetes. Diabetes. 2008 Jul;57(7):1774-83.